

STEREOGRAPHIC MARKOV CHAIN MONTE CARLO

JUN YANG¹, KRZYSZTOF ŁATUSZYŃSKI², AND GARETH O. ROBERTS²

ABSTRACT. High dimensional distributions, especially those with heavy tails, are notoriously difficult for off the shelf MCMC samplers: the combination of unbounded state spaces, diminishing gradient information, and local moves, results in empirically observed "stickiness" and poor theoretical mixing properties – lack of geometric ergodicity. In this paper, we introduce a new class of MCMC samplers that map the original high dimensional problem in Euclidean space onto a sphere and remedy these notorious mixing problems. In particular, we develop random-walk Metropolis type algorithms as well as versions of Bouncy Particle Sampler that are uniformly ergodic for a large class of light and heavy tailed distributions and also empirically exhibit rapid convergence in high dimensions. In the best scenario, the proposed samplers can enjoy the "blessings of dimensionality" that the mixing time decreases with dimension.

CONTENTS

1. Introduction	2
2. Stereographic Markov Chain Monte Carlo	4
3. SPS: Isotropic Targets	10
4. SPS: Extension to Elliptical Targets	13
5. SPS in High-dimensional Problems	16
6. Simulations	21
7. Discussions	25
Acknowledgement	26
A. Proofs of Main Results	27
B. Additional Simulations	69
References	84

¹DEPARTMENT OF STATISTICS, UNIVERSITY OF OXFORD, UK

²DEPARTMENT OF STATISTICS, UNIVERSITY OF WARWICK, UK

E-mail addresses: jun.yang@stats.ox.ac.uk, k.g.latuszynski@warwick.ac.uk, gareth.o.roberts@warwick.ac.uk.

1. INTRODUCTION

Bayesian analysis relies heavily on Markov chain Monte Carlo (MCMC) methods to explore complex posterior distributions. In most settings, such distributions typically have support contained within a subset S of \mathbb{R}^d for some $d > 0$, then it is natural to construct appropriate MCMC algorithms directly on S . In practice this is how the vast majority of algorithms are constructed, although there are intrinsic problems with this approach. For instance, it is now well-established [MT96] that the popular vanilla MCMC workhorse, the random-walk Metropolis (RWM) algorithm fails to be uniformly ergodic for any target density π when S is unbounded. In fact all existing generic MCMC methods are built upon local proposal mechanisms and are similarly afflicted. Lack of uniform ergodicity results in sensitivity of the algorithm's convergence to its starting value, and potentially long burn-in periods.

Moreover, these convergence problems are exacerbated for target distributions with heavy (heavier than exponential) tails. For instance in such cases, RWM and the Metropolis-adjusted Langevin Algorithm (MALA) fail to be even geometrically ergodic (i.e., they converge at a rate slower than any geometric rate) [RT96b; JH00; RT96a]. In practice this manifests itself on the algorithm trajectories by the presence of infrequent excursions of heavy-tailed duration into the target distribution tails. This can lead to further theoretical and practical problems, e.g., the non-existence of a Central Limit Theorem (CLT), for example [JR07], and unstable Monte Carlo estimators with large and difficult to quantify mean square errors which are highly sensitive to initial values.

Important modern innovations in MCMC algorithms have come from Piecewise Deterministic Markov Processes (PDMPs) [BKW09; BCVD18; BFR19] which offer for the first time generic recipes for non-reversible MCMC and offering substantial gains in algorithm efficiency as a result. Although not completely necessary, it turns out to be convenient and natural to construct PDMPs as continuous time algorithms. While the practical use of PDMPs for posterior exploration is still in its infancy, these methods offer substantial promise. However PDMPs are still localised algorithms and as such usually suffer from the lack of uniform and/or geometric ergodicity [VR21a; VR21b; ADW21; And+21].

In contrast, when the target density tails are exponential or lighter, RWM, MALA, and related algorithms are generally geometrically ergodic under weak regularity conditions [RT96b; JH00]. Some transformation strategies for achieving this are described in [SFR10; JG12] with closely related strategies being proposed in [Kam18], although these approaches are unlikely to regain uniform ergodicity. When S is bounded, then MCMC algorithms are generally easily shown to be uniformly ergodic (see for example [MT96] for RWM). This naturally suggests that transformations designed to compactify S might facilitate the construction of more robust families of MCMC algorithms. However, finding generic solutions to the construction of such

transformations which lead to well-behaved densities on the transformed space is challenging.

It is, however, far easier to construct general transformations to transform \mathbb{R}^d to a *pre-compact* space. The most celebrated of such transformations is stereographic projection which was known to the ancient Egyptians, see [Cox61] for a modern description. It maps $\mathbb{R}^d \rightarrow \mathbb{S}^d \setminus N$, i.e., the d -sphere excluding its North Pole. This paper will explore the use of stereographically projected algorithms. One iteration of such an algorithm takes the current state $\mathbf{x} \in \mathbb{R}^d$, transforms to $\mathbb{S}^d \setminus N$ through inverse stereographic projection, carrying out an appropriately constructed MCMC step on $\mathbb{S}^d \setminus N$ before returning to \mathbb{R}^d by stereographic projection. The contributions of our work are as follows.

- (1) We present the Stereographic Projection Sampler (SPS) efficient and practical implementation of the above programme for RWM, including a simple reprojection step to ensure the Markov chain remains on $\mathbb{S}^d \setminus N$. We provide a dimension and scale dependant recipe for choosing the radius of S . See Section 2.1.
- (2) We prove that for continuous positive densities, π on \mathbb{R}^d with tails no heavier than those of a d -dimensional multivariate student's t distribution with d degrees of freedom, SPS is uniformly ergodic. The tail conditions on π are in fact necessary for geometric ergodicity. See Theorem 2.2 and Remark 2.4.
- (3) We give a high-dimensional analysis of SPS for the stylised family of product i.i.d. form targets, by maximizing the expected squared jumping distance (ESJD) as well as by showing for a variant of SPS that each component converges (as $d \rightarrow \infty$) to a Langevin diffusion. This affords a direct and uniformly favourable comparison with the Euclidean RWM algorithm. See Section 5.
- (4) We also introduce the Stereographic Bouncy Particle Sampler (SBPS) which replaces the random walk move in SPS with a PDMP algorithm which follows great circle trajectories interspersed with abrupt direction changes. See Section 2.2.
- (5) We prove uniform ergodicity of SBPS under weaker conditions than those for SPS, specifically requiring tails to be lighter than those of a d -dimensional multivariate student's t distribution with $d - 1/2$ degrees of freedom. See Theorem 2.6 and Corollary 2.7.
- (6) For isotropic targets (i.e., spherically symmetric targets), we demonstrate that both light- and heavy-tailed, the proposed SPS and SBPS can enjoy the *blessings of dimensionality*. For example, the mixing times of SPS and SBPS can actually *decrease* as the dimension increases. See Section 3 and Section 6.
- (7) We introduce generalizations of stereographic projection which are suitable for elliptical targets. See Section 4. The framework we established in this paper

opens opportunities for developing other mappings from \mathbb{R}^d to \mathbb{S}^d for other classes of targets. See Section 7.

In very recent work, [Lie+21] presents related methodology for exploring distributions defined directly on a manifold, providing supporting theory showing that under suitable conditions their method’s spectral gap is dimension-independent. However, the focus of their work is very different. Their work uses a different reprojection scheme based on [Cot+13] and does not consider distributions defined directly on \mathbb{R}^d . Moreover, they consider densities which are absolutely continuous with respect to a Gaussian measure in the infinite dimensional limit. This is an arguably very restrictive class. So their dimension-independent results are not really comparable with our results. An alternative reprojection scheme is introduced in [ZHCG18]. Compared to that method, the reprojection scheme used in this paper has the advantage that reprojection from a fixed point on the tangent space is always possible and is a much more natural approach for the hypersphere. The [ZHCG18] method does have advantages for use in more general manifolds, but this is not of any use to us here.

There are strong theoretical reasons for wanting to construct the algorithm dynamics directly on a manifold of positive curvature such as a hypersphere [MS18; Oli09; MMB18]. However quite naturally, the existing literature has concentrated primarily on the case of Brownian motion which clearly has uniform invariant distribution on S , and which maps via stereographic projection to a spherically symmetric multivariate distribution on \mathbb{R}^d . Therefore we can immediately lift theory from existing theory to show that SPS on such target densities has a dimension-free convergence time. In our paper we go further. Rapid convergence extends to a large family of spherically symmetric target densities (essentially excluding only very heavy-tailed distributions).

Our paper is structured as follows. Section 2 introduces both SPS and SBPS algorithms and presents formal ergodicity and uniform ergodicity results for both methods. Sections 3 to 5 provide additional results for SPS and its generalisations. In Section 3 a detailed analysis of SPS for isotropic densities is provided, while in Section 4, a generalised version of the algorithm is introduced. Section 4 also gives robustness results to departures from isotropy. In Section 5 we provide a high dimensional analysis of SPS for the stylised family of product i.i.d. target densities and give positive comparisons to the Euclidean RWM algorithm. Numerical studies on both SPS and SBPS are provided in Section 6 to illustrate our theory and we conclude with the discussions on SPS and SBPS in Section 7. The supplementary materials contain all the technical proofs and some additional simulations.

2. STEREOGRAPHIC MARKOV CHAIN MONTE CARLO

2.1. Stereographic Projection Sampler (SPS). We begin by giving a brief description of stereographic projection and then describe in detail two novel MCMC samplers which exploit the properties of stereographic projection.

Let \mathbb{S}^d denote the *unit sphere* in \mathbb{R}^{d+1} centered at the origin. A stereographic projection describes a bijection from $\mathbb{S}^d \setminus \{(0, \dots, 0, 1)\}$ to \mathbb{R}^d . Within this paper, we shall restrict attention to projections indexed by a single parameter $R \in \mathbb{R}^+$ and described by the mapping

$$x = \text{SP}(z) := \left(R \frac{z_1}{1 - z_{d+1}}, \dots, R \frac{z_d}{1 - z_{d+1}} \right)^T,$$

with Jacobian determinant at $x \in \mathbb{R}^d$ satisfying

$$J_{\text{SP}}(x) \propto (R^2 + \|x\|^2)^d, \quad (1)$$

and inverse $\text{SP}^{-1} : \mathbb{R}^d \rightarrow \mathbb{S}^d \setminus \{(0, \dots, 0, 1)\}$ given by

$$z_i = \frac{2Rx_i}{\|x\|^2 + R^2}, \quad \forall 1 \leq i \leq d, \quad z_{d+1} = \frac{\|x\|^2 - R^2}{\|x\|^2 + R^2}. \quad (2)$$

See Fig. 1 for a geometric illustration of this stereographic projection (in the case $d = 1$ for simplicity) and Appendix A.13 for the proof of the Jacobian determinant Eq. (1).

Now suppose we wish to sample from a target density $\pi(x)$ where $x \in \mathbb{R}^d$. Our aim will be to take advantage of our stereographic bijection to construct an MCMC sampler directly on \mathbb{S}^d , projecting the output back onto \mathbb{R}^d . We denote the transformed target as $\pi_S(z)$ then for $x = \text{SP}(z)$ we have

$$\pi_S(z) \propto \pi(x)(R^2 + \|x\|^2)^d. \quad (3)$$

First, we just consider a random-walk Metropolis algorithm with normalized step size h on the unit sphere. Fig. 2 illustrates how the algorithm moves are constructed on

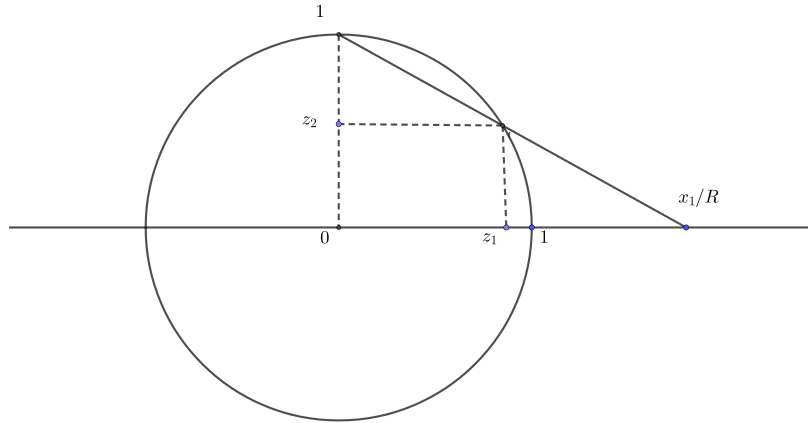


FIGURE 1. Illustration of Stereographic Projection $\text{SP} : \mathbb{S} \rightarrow \mathbb{R}$.

the sphere. (Note that we could very easily have constructed more general Metropolis–Hastings algorithms.)

Algorithm 1 Stereographic Projection Sampler (SPS)

- Let the current state be $X^d(t) = x$;
 - Compute the proposal \hat{X} :
 - Let $z := \text{SP}^{-1}(x)$;
 - Sample independently $d\tilde{z} \sim \mathcal{N}(0, h^2 I_{d+1})$;
 - Let $dz := d\tilde{z} - \frac{(z^T \cdot d\tilde{z})z}{\|z\|^2}$ and $\hat{z} := \frac{z+dz}{\|z+dz\|}$;
 - The proposal $\hat{X} := \text{SP}(\hat{z})$.
 - $X^d(t+1) = \hat{X}$ with probability $1 \wedge \frac{\pi(\hat{X})(R^2 + \|\hat{X}\|^2)^d}{\pi(x)(R^2 + \|x\|^2)^d}$; otherwise $X^d(t+1) = x$.
-

The symmetry of the re-projection mechanism in the proposal of the algorithm means that SPS is indeed a valid MCMC algorithm for π . More formally, we have the following result.

Proposition 2.1. *If $\pi(x)$ is positive and continuous in \mathbb{R}^d , then SPS gives rise to an ergodic Markov chain on \mathbb{R}^d with invariant distribution π .*

Proof. See Appendix A.1. □

It is long recognised that random-walk Metropolis (RWM) algorithms on bounded spaces are usually uniformly ergodic, while the same algorithms on unbounded spaces are never uniformly ergodic [MT96]. Therefore, given the compactness of \mathbb{S}^d , it

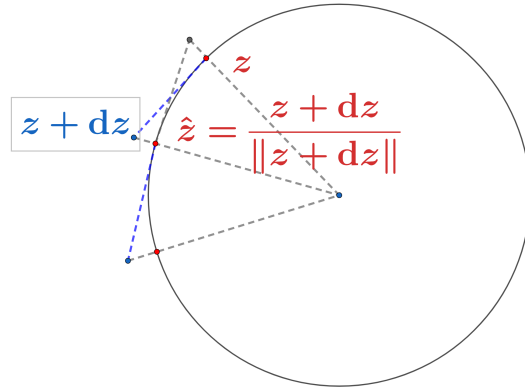


FIGURE 2. Illustration of SPS proposing $\hat{z} = \text{SP}^{-1}(\hat{X})$ from $z = \text{SP}^{-1}(x)$. By symmetricity, the proposal distribution is the same as proposing z from \hat{z} .

is reasonable to hope that SPS might be uniformly ergodic under mild regularity conditions on π . Since the actual state space of SPS is in fact $\mathbb{S}^d \setminus N$ (where N denotes the *North Pole*: $(0, \dots, 0, 1)$) which is not compact, this question is more complicated than in the Euclidean state space case as we need to consider the properties of the transformed density near N . However our first main result confirms that we do get uniform ergodicity if and only if the transformed density on the sphere is bounded at N .

Theorem 2.2. *If $\pi(x)$ is positive and continuous in \mathbb{R}^d , then SPS is uniformly ergodic if and only if*

$$\sup_{x \in \mathbb{R}^d} \pi(x)(R^2 + \|x\|^2)^d < \infty. \quad (4)$$

Proof. See Appendix A.2. □

Example 2.3. If the target $\pi(x)$ where $x \in \mathbb{R}^d$ is multivariate student's t distribution with degree of freedom no smaller than d , then the SPS algorithm is *uniformly ergodic*. ◁

Remark 2.4. We make the following remarks:

- (1) The condition Eq. (4) is necessary: if $\sup_{x \in \mathbb{R}^d} \pi(x)(R^2 + \|x\|^2)^d = \infty$, then the chain is not even geometric ergodic [RT96b];
- (2) The traditional RWM algorithm is *not* uniformly ergodic if the support of π is \mathbb{R}^d [MT96] and *not* geometrically ergodic for any heavy-tailed target distribution [JH00];
- (3) The condition that $\pi(x)$ is positive and continuous in \mathbb{R}^d in both Proposition 2.1 and Theorem 2.2 can be relaxed. We used it here just for the simplicity of the proof.

◁

2.2. Stereographic Bouncy Particle Sampler (SBPS). Many recent innovations in MCMC algorithm construction have focused on non-reversible methods, most particularly those described by *piecewise deterministic Markov processes* (PDMPs) (see for example [BCVD18; BFR19]). In this subsection we shall demonstrate that we can readily incorporate these methods within our projective framework. We shall concentrate on a version of the *Bouncy Particle Sampler* (BPS) [BCVD18] as this adapts naturally to our context. The algorithm is described as follows.

PDMPs are continuous-time algorithms which introduce an auxiliary random variable v , which in the case of the Stereographic Bouncy Particle Sampler (SBPS) has stationary distribution uniformly distributed on \mathbb{S}^d and independently of x . One feature of PDMP algorithms such as SBPS is the option to include *refresh* moves which (according to some possibly x -dependent hazard rate) which independently refresh

v by sampling it from its invariant distribution (uniform on \mathbb{S}^d). In the description below, we restrict ourselves to the case where this refresh rate is constant.

Algorithm 2 Stereographic Bouncy Particle Sampler (SBPS)

- Initialize $z^{(0)}$ arbitrarily on \mathbb{S}^d then $v^{(0)}$ arbitrarily with $v^{(0)} \cdot z^{(0)} = 0$ and $\|v^{(0)}\| = 1$.
 - For $i = 1, 2, \dots$
 - Simulate bounce time τ_{bounce} of a Poisson process of intensity $\chi(t) = \lambda(\sin(t)v^{(i-1)} + \cos(t)z^{(i-1)}, \cos(t)v^{(i-1)} - \sin(t)z^{(i-1)})$, where
$$\lambda(z, v) := \max\{0, [-v \cdot \nabla_z \log \pi_S(z)]\}.$$
 - Simulate refreshment time $\tau_{\text{refresh}} \sim \text{Exponential}(\lambda_{\text{refresh}})$.
 - Let $\tau_i = \min\{\tau_{\text{bounce}}, \tau_{\text{refresh}}\}$ and
$$z^{(i)} = \sin(\tau_i)v^{(i-1)} + \cos(\tau_i)z^{(i-1)}.$$
 - If $\tau_i = \tau_{\text{refresh}}$, sample new $v^{(i)}$ independently
$$v^{(i)} \sim \text{Uniform}\{v : z^{(i)} \cdot v = 0, \|v\| = 1\}$$
 - If $\tau_i = \tau_{\text{bounce}}$, compute
$$v^{(i)} = v_{\text{temp}} - 2 \left[\frac{v_{\text{temp}} \cdot \tilde{\nabla}_z \log \pi_S(z^{(i)})}{\tilde{\nabla}_z \log \pi_S(z^{(i)}) \cdot \tilde{\nabla}_z \log \pi_S(z^{(i)})} \right] \tilde{\nabla}_z \log \pi_S(z^{(i)}),$$
where
$$v_{\text{temp}} = \cos(\tau_i)v^{(i-1)} - \sin(\tau_i)z^{(i-1)}$$

$$\tilde{\nabla}_z \log \pi_S(z^{(i)}) = \nabla_z \log \pi_S(z^{(i)}) - [z^{(i)} \cdot \nabla_z \log \pi_S(z^{(i)})] z^{(i)}.$$
 - If $\sum_{j=1}^i \tau_j \geq T$ (where T is some constant time), exit.
-

Again we demonstrate that SBPS is indeed a valid MCMC algorithm, at least under certain conditions on π and the refresh rate in the algorithm. Note that the conditions on π and λ_{refresh} in Proposition 2.5 are not required for invariance, only for ensuring ϕ -irreducibility of the algorithm.

Proposition 2.5. *Suppose that $\lambda_{\text{refresh}} > 0$ and $\pi > 0$ for all $x \in \mathbb{R}^d$. Then SBPS gives rise to an ergodic Markov chain on \mathbb{R}^d with invariant distribution for (x, v) with joint density on $\mathbb{R}^d \times \mathbb{S}^d$. The marginal density on \mathbb{R}^d is proportional to $\pi(x)$.*

Proof. The proof of this result is routine (but tedious), following the lines of existing results for PDMPs in the literature. We give a sketch proof in Appendix A.3. \square

In this subsection, we shall prove a uniform ergodicity result analogous to that of Theorem 2.2.

Theorem 2.6. *If $\pi(x)$ is positive in \mathbb{R}^d with continuous first derivative in all components, then SBPS is uniformly ergodic if*

$$\limsup_{\{x: \|x\| \rightarrow \infty\}} \sum_{i=1}^d \left(\frac{\partial \log \pi(x)}{\partial x_i} x_i \right) + 2d < \frac{1}{2}.$$

Proof. See Appendix A.4. □

Corollary 2.7. *If the target $\pi(x)$ where $x \in \mathbb{R}^d$ is multivariate student's t distribution with degree of freedom larger than $d - \frac{1}{2}$, then the SBPS algorithm is uniformly ergodic.*

Proof. See Appendix A.5. □

Remark 2.8. We make the following remarks:

- (1) This is the first known PDMP algorithm that is uniformly ergodic for a large family of target distributions including heavy-tailed targets. For comparison, the traditional BPS is only known to be geometrically ergodic under certain restrictive conditions on the target [DBCD19; DGM20] and is known not to be geometrically ergodic for any heavy-tailed target distribution [VR21b].
- (2) We conjecture that the best possible condition for Theorem 2.6 is

$$\limsup_{\{x: \|x\| \rightarrow \infty\}} \sum_{i=1}^d \left(\frac{\partial \log \pi(x)}{\partial x_i} x_i \right) + 2d < 1.$$

We explain the reason for our conjecture in Appendix A.6. Therefore, we conjecture that Corollary 2.7 is only loose by 1/2 degree. That is, if the target $\pi(x)$ where $x \in \mathbb{R}^d$ is multivariate student's t distribution with degree of freedom larger than $d - 1$, then the SBPS algorithm is conjectured to be *uniformly ergodic*. ◁

To finish this section, we present some typical sample paths obtained by implementing SBPS.

Example 2.9. In Fig. 3, we show the proposed SBPS without and with refreshment for standard Gaussian target in two dimensions. Note that the SBPS without refreshment is not irreducible in this case. The same issue exists for the traditional BPS for standard Gaussian targets. This issue can be fixed by adding the refreshment. ◁

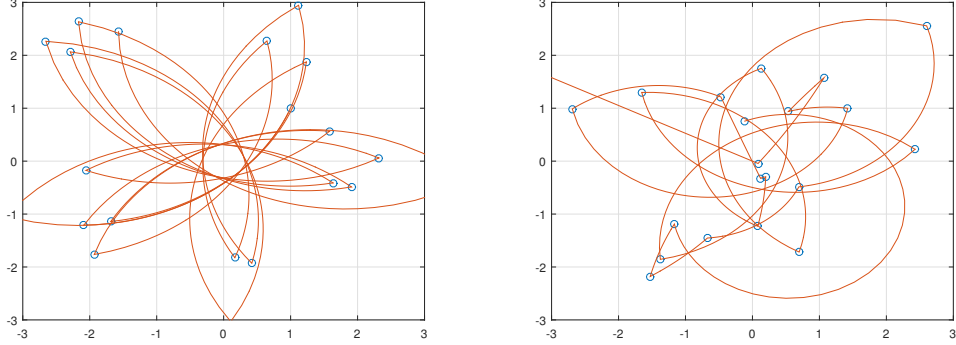


FIGURE 3. SBPS without (left) and with (right) refreshment for target distribution $\mathcal{N}(0, I_2)$. Note that the SBPS chain is not irreducible without refreshment.

3. SPS: ISOTROPIC TARGETS

In this section, we consider *isotropic targets*, which is also called spherical symmetric targets¹. That is, $\pi(x)$ is only a function of $\|x\|$. Recall the mapping and Eq. (2) and the transformed target $\pi_S(z)$ in Eq. (3). We can see that, for any isotropic target, the transformed target $\pi_S(z)$ is only a function of the “latitude” z_{d+1} .

We shall assume that all second moments exist, and without loss of further generality, we suppose $\pi(x)$ satisfies that

$$\mathbb{E}_{X \sim \pi}[\|X\|^2] = d.$$

Throughout this section, we assume $R = \sqrt{d}$.

Under the above assumptions, it suffices to study the path of the absolute value of the “latitude” z_{d+1} of SPS. Informally, the “stationary phase” of SPS is the period in which $z_{d+1} = \mathcal{O}(d^{-1/2})$ and the “transient phase” is the period in which $|z_{d+1}|$ is larger than $\mathcal{O}(d^{-1/2})$. Somehow surprisingly, by analyzing the proposed “latitude” \hat{z}_{d+1} , we can show that the SPS enjoys the *blessings of dimensionality*: the number of iterations for the “latitude” of SPS to decrease to $\mathcal{O}(d^{-1/2})$ decreases with the dimension d . This implies (informally) the “transient phase” of SPS is $\mathcal{O}(1)$.

3.1. Analysis of the proposal distribution. We assume the chain starts from either the “north pole” or the “south pole”. By the assumptions, the chain is in the “stationary phase” once it is around the “equator”.

¹Note that in some literature, isotropic distribution could be used to denote a distribution with zero mean and identity covariance matrix, which is different from our definition in this paper.

In the following, we give useful approximations for the proposed “latitude” \hat{z}_{d+1} in both transient phase and stationary phase. This can be used to analyze the behavior of isotropic targets. See Fig. 4 for some simulations using the result from Lemma 3.1.

Lemma 3.1. *Let z_i be the current i -th coordinate and \hat{z}_i be the i -th coordinate of the proposal, where $i = 1, \dots, d+1$. Then if $h = \mathcal{O}(1)$, we have the following approximation*

$$\hat{z}_i = \frac{1}{\sqrt{1+h^2d}} \left(z_i + \sqrt{1-z_i^2}hU \right) (1 + \mathcal{O}_{\mathbb{P}}(d^{-1/2})), \quad (5)$$

where $U \sim \mathcal{N}(0,1)$. Furthermore, if $h = \mathcal{O}(d^{-1/2})$, then we have the following coordinate-wise approximation

$$\hat{z}_i = \frac{1}{\sqrt{1+h^2(d-1)}} \left[\left(1 - \frac{1}{2}h^2U^2 \right) z_i - \sqrt{1-z_i^2}hU \right] + \mathcal{O}_{\mathbb{P}}(h^3). \quad (6)$$

As special cases of Eq. (6), z_{d+1} is the current “latitude” and \hat{z}_{d+1} be the proposed “latitude”. Then, in the transient phase, if $z_{d+1}^2 = 1 - o(h^2)$, we have

$$\hat{z}_{d+1} = \frac{1}{\sqrt{1+h^2(d-1)}} \left(1 - \frac{1}{2}h^2U^2 \right) z_{d+1} + o_{\mathbb{P}}(d^{-1}), \quad (7)$$

and in the stationary phase, if $z_{d+1} = \mathcal{O}(d^{-1/2})$, we have

$$\hat{z}_{d+1} = \frac{1}{\sqrt{1+h^2(d-1)}} (z_{d+1} - hU) + o_{\mathbb{P}}(d^{-1}). \quad (8)$$

Proof. See Appendix A.7. □

The above lemma suggest that in the transient phase, the proposed “latitude” is almost deterministic, whereas in the stationary phase, the proposed “latitude” approximately follows an autoregressive process. For example, if we take h to be constant and $i = d+1$, then Eq. (5) shows that the proposal “latitude” \hat{z}_{d+1} decreases to $\mathcal{O}(d^{-1/2})$ faster when dimension is larger. If the proposals will be accepted a probability bounded away from 0, the “transient phase” of SPS only involve $\mathcal{O}(1)$ iterations and the number even decreases with the dimension. In the next subsection, we show a class of examples of targets such that the SPS enjoys the *blessings of dimensionality*.

3.2. Examples of Isotropic Targets. We denote the multivariate student’s t distributions by $\pi_{\nu}(x)$ where ν is the degree of freedom. We denote the standard multivariate Gaussian as the limit $\pi_{\infty}(x)$. That is,

$$\pi_{\nu}(x) \propto \left(1 + \frac{1}{\nu} \|x\|^2 \right)^{-(\nu+d)/2}, \quad \pi_{\infty}(x) \propto \exp \left(-\frac{1}{2} \|x\|^2 \right)$$

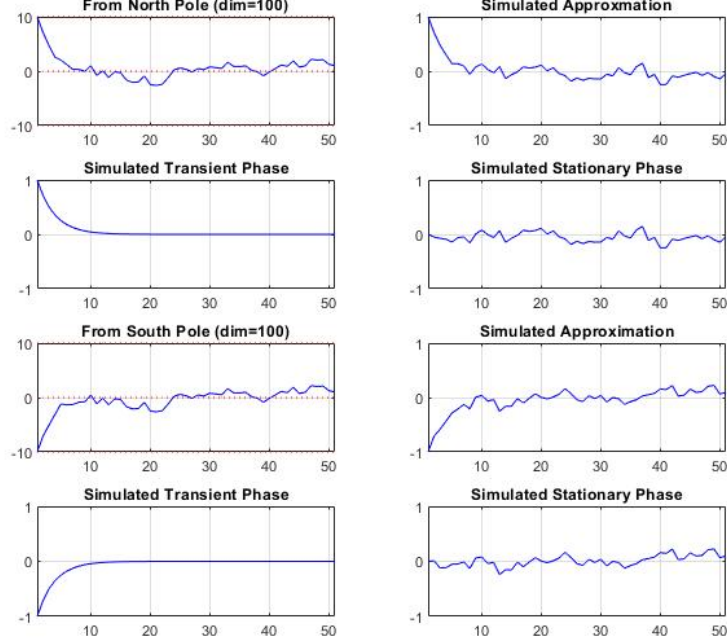


FIGURE 4. We consider $h = 0.1$ and $d = 100$ and two cases for the initial state: from North Pole (up) and from South Pole (down). For each case, the first subplot is the traceplot of the proposal latitudes. The other three are approximations using Eq. (6), Eq. (7), and Eq. (8) from Lemma 3.1.

Then the logarithm of the likelihood ratio can be written as a function of z_{d+1} and \hat{z}_{d+1} :

$$\log \frac{\pi_\nu(\hat{X})}{\pi_\nu(x)} + d \log \frac{R^2 + \|\hat{X}\|^2}{R^2 + \|x\|^2} = d(g_{\nu/d}(z_{d+1}) - g_{\nu/d}(\hat{z}_{d+1})),$$

where $g_k(z) := \frac{k+1}{2} \log(k + \frac{1+z}{1-z}) + \log(1-z)$. If $k = \nu/d \rightarrow \infty$, we have $g_k(z)$ converges to $g_\infty(z) := \frac{1}{1-z} - \frac{1}{2} + \log(1-z)$ up to a constant. See Appendix B.1 for the plots of function of $g_k(z)$ for different values of k .

Example 3.2. (Multivariate student's t distribution with DoF $\nu = d$) It can be easily verified that $g_1(z) = \log(2)$. Therefore, any proposal will be accepted since the acceptance rate is always 1 whatever h is. \triangleleft

Example 3.3. (Multivariate student's t distribution with DoF $\nu > d$, including Gaussian) From Lemma 3.1, one can conclude: (i) in *transient phase*, the acceptance

probability is almost 1 starting from either the “north pole” or the “south pole”; (ii) In *stationary phase*, the acceptance rate is close to 1. This suggests that as long as the target has “lighter tail” than multivariate student’s t with DoF d , the “transient phase” only takes $\mathcal{O}(1)$ steps. For comparison, for the standard multivariate Gaussian target, the “transient phase” of the traditional RWM takes $\mathcal{O}(d)$ steps [CRR05]. \triangleleft

Remark 3.4. Our theoretical results don’t cover the cases of SPS for targets with heavier tails, such as multivariate student’s t with DoF $\nu < d$. In this case, the SPS cannot start from the “north pole” since the first proposal of the SPS will be rejected with probability 1. One might consider to start from the “south pole”. However, the SPS could get stuck at the “south pole” if the proposal variance is large (even if the origin is the mode of the target density). See Appendix A.12 for comments. In practice, we suggest to choose the initial state of the SPS as a random state uniformly sampled on the sphere. \triangleleft

4. SPS: EXTENSION TO ELLIPTICAL TARGETS

4.1. Extensions of Stereographic Projection. Same as previous section, we denote the state of the Markov chain by $x = (x_1, \dots, x_d)^T \in \mathbb{R}^d$. Suppose $z = (z_1, \dots, z_{d+1})^T$ is the coordinates of a *unit sphere in \mathbb{R}^{d+1}* (that is, $\|z\| = 1$).

Now, we map $z \in \mathbb{S}^d$ to $x \in \mathbb{R}^d$ by the generalized stereographic projection (GSP)

$$x = \text{GSP}(z) := Q \left(R\sqrt{\lambda_1} \frac{z_1}{1 - z_{d+1}}, \dots, R\sqrt{\lambda_d} \frac{z_d}{1 - z_{d+1}} \right)^T,$$

where R is the radius parameter, $Q^T = Q^{-1} \in \mathbb{R}^{d \times d}$ is a rotation matrix, $\{\lambda_1, \dots, \lambda_d\}$ are non-negative constants. That is, the GSP is obtained by “stretching” via $\{\lambda_i\}$ and “rotating” via Q from the SP.

Defining the norm

$$\|x\|_{\Lambda, Q}^2 := x^T Q \Lambda^{-1} Q^T x,$$

where $\Lambda = \text{Diag}\{\lambda_1, \dots, \lambda_d\}$, we have the following Generalized Stereographic Projection Sampler (GSPS) with parameters R, h, Λ, Q .

The following example shows that we can extend isotropic targets to elliptical targets using the GSPS.

Example 4.1. Suppose $\pi(x)$ is multivariate student’s t with covariance matrix $\Sigma = Q\Lambda Q^T$ where $\Lambda = \text{Diag}\{\lambda_1, \dots, \lambda_d\}$:

$$\pi(x) \propto \left(1 + \frac{1}{\nu} x^T \Sigma^{-1} x \right)^{-(\nu+d)/2}$$

Then, for the GSPS with the corresponding Q and Λ , and $R^2 = \sum_i \lambda_i$, the acceptance rate is always 1 for any h . \triangleleft

Algorithm 3 Generalized Stereographic Projection Sampler (GSPS)

-
- Let the current state be $X^d(t) = x$;
 - Compute the proposal \hat{X} :
 - Let $z := \text{GSP}^{-1}(x)$;
 - Sample independently $d\tilde{z} \sim \mathcal{N}(0, h^2 I_{d+1})$;
 - Let $dz := d\tilde{z} - \frac{(z^T \cdot d\tilde{z})z}{\|z\|^2}$ and $\hat{z} := \frac{z+dz}{\|z+dz\|}$;
 - The proposal $\hat{X} := \text{GSP}(\hat{z})$.
 - $X^d(t+1) = \hat{X}$ with probability $1 \wedge \frac{\pi(\hat{X})(R^2 + \|\hat{X}\|_{\Lambda, Q}^2)^d}{\pi(x)(R^2 + \|x\|_{\Lambda, Q}^2)^d}$; otherwise $X^d(t+1) = x$.
-

The GSPS naturally suggests that one can estimate the covariance matrix $\Sigma = Q\Lambda Q^T$ under the adaptive MCMC framework, which results in adaptive GSPS. Indeed, if both Λ and Q is known, then one can normalize GSPS and reduce it to SPS, which is GSPS with $\Sigma = I_d$.

As the robustness to estimations of the mean and the covariance matrix of the target is the key to the success of adaptive GSPS, we study the robustness for Gaussian targets in the next section.

4.2. Robustness for Gaussian Targets. We consider multivariate Gaussian targets with mean vector μ and covariance matrix Σ :

$$\pi_{\mu, \Sigma}(x) \propto \exp\left(-\frac{1}{2}(x - \mu)^T \Sigma^{-1}(x - \mu)\right),$$

where

$$\Sigma = \text{Diag}(\lambda_1, \dots, \lambda_d), \quad \mu = (\mu_1, \dots, \mu_d)^T.$$

We are interested in the robustness to $\mu \neq 0$ and $\Sigma \neq I_d$.

For comparison with the traditional RWM in \mathbb{R}^d on the orders of stepsize, we recall that the optimal scaling theory gives an optimal stepsize of $\mathcal{O}(d^{-1/2})$ for RWM [RGG97]. Our stepsize h is defined on unit sphere. When projecting to \mathbb{R}^d , we multiply by $R = \mathcal{O}(d^{1/2})$. Therefore, the optimal stepsize of RWM roughly corresponds to $h = \mathcal{O}(d^{-1})$ in our setting. In this subsection, we study how large the stepsize h can be so the expected acceptance probability of SPS goes to 1. This roughly corresponds to a stepsize of $\mathcal{O}(hd^{1/2})$ in \mathbb{R}^d . Our results show that the order of the stepsize of SPS when projected back to \mathbb{R}^d is always no smaller than the order of the optimal stepsize of RWM.

Theorem 4.2. Assume there exist constants $C < \infty$ and $c > 0$ such that $c \leq \lambda_i \leq C$ and $|\mu_i| \leq C$ for all $i = 1, \dots, d$. Furthermore, assume $R = d^{1/2}$ and

$$\left| \sum_{i=1}^d \mu_i^2 - \sum_{i=1}^d (1 - \lambda_i) \right| = \mathcal{O}(d^\alpha), \quad (9)$$

where $\alpha \leq 1$. Then, under stationarity that $X \sim \pi$, the expected acceptance probability converges to 1 as $d \rightarrow \infty$

$$\mathbb{E}_{X \sim \pi_{\mu, \Sigma}} \mathbb{E}_{\hat{X} | X} \left[1 \wedge \frac{\pi_{\mu, \Sigma}(\hat{X})(R^2 + \|\hat{X}\|^2)^d}{\pi_{\mu, \Sigma}(X)(R^2 + \|X\|^2)^d} \right] \rightarrow 1,$$

for all h such that

$$h = o \left(\frac{d^{-1}}{\sqrt{\max \left\{ \frac{1}{d} \sum_i |1 - \lambda_i|, \frac{1}{d} \sum_i \mu_i^2 \right\}}} \wedge d^{-(\frac{1}{2} \vee \alpha)} \right). \quad (10)$$

Proof. See Appendix A.8. \square

Note that for standard Gaussian target, we know that the acceptance rate goes to 1 as $d \rightarrow \infty$ for any h . Recall that for traditional RWM in dimension k , the optimal stepsize is $\mathcal{O}(k^{-1/2})$ in \mathbb{R}^k under the optimal scaling framework [RGG97], which corresponds to $h = \mathcal{O}(k^{-1/2}d^{-1/2})$ in the SPS setting. Therefore, Theorem 4.2 suggests that the “effective dimension” is determined by $\{\mu_i\}$ and $\{\lambda_i\}$: as long as $\{\lambda_i\}$ and $\{\mu_i\}$ are uniformly bounded, the “effective dimension” of SPS is never larger than d , which is the “effective dimension” of the traditional RWM. Furthermore, we can compare the “effective dimension” for SPS with d using Theorem 4.2 under different settings.

Example 4.3. Suppose $\mu_i = 0$ for all $i = 1, \dots, d$. Moreover, $\lambda_1 = \lambda_2 = \dots = \lambda_k = 2$ and $\lambda_{k+1} = \dots = \lambda_d = 1$, then as long as k is a fixed number, $\frac{1}{d} \sum_i |1 - \lambda_i| = \mathcal{O}(kd^{-1})$. By Theorem 4.2, when $h = o(k^{-1/2}d^{-1/2})$ then the acceptance rate goes to 1 as $d \rightarrow \infty$. This suggests that the “effective dimension” for SPS is no more than k . \triangleleft

Example 4.4. Suppose $\lambda_i = 0$ for all $i = 1, \dots, d$. Furthermore, $\mu_1 = \mu_2 = \dots = 1$ and $\mu_{k+1} = \dots = \mu_d = 0$ where k is a fixed number. Then we have $\frac{1}{d} \sum_i \mu_i^2 = \mathcal{O}(kd^{-1})$. By Theorem 4.2, the acceptance rate goes to 1 when $h = o(k^{-1/2}d^{-1/2})$, which implies the “effective dimension” for SPS is no more than k . \triangleleft

One can consider Theorem 4.2 in the context of adaptive MCMC, in which $\{\mu_i\}$ and $\{1 - \lambda_i\}$ represent the “estimation errors” of the coordinate means and eigenvalues of the covariance matrix of the target. One can choose the “radius” R of the stereographic projection properly to satisfy Eq. (9) with $\alpha = \frac{1}{2}$. This is to properly scale R so

that the “latitude” on the unit sphere of the SPS is $\mathcal{O}_{\mathbb{P}}(d^{-1/2})$. Then, according to Theorem 4.2, the “effective dimension” of SPS is smaller than d if $\frac{1}{d} \sum_i |1 - \lambda_i| = o(1)$ and $\frac{1}{d} \sum_i \mu_i^2 = o(1)$.

Finally, we show two examples that the result of Theorem 4.2 is tight. First, consider the special case that $\mu_i = \mu > 0$ and $\lambda_i = \sigma^2$ for all i . We assume $\mu^2 = 1 - \sigma^2$ so that Eq. (9) holds for any $\alpha \leq 1/2$. Then Eq. (10) suggests that the acceptance probability goes to zero if $h = o(d^{-1}/\mu)$. On the other hand, the target in this special case is a product i.i.d. target with marginal distribution $\mathcal{N}(\mu, 1 - \mu^2)$. By our optimal scaling results in Section 5, we know that the acceptance probability does not go to zero if $h = \mathcal{O}(d^{-1}/\mu)$ (see Lemma 5.2 and Corollary 5.7). Therefore, Eq. (10) is tight. Second, consider the special case that $\mu_i = \mu = 0$ and $\lambda_i = \sigma^2 \neq 1$ for all i . Then Eq. (9) holds for $\alpha = 1$. In this case, Eq. (10) suggests that the acceptance probability goes to zero if $h = o(d^{-\alpha}) = o(d^{-1})$. On the other hand, the target in this special case is a product i.i.d. target with marginal $\mathcal{N}(0, \sigma^2)$ where $\sigma^2 \neq 1$. If we properly rescale R and σ^2 , it reduces to the case of Lemma 5.2 where the target is the standard Gaussian but $R \neq d^{1/2}$. Therefore, by Lemma 5.2, the acceptance probability doesn’t converge to zero if $h = \mathcal{O}(d^{-1})$. Therefore, Eq. (10) is again tight.

5. SPS IN HIGH-DIMENSIONAL PROBLEMS

In this section we shall give a case study of the behaviour of SPS for high-dimensional target densities. We shall consider various limits of SPS as $d \rightarrow \infty$ though to have tractability of this limit we need to consider a very specialised class of target densities. To this end, analogous to [RGG97] we assume the target $\pi(x)$ has a product i.i.d. form.

5.1. Assumptions on π . We assume the target $\pi(x)$ has a product i.i.d. form:

$$\pi(x) = \prod_{i=1}^d f(x_i). \quad (11)$$

Without loss of generality, we assume f is normalised such that

$$\mathbb{E}_f(X^2) = \int x^2 f(x) dx = 1, \quad \mathbb{E}_f(X^6) < \infty. \quad (12)$$

We further assume f'/f is Lipschitz continuous, $\lim_{x \rightarrow \pm\infty} x f'(x) = 0$, and

$$\mathbb{E}_f \left[\left(\frac{f'(X)}{f(X)} \right)^8 \right] < \infty, \quad \mathbb{E}_f \left[\left(\frac{f''(X)}{f(X)} \right)^4 \right] < \infty, \quad \mathbb{E}_f \left[\left(\frac{X f'(X)}{f(X)} \right)^4 \right] < \infty. \quad (13)$$

Remark 5.1. Under the assumption $\mathbb{E}_f(X^2) = 1$, by Cauchy–Schwarz inequality

$$\mathbb{E}_f \left[((\log f)')^2 \right] \geq 1$$

TABLE 1. Examples of C_ν and $C_\nu/(C_\nu - 1)$ for different ν in Remark 5.1 and Remark 5.8

	$\nu = 3$	$\nu = 5$	$\nu = 10$	$\nu = 20$	$\nu = 50$	$\nu = 100$
C_ν	7.1285	3.0187	1.7521	1.3336	1.1250	1.0612
$C_\nu/(C_\nu - 1)$	1.1632	1.4954	2.3297	3.9977	8.9990	17.3328

where the equality is achieved by standard Gaussian (or truncated standard Gaussian). For univariate student's t distribution with any DoF = $\nu > 2$, rescaling by a factor $\sqrt{\frac{\nu-2}{\nu}}$, we can obtain a target density f_ν with $\mathbb{E}_{f_\nu}(X^2) = 1$ and

$$C_\nu := \mathbb{E}_{f_\nu} \left[((\log f_\nu)')^2 \right] = \left(\frac{\nu}{\nu-2} \right) \left(\frac{\nu+1}{\nu} \right) \left(\frac{\nu+4}{\nu+3} \right) \sqrt{\frac{\nu+4}{\nu}} > 1.$$

where $\nu \rightarrow \infty$ recovers the case for standard Gaussian target. See Table 1 for values of C_ν for different ν . One can see that C_ν is very close to 1 for even medium size of ν . \triangleleft

In this section, we consider f has full support in \mathbb{R} . Then the product i.i.d. target π is not isotropic unless it is the standard Gaussian.

5.2. Acceptance Probability. To make progress, we need a detailed understanding of the high-dimensional behaviour of the acceptance probability of SPS. It turns out that to optimally apply SPS, we need to scale R to be $\mathcal{O}(d^{1/2})$. Not doing this will concentrate mass at either the North or South poles in an ultimately degenerate way. We shall thus assume R to be scaled in this way in what follows.

Lemma 5.2. *Under the assumptions on π in Section 5.1, suppose the current state $X \sim \pi$, and the parameter of the algorithm $R = \sqrt{\lambda d}$, where $\lambda > 0$ is a fixed constant. We further re-parameterize the other parameter h using ℓ via*

$$\frac{1}{\sqrt{1 + h^2(d-1)}} = 1 - \frac{\ell^2}{2d} \frac{4\lambda}{(1+\lambda)^2}.$$

Then, if either $\lambda \neq 1$ or f is not the standard Gaussian density, there exists a sequence of sets $\{F_d\}$ such that $\pi(F_d) \rightarrow 1$ and

$$\sup_{X \in F_d} \mathbb{E}_{\hat{X}|X} \left[\left| 1 \wedge \frac{\pi(\hat{X})(R^2 + \|\hat{X}\|^2)^d}{\pi(X)(R^2 + \|X\|^2)^d} - 1 \wedge \exp(W_{\hat{X}|X}) \right| \right] = o(d^{-1/4} \log(d)),$$

where $W_{\hat{X}|X} \sim \mathcal{N}(\mu, \sigma^2)$ and

$$\mu = \frac{\ell^2}{2} \left\{ \frac{4\lambda}{(1+\lambda)^2} - \mathbb{E}_f \left[((\log f)')^2 \right] \right\}, \quad \sigma^2 = \ell^2 \left\{ \mathbb{E}_f \left[((\log f)')^2 \right] - \frac{4\lambda}{(1+\lambda)^2} \right\}.$$

Proof. See Appendix A.9. \square

Remark 5.3. Lemma 5.2 requires either $\lambda \neq 1$ or π is not the standard multivariate Gaussian. If $\lambda = 1$ and π is the standard multivariate Gaussian, the case reduces to isotropic targets discussed in Section 3.2, so the Gaussian approximation in Lemma 5.2 doesn't hold. \triangleleft

Remark 5.4. Lemma 5.2 suggests that the expected acceptance probability in the stationary phase

$$\mathbb{E}_{X \sim \pi} \mathbb{E}_{\hat{X} | X} \left[1 \wedge \frac{\pi(\hat{X})(R^2 + \|\hat{X}\|^2)^d}{\pi(X)(R^2 + \|X\|^2)^d} \right] \rightarrow 2\Phi\left(-\frac{\sigma}{2}\right).$$

Furthermore, one can show that $\mathbb{E}[\|\hat{X} - X\|^2] \rightarrow \ell^2$. Then, we obtain the commonly used approximation of ESJD as

$$\begin{aligned} & \mathbb{E}[\|\hat{X} - X\|^2] \cdot \mathbb{E} \left[1 \wedge \frac{\pi(\hat{X})(R^2 + \|\hat{X}\|^2)^d}{\pi(X)(R^2 + \|X\|^2)^d} \right] \\ & \rightarrow 2\ell^2 \cdot \Phi \left(-\frac{\ell}{2} \sqrt{\mathbb{E}_f [((\log f)')^2]} - \frac{4\lambda}{(1+\lambda)^2} \right). \end{aligned}$$

By maximizing over ℓ , one can see the following observations:

- (1) When $\lambda \rightarrow 0$ or $\lambda \rightarrow \infty$, one recovers the maximum ESJD for the traditional RWM [RGG97];
- (2) For any fixed $\lambda > 0$, the approximated ESJD of SPS is strictly larger than the maximum ESJD of RWM;
- (3) If π is not standard Gaussian target, the maximum approximated ESJD of SPS is achieved at $\lambda = 1$ (that is, $R = \sqrt{d}$).

We will make the last statement precise in Theorem 5.6. \triangleleft

5.3. Maximizing ESJD. This subsection will obtain an explicit limiting expression for the expected squared jumping distance for SPS and demonstrate (again analogously to [RGG97]) that its limit is optimised by targeting an acceptance probability of 0.234.

Definition 5.5. Expected Squared Jumping Distance (ESJD):

$$\text{ESJD} := \mathbb{E}_{X \sim \pi} \mathbb{E}_{\hat{X} | X} \left[\|\hat{X} - X\|^2 \left(1 \wedge \frac{\pi(\hat{X})(R^2 + \|\hat{X}\|^2)^d}{\pi(X)(R^2 + \|X\|^2)^d} \right) \right].$$

Theorem 5.6. Under the assumptions on the target in Section 5.1, suppose f is not the standard Gaussian density and the SPS chain is in the stationary phase and

the radius parameter is chosen as $R = \sqrt{d}$. We further re-parameterize the other parameter h using ℓ via

$$\frac{1}{\sqrt{1 + h^2(d-1)}} = 1 - \frac{\ell^2}{2d}.$$

Then, as $d \rightarrow \infty$, we have

$$\text{ESJD} \rightarrow 2\ell^2 \cdot \Phi \left(-\frac{\ell}{2} \sqrt{\mathbb{E}_f [((\log f)')^2] - 1} \right).$$

Proof. See Appendix A.10. □

Corollary 5.7. *The maximum ESJD is approximately $\frac{1.3}{\mathbb{E}_f [((\log f)')^2] - 1}$, which is achieved when the acceptance rate is about 0.234. The optimal $\hat{\ell} \approx \frac{2.38}{\sqrt{\mathbb{E}_f [((\log f)')^2] - 1}}$ and the optimal \hat{h} is given by*

$$\hat{h} = \frac{1}{\sqrt{d-1}} \sqrt{\left(1 - \frac{\hat{\ell}^2}{2d}\right)^{-2} - 1} \approx \frac{\hat{\ell}}{\sqrt{d(d-1)}} \approx \frac{2.38}{\sqrt{d(d-1)}} \frac{1}{\sqrt{\mathbb{E}_f [((\log f)')^2] - 1}} = \mathcal{O}(d^{-1}).$$

Remark 5.8. Comparing with the maximum ESJD of RWM, the maximum ESJD of SPS is $\frac{\mathbb{E}_f [((\log f)')^2]}{\mathbb{E}_f [((\log f)')^2] - 1}$ times larger. For example, for the class of distributions defined in Remark 5.1 indexed by ν , we can compute $C_\nu/(C_\nu - 1)$. See Table 1 for examples of $C_\nu/(C_\nu - 1)$ for different ν . One can see that the maximum ESJD of SPS can be much larger than the maximum ESJD of RWM even for medium size of ν . ◁

5.4. Diffusion Limit. Continuing our analogy to the Euclidean RWM case, we shall provide a diffusion limit result, giving a more explicit description of SPS for high-dimensional situations. However it is difficult to obtain a diffusion limit directly for SPS. Instead we shall slightly changed the original SPS algorithm in a way which is asymptotically negligible (as d gets large) but which greatly facilitates our limiting diffusion approach. The revised algorithm is called RSPS.

Theorem 5.9. *Under the assumptions on π in Section 5.1, suppose f is not the standard Gaussian density and the RSPS chain $\{X^d(t)\}$ starts from the stationarity, i.e. $X^d(0) \sim \pi$, and the radius parameter is chosen as $R = \sqrt{d}$. We further re-parameterize the other parameter h using ℓ via*

$$\frac{1}{\sqrt{1 + h^2(d-1)}} = 1 - \frac{\ell^2}{2d}.$$

Writing $X^d(t) = (X_1^d(t), \dots, X_d^d(t))$, we let $U^d(t) := X_1^d(\lfloor dt \rfloor)$ be the sequence of the first coordinates of $\{X^d(t)\}$ sped-up by a factor of d . Then, as $d \rightarrow \infty$, we have

Algorithm 4 Revised Stereographic Projection Sampler (RSPS)

-
- Let the current state be $X^d(t) = x$;
 - Compute the proposal \hat{X} :
 - Let $z := \text{SP}^{-1}(x)$;
 - Sample independently $d\tilde{z}', d\tilde{z}'' \sim \mathcal{N}(0, h^2 I_{d+1})$;
 - Let $dz' := d\tilde{z} - \frac{(z^T \cdot d\tilde{z}')z}{\|z\|^2}$ and $dz'' := d\tilde{z} - \frac{(z^T \cdot d\tilde{z}'')z}{\|z\|^2}$;
 - Let $\hat{z}' := \frac{z+dz'}{\|z+dz'\|}$ and $\hat{z}'' := \frac{z+dz''}{\|z+dz''\|}$;
 - Two independent proposals $\hat{X}' := \text{SP}(\hat{z}')$ and $\hat{X}'' := \text{SP}(\hat{z}'')$;
 - The proposal $\hat{X} := (\hat{X}'_1, \hat{X}''_{2:d})$.
 - $X^d(t+1) = \hat{X}$ with probability $1 \wedge \frac{\pi(\hat{X})(R^2 + \|\hat{X}\|^2)^d}{\pi(x)(R^2 + \|x\|^2)^d}$; otherwise $X^d(t+1) = x$.
-

$U^d \Rightarrow U$, where \Rightarrow denotes weak convergence in Skorokhod topology, and U satisfies the following Langevin SDE

$$dU(t) = (s(\ell))^{1/2} dB(t) + s(\ell) \frac{f'(U(t))}{2f(U(t))} dt,$$

where

$$s(\ell) := 2\ell^2 \Phi \left(-\ell \frac{\sqrt{\mathbb{E}_f [((\log f)')^2] - 1}}{2} \right)$$

is the speed measure for the diffusion process, and $\Phi(\cdot)$ being the standard Gaussian cumulative density function.

Proof. See Appendix A.11. □

Corollary 5.10. *The optimal acceptance rate for RSPS is 0.234 and the maximum speed of the diffusion limit is*

$$s(\hat{\ell}) \approx \frac{1.3}{\mathbb{E}_f [((\log f)')^2] - 1}$$

where $\hat{\ell} \approx \frac{2.38}{\sqrt{\mathbb{E}_f [((\log f)')^2] - 1}}$. The optimal \hat{h} is given by

$$\hat{h} = \frac{1}{\sqrt{d-1}} \sqrt{\left(1 - \frac{\hat{\ell}^2}{2d}\right)^{-2} - 1} \approx \frac{\hat{\ell}}{\sqrt{d(d-1)}} \approx \frac{2.38}{\sqrt{d(d-1)}} \frac{1}{\sqrt{\mathbb{E}_f [((\log f)')^2] - 1}} = \mathcal{O}(d^{-1}).$$

Remark 5.11. Comparing with the maximum speed of the diffusion limit of RWM [RGG97], the maximum speed of the diffusion limit of RSPS is $\frac{\mathbb{E}_f[(\log f')^2]}{\mathbb{E}_f[(\log f')^2]-1}$ times larger. \triangleleft

Remark 5.12. A reasonable conjecture is that the same diffusion limit holds for original SPS algorithm. In order to establish the same diffusion limit, if we follow the same arguments as in the proof of Theorem 5.6, it is required to show the acceptance rate term becomes “asymptotically independent” with the first coordinate as a rate of $\mathcal{O}(d^{-1/2})$. However, our current technical arguments in Theorem 5.6 can achieve a rate of $\mathcal{O}(d^{-1/8})$ which is not enough for establishing the weak convergence to a diffusion limit. Therefore, we only prove the diffusion limit for RSPS in this paper and leave the proof for SPS as an open problem. \triangleleft

6. SIMULATIONS

In this section, we study the proposed SPS and SBPS through numerical examples. In most of the examples, we consider $d = 100$ dimensions and two choices of target distributions, the heavy tailed multivariate student’s t target with d degree of freedom and the standard Gaussian target. By default, we choose $R = \sqrt{d}$ for SPS and SBPS. We refer to Appendix B for additional simulations such as different choices of R .

6.1. SPS: traceplot and ACF. In this example, Fig. 5 shows traceplots and ACFs of SPS (first column) and RWM (the last three columns). SPS starts from the north pole and RWM starts from different initial states (c, c, \dots, c) where $c = 10, 20, 50$, respectively (see the last three columns of Fig. 5). For SPS starting from the south pole compared with RWM, we refer to Appendix B. We plot the traceplots and ACFs of the 1-st coordinate and negative log-target density, as well as traceplots of the first two coordinates. The target is standard Gaussian in $d = 100$ dimensions. The proposal variance for RWM is tuned such that the acceptance rate is about 0.234, which is known to be the optimal acceptance rate [RGG97]. For SPS, the acceptance rate is roughly 0.78, which is the lowest acceptance rate possible.

According to Fig. 5, the SPS mixes almost immediately. Indeed, the transient phase of SPS in $d = 100$ dimensions is less than 10 iterations. Comparing with SPS, the mixing time of RWM relies on the initial value. For example, in the last column of Fig. 5, the RWM hasn’t mixed after 5000 iterations. In the stationary phase, with an acceptance rate of 0.78, SPS generates almost uncorrelated samples according to the ACFs. Comparing with SPS, the samples from RWM with optimal acceptance rate 0.234 are highly correlated in high dimensions.

6.2. SPS: ESJD per dimension. In this example, we study the ESJD for SPS and its robustness to the choice of the radius R . We first tune the proposal stepsize h of SPS to get different acceptance rates. Then we plot ESJD per dimension for

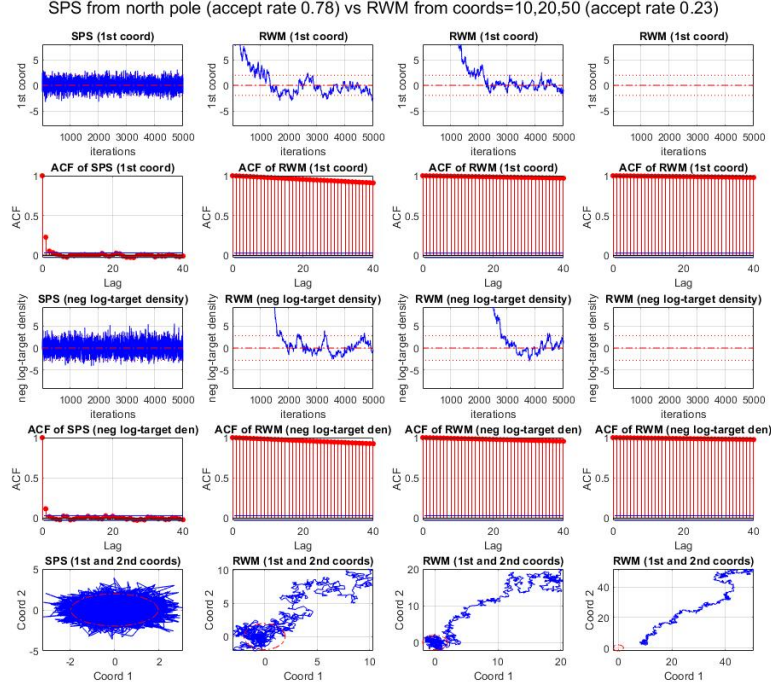


FIGURE 5. Traceplots and ACFs of the 1-st coordinate, negative log-target density, and the first two coordinates, for standard Gaussian target in 100 dimensions: SPS starts from the north pole (first column) vs RWM starts from different initial states (c, c, \dots, c) where $c = 10, 20, 50$ (the last three columns).

varying acceptance rates as the efficiency curve of SPS. Fig. 6 shows eight efficiency curves for different choices of R . The target distribution is multivariate student's t distribution with $d = 100$ degrees of freedom. In this setting, $R = \sqrt{d}$ is optimal. The four subplots in the first column are for $R < \sqrt{d}$ and the second column contains four cases of $R > \sqrt{d}$.

Although we do not plot the ESJD for RWM, the maximum ESJD per dimension for RWM is known to have an order of $\mathcal{O}(d^{-1})$. In all cases in Fig. 6, SPS has much larger ESJD than RWM. For the two subplots in the first row of Fig. 6, since R is closer to \sqrt{d} , the acceptance rate cannot be lower than 0.5 whatever the proposal variance is. For all the other efficiency curves, an interesting observation is that, the maximum ESJDs are always achieved when the acceptance rate is around 0.234. This suggests the optimal acceptance rate 0.234 is quite robust and not limited to product

i.i.d. targets, which is similar to the case of optimal acceptance rate 0.234 for RWM [YRR20].

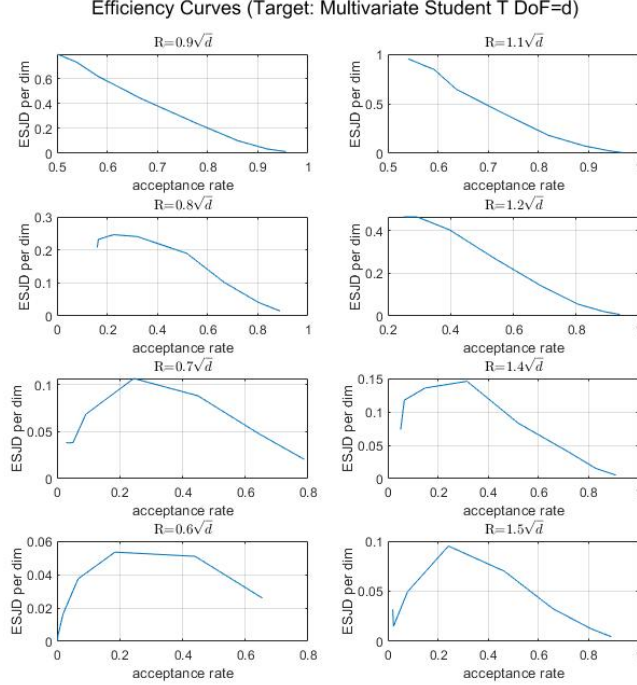


FIGURE 6. Efficiency Curves (ESJD per dimension) as functions of the acceptance rate of SPS for different choices of R . Target distribution is multivariate student's t distribution with $\text{DoF} = d = 100$. When R is close to \sqrt{d} (such as $R = 0.9\sqrt{d}$ and $R = 1.1\sqrt{d}$), the acceptance rate is always larger than 0.234.

6.3. SBPS: traceplot and ACF. In this example, we study SBPS via the traceplots and ACFs for the 1-st coordinate, the negative log-density, and the squared 1-st coordinate, respectively. In Fig. 7, the target is multivariate student's t distribution with $d = 100$ degrees of freedom. Since SBPS is a continuous-time process, for the traceplot and ACF, we further discretize every unit time into 5 samples. $N = 1000$ events are simulated and low refresh rate 0.2 is chosen. For other settings such as high refresh rate, light-tailed targets, and different covariance matrices, we refer to Appendix B for additional simulations for SBPS.

There are several interesting observations from Fig. 7. The ACFs for all three cases have certain periodic behavior, and can take negative values for the first two cases.

We also include the Effective Sample Size (ESS) per Switch for the three cases. The definition of ESS is in Appendix B which is the same as in [BFR19, supplemental material]. As a result of negative ACFs, the ESS per Switch is larger than 1 in the first two cases. This suggests asymptotic variance for estimating the 1-st coordinate or the negative log-density using SBPS is even smaller than the variance using N independent samples from the target.

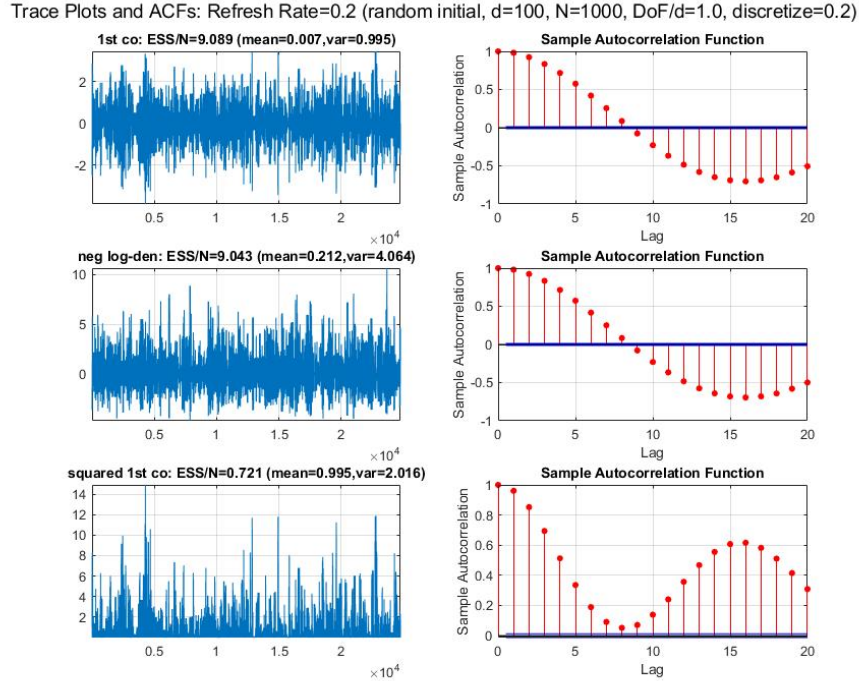


FIGURE 7. Trace plots and ACFs for the 1-st coordinate, the negative log-density, and the squared 1-st coordinate. Target distribution is multivariate student's t distribution with DoF = $d = 100$. Every unit time is discretized into 5 samples. $N = 1000$ events are simulated. Low refresh rate = 0.2. The ESS per switch is larger than 1 and the ACF can be negative in the first two cases.

6.4. SBPS: ESS per Switch. In this example, we study efficiency curves of SBPS and BPS in terms of ESS per Switch versus the refresh rate. The first subplot of Fig. 8 contains the proportion of refreshments in all the N events for varying refresh rates. It is clear that as the refresh rate increases, the proportion of refreshments increases. In the other three subplots of Fig. 8, we plot the logarithm of ESS per

Switch as a function of the refresh rate for three cases, the 1-st coordinate, the negative log-density, and the squared 1-st coordinate, respectively. For each efficiency curve, $N = 1000$ events are simulated. We use random initial states for our SBPS. For comparison, BPS starts from stationarity to avoid slow mixing. As SBPS and BPS are continuous-time processes, each unit time is discretized into 5 samples. The target is standard Gaussian with $d = 100$. We refer to Appendix B for additional efficiency curves for heavy-tailed targets.

According to Fig. 8, the ESS per Switch of SBPS is much larger than the ESS per Switch of BPS for all cases (actually the gap becomes larger in higher dimensions). For both the 1-st coordinate and the negative log-target density, the ESS per Switch of SBPS can be larger than 1 if the refresh rate is relatively low. For BPS, however, even starting from stationarity, the ESS per Switch is always much smaller than 1.

7. DISCUSSIONS

We have explored the use of stereographically projected algorithms and developed SPS and SBPS that are uniformly ergodic for a large class of light and heavy tailed targets and also exhibit fast convergence in high dimensions. The framework we established in this paper opens new opportunities for developing MCMC algorithms for sampling high-dimensional and/or heavy-tailed distributions. We finish the paper by some potentially interesting future directions.

- *Adaptive MCMC*: the proposed GSPS algorithm fits the adaptive MCMC framework very well [RR09]. The tuning parameters of GSPS such as the covariance matrix, the location and radius of the sphere can be tuned adaptively. Empirical study of the sensitivity of GSPS to the tuning parameters and extending GSPS for sampling multimodal distributions [PHL20] are important future directions.
- *Quantitative bounds*: we know SPS is uniform ergodicity for a large class of targets and dimension-free for isotropic targets. However, we do not establish quantitative bounds for the mixing time. The mixing time quantitative bounds and its dimension dependence (i.e, the “convergence complexity” [YR17]) would be an interesting direction for future work.
- *Scaling limit for SBPS*: we know SBPS is dimension-free for isotropic targets. For product i.i.d. targets, we establish optimal scaling results for SPS but not for SBPS. Recently, scaling limits for the traditional BPS has been developed in different settings [BKR18; Del+21]. It would be interesting to obtain such scaling limits for SBPS for non-isotropic targets and compare with BPS directly.
- *Stereographic MALA, HMC, and others*: another interesting future direction is to develop new MCMC samplers based on other popular MCMC algorithms, such as (Riemann) MALA and Hamiltonian Monte Carlo (HMC) [GC11] and

Efficiency Curves: ESS/N vs refresh rate (Gaussian target)

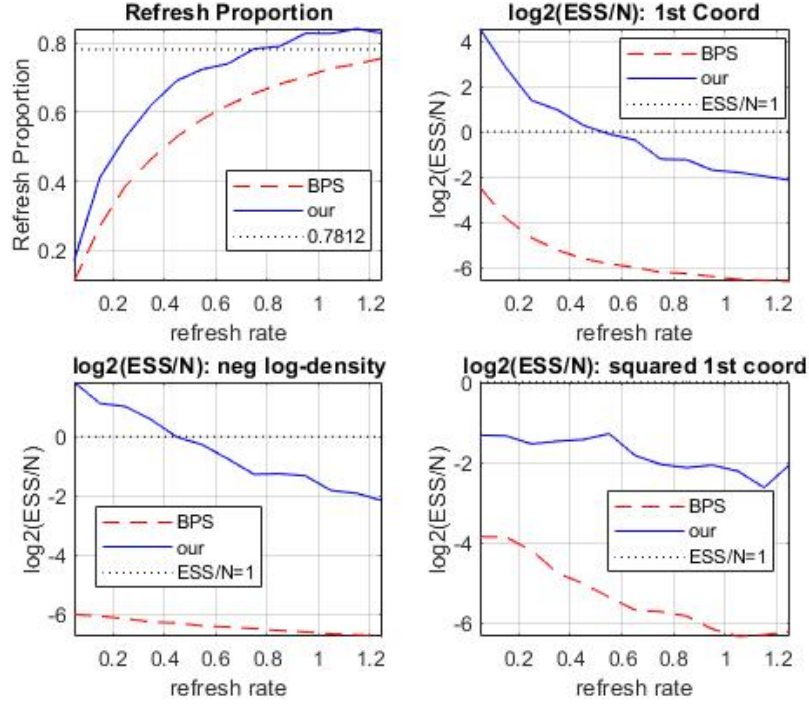


FIGURE 8. Efficiency curves (ESS per Switch) for SBPS and BPS for varying refresh rate. $N = 1000$ events are simulated, Random initial values for SBPS and BPS starts from stationarity. Each unit time is discretized to 5 samples. Target distribution: standard Gaussian with $d = 100$. The first subplot is the proportion of refreshment events in all N events. The other three subplots are ESS for the 1-st coordinate, the negative log-density, and the squared 1-st coordinate.

other PDMPs, or based on other mappings from \mathbb{R}^d to \mathbb{S}^d than the (generalized) stereographic projection.

ACKNOWLEDGEMENT

JY was supported by the Florence Nightingale Fellowship, the Lockey Fund from University of Oxford, and St Peter's College Research Fund (O'Connor Fund). KL has been supported by the Royal Society through the Royal Society University Research Fellowship. GOR was supported by EPSRC grants Bayes for Health (R018561) and CoSInES (R034710).

A. PROOFS OF MAIN RESULTS

A.1. Proof of Proposition 2.1.

Proof. If $\pi(x) > 0, \forall x \in \mathbb{R}^d$ and π being continuous, then $\pi_S(z)$ is continuous and $\pi_S(z) > 0$ for all $z \in \mathbb{S}^d$ except the north pole. According to [MT12, Theorem 13.0.1], it suffices to prove the existence of a stationary distribution, aperiodicity, π -irreducibility, and positive Harris recurrence.

The existence of a stationary distribution comes from the detailed balance of Metropolis–Hastings chain. SPS is aperiodic by [RS94, Theorem 3(i)] using the facts that the acceptance probability does not equal to zero and the proposal distribution as a Markov kernel is aperiodic. Furthermore, π -irreducibility comes from [RS94, Theorem 3(ii)] using the fact that the proposal distribution as a Markov kernel is π -irreducible. Next, in Appendix A.2, we prove a 3-step minorization condition for the transitional kernel. That is, for $z \in \mathbb{S}^d$, we have $P^3(z, A) \geq \epsilon Q(A)$ for all Borel measurable set A , where $Q(\cdot)$ is a fixed probability measure on \mathcal{S}^d and $\epsilon > 0$. Then, for any measurable set A with $\pi(A) > 0$, for every three steps there is at least a non-zero constant probability to hit A . This implies any such set A is Harris recurrent so the π -irreducible chain is Harris recurrent [MT12, ch.9, pp.199]. Finally, since for every three steps there is at least a non-zero constant probability to hit A from any point on \mathbb{S}^d , the expected number of steps for returning to A is finite (which equals to the expectation of a geometric random variable). Therefore, by [MT12, Theorem 10.4.10(ii)], the chain is positive recurrent. \square

A.2. Proof of Theorem 2.2.

Proof. If there exists x such that $\sup_{x \in \mathbb{R}^d} \pi(x)(R^2 + \|x\|^2)^d = \infty$, then the chain is not even geometric ergodic by [RT96b, Proposition 5.1]. This implies that Eq. (4) is necessary. Therefore, it suffices to prove Eq. (4) is also a sufficient condition.

We prove uniform ergodicity by showing the whole \mathbb{S}^d is a small set. More precisely, we will show the 3-step transitional kernel satisfies the following minorization condition:

$$P^3(z, A) \geq \epsilon Q(A)$$

for all measurable set A , where $Q(\cdot)$ is a fixed probability measure on \mathbb{S}^d and $\epsilon > 0$.

We use the following notations:

- (1) We use $\text{AC}(\epsilon) := \{z \in \mathbb{S}^d : z_{d+1} \geq 1 - \epsilon\}$ to denote the “Arctic Circle” with “size” $\epsilon \geq 0$.
- (2) We use $\text{HS}(z, 0) := \{z' \in \mathbb{S}^d : z^T z' \geq 0\}$ to denote the “hemisphere” from z . and $\text{HS}(z, \epsilon') := \{z' \in \mathbb{S}^d : z^T z' \geq \epsilon'\}$ to denote the area left after “cutting” the hemisphere’s boundary of “size” $\epsilon' \geq 0$.

Now consider the 3-step path $z \rightarrow z_1 \rightarrow z_2 \rightarrow z' \in A$ where $z \in \mathbb{S}^d$ is the starting point, z_1 and z_2 are two intermediate points, and $z' \in A$ is final point. Denoting $q(z, \cdot)$

as the proposal density, we have

$$p(z, z') \geq q(z, z') \left(1 \wedge \frac{\pi_S(z')}{\pi_S(z)} \right).$$

Then the 3-step transition kernel can be bounded below by

$$\begin{aligned} P^3(z, A) &\geq \int_{z' \in A} \int_{z_2 \in \mathbb{S}^d} \int_{z_1 \in \mathbb{S}^d} q(z, z_1) q(z_1, z_2) q(z_2, z') \\ &\quad \cdot \left(1 \wedge \frac{\pi_S(z_1)}{\pi_S(z)} \right) \left(1 \wedge \frac{\pi_S(z_2)}{\pi_S(z_1)} \right) \left(1 \wedge \frac{\pi_S(z')}{\pi_S(z_2)} \right) \nu(dz_1) \nu(dz_2) \nu(dz') \end{aligned}$$

where $\nu(\cdot)$ denotes the Lebesgue measure on \mathbb{S}^d .

By the conditions of Theorem 2.2, $\pi(x) > 0$ is continuous in \mathbb{R}^d , which implies $\pi_S(z)$ is positive and continuous in any compact subset of $\mathbb{S}^d \setminus N$ where N denotes the north pole. Then using the fact that a continuous function on a compact set is bounded, if we rule out $\text{AC}(\epsilon)$, then $\pi_S(z)$ is bounded away from 0. That is,

$$\inf_{z \notin \text{AC}(\epsilon)} \pi_S(z) \geq \delta_\epsilon > 0, \forall \epsilon \in (0, 1),$$

where $\delta_\epsilon \rightarrow 0$ as $\epsilon \rightarrow 0$.

Furthermore, since the surface area of \mathbb{S}^d is finite and $\pi_S(z) \propto \pi(x)(R^2 + \|x\|^2)^d$ where $x = \text{SP}(z)$, we know $\sup_{x \in \mathbb{R}^d} \pi(x)(R^2 + \|x\|^2)^d < \infty$ implies that $M := \sup \pi_S(z) < \infty$. Therefore, we have

$$\begin{aligned} P^3(z, A) &\geq \int_{z' \in A} \int_{z_2 \in \mathbb{S}^d \setminus \text{AC}(\epsilon)} \int_{z_1 \in \mathbb{S}^d \setminus \text{AC}(\epsilon)} q(z, z_1) q(z_1, z_2) q(z_2, z') \\ &\quad \cdot \left(1 \wedge \frac{\delta_\epsilon}{M} \right)^2 \left(1 \wedge \frac{\pi_S(z')}{M} \right) \nu(dz_1) \nu(dz_2) \nu(dz'). \end{aligned}$$

Next, we consider the term $q(z, z_1) q(z_1, z_2) q(z_2, z')$. For our algorithm, the proposal can cover the whole hemisphere except the boundary, by “cutting” the boundary a little bit, the proposal density will be bounded below. That is, we have

$$q(z, z') \geq \delta'_{\epsilon'} > 0, \quad \forall z' \in \text{HS}(z, \epsilon'), \epsilon' \in (0, 1),$$

where $\delta'_{\epsilon'} \rightarrow 0$ as $\epsilon' \rightarrow 0$.

Therefore, if $z_1 \in \text{HS}(z, \epsilon')$ and $z_2 \in \text{HS}(z', \epsilon')$ then $q(z, z_1) \geq \delta'_{\epsilon'}$ and $q(z_2, z') \geq \delta'_{\epsilon'}$. Then we have

$$\begin{aligned} &\int_{z_2 \in \text{HS}(z', \epsilon') \setminus \text{AC}(\epsilon)} \int_{z_1 \in \text{HS}(z, \epsilon') \setminus \text{AC}(\epsilon)} q(z, z_1) q(z_1, z_2) q(z_2, z') \nu(dz_1) \nu(dz_2) \\ &\geq (\delta'_{\epsilon'})^3 \int_{z_2 \in \text{HS}(z', \epsilon') \setminus \text{AC}(\epsilon)} \int_{z_1 \in \text{HS}(z, \epsilon') \setminus \text{AC}(\epsilon)} \mathbf{1}_{z_1 \in \text{HS}(z_2, \epsilon')} \nu(dz_1) \nu(dz_2). \end{aligned}$$

Note that 3 steps are enough to reach any point z' from any z on the sphere. It is clear that under the Lebesgue measure ν on \mathbb{S}^d , we can define the following positive constant C :

$$C := \inf_{z, z' \in \mathbb{S}^d} \int_{z_2 \in \text{HS}(z', 0) \setminus \text{AC}(0)} \int_{z_1 \in \text{HS}(z, 0) \setminus \text{AC}(0)} \mathbf{1}_{z_1 \in \text{HS}(z_2, 0)} \nu(dz_1) \nu(dz_2) > 0.$$

Now consider the following function of $\epsilon \geq 0$ and $\epsilon' \geq 0$

$$C_{\epsilon, \epsilon'} := \inf_{z, z' \in \mathbb{S}^d} \int_{z_2 \in \text{HS}(z', \epsilon') \setminus \text{AC}(\epsilon)} \int_{z_1 \in \text{HS}(z, \epsilon') \setminus \text{AC}(\epsilon)} \mathbf{1}_{z_1 \in \text{HS}(z_2, \epsilon')} \nu(dz_1) \nu(dz_2).$$

It is clear that $C \geq C_{\epsilon, \epsilon'}$. The difference between them can be bounded by

$$\begin{aligned} C - C_{\epsilon, \epsilon'} &\leq \sup_{z \in \mathbb{S}^d} \nu(\{z_1 : z_1 \in (\text{HS}(z, 0) \setminus \text{HS}(z, \epsilon')) \cap (\text{AC}(\epsilon) \setminus \text{AC}(0))\}) \\ &\quad + \sup_{z' \in \mathbb{S}^d} \nu(\{z_2 : z_2 \in (\text{HS}(z', 0) \setminus \text{HS}(z', \epsilon')) \cap (\text{AC}(\epsilon) \setminus \text{AC}(0))\}) \\ &\quad + \sup_{z_2 \in \mathbb{S}^d} \nu(\{z_1 : z_1 \in \text{HS}(z_2, 0) \setminus \text{HS}(z_2, \epsilon')\}). \end{aligned}$$

Then clearly the upper bound is continuous w.r.t. both ϵ and ϵ' and goes to zero when $\epsilon \rightarrow 0$ and $\epsilon' \rightarrow 0$. Therefore, there exists $\epsilon > 0$ and $\epsilon' > 0$ such that $C - C_{\epsilon, \epsilon'} \leq \frac{1}{2}C$, that is

$$C_{\epsilon, \epsilon'} \geq \frac{1}{2}C > 0.$$

Using such ϵ and ϵ' we have

$$\int_{z_2 \in \text{HS}(z', \epsilon') \setminus \text{AC}(\epsilon)} \int_{z_1 \in \text{HS}(z, \epsilon') \setminus \text{AC}(\epsilon)} q(z, z_1) q(z_1, z_2) q(z_2, z') \nu(dz_1) \nu(dz_2) \geq \frac{1}{2}C(\delta'_{\epsilon'})^3 > 0.$$

Then we have

$$P^3(z, A) \geq \left(1 \wedge \frac{\delta_{\epsilon}}{M}\right)^2 \frac{1}{2}C(\delta'_{\epsilon'})^3 \int_{z' \in A} \left(1 \wedge \frac{\pi_S(z')}{M}\right) \nu(dz')$$

Note that $\pi_S(z') > 0$ almost surely w.r.t. ν . Denoting

$$g(z') := \left(1 \wedge \frac{\delta_{\epsilon}}{M}\right)^2 \frac{1}{2}C(\delta'_{\epsilon'})^3 \left(1 \wedge \frac{\pi_S(z')}{M}\right),$$

we have established

$$P^3(z, A) \geq \int_{z' \in A} g(z') \nu(dz'),$$

where $g(z) > 0$ almost surely w.r.t. ν . Then we can define

$$\int_A g(z') \nu(dz') = \int_{\mathbb{S}^d} g(z') \nu(dz') \frac{\int_A g(z') \nu(dz')}{\int_{\mathbb{S}^d} g(z') \nu(dz')} =: \epsilon Q(A),$$

where $\epsilon = \int_{\mathbb{S}^d} g(z') \nu(dz') > 0$ and $Q(A) := \frac{\int_A g(z') \nu(dz')}{\int_{\mathbb{S}^d} g(z') \nu(dz')}$ is a probability measure. This proves the desired minorization condition, which completes the proof. \square

A.3. Sketch proof of Proposition 2.5.

Proof. In this proof, for two vectors a and b , we use $a \cdot b$ to denote the inner product. We denote the generator of our PDMP and its adjoint (see [Fea+18, Section 2.2] or [Lig10]) as \mathcal{A} and \mathcal{A}^* , respectively. Then, we can divide the generator \mathcal{A} into two parts

$$\mathcal{A} = \mathcal{A}_D + \mathcal{A}_J,$$

where the first term \mathcal{A}_D is the generator of the deterministic dynamics (moving along a greatest circle) and the second term \mathcal{A}_J relates the jumping process (that is, the change in expectation at bounce or refreshment events).

Then it can be easily derived that, for suitable functions $f(z, v)$ and $g(z, v)$, where $v \perp z$ and $\|v\| = \|z\| = 1$, the generator \mathcal{A}_D and its adjoint \mathcal{A}_D^* of the deterministic process satisfy

$$\begin{aligned}\mathcal{A}_D f &= \nabla_z f \cdot v - \nabla_v f \cdot z, \\ \mathcal{A}_D^* g &= \nabla_v g \cdot z - \nabla_z g \cdot v.\end{aligned}$$

Denoting $|\mathbb{S}^{d-1}|$ as the volume of the \mathbb{S}^{d-1} , we substitute the following joint distribution on $\mathbb{S}^d \times \mathbb{S}^d$:

$$\pi(z, v) = \pi_S(z) p(v | z) = \pi_S(z) \frac{\mathbf{1}_{v \cdot z = 0}}{|\mathbb{S}^{d-1}|}, \quad \forall (z, v) \in \mathbb{S}^d \times \mathbb{S}^d.$$

For any $(z, v) \in \mathbb{S}^d \times \mathbb{S}^d$ such that $z \perp v$, we have

$$\begin{aligned}\mathcal{A}_D^*[\pi(z, v)] &= 0 \cdot z - \frac{1}{|\mathbb{S}^{d-1}|} \nabla_z \pi_S(z) \cdot v \\ &= -\pi_S(z) \frac{\mathbf{1}_{v \cdot z = 0}}{|\mathbb{S}^{d-1}|} [v \cdot \nabla_z \log \pi_S(z)] \\ &= -\pi(z, v) [v \cdot \nabla_z \log \pi_S(z)].\end{aligned}$$

For \mathcal{A}_J , since the refreshment clearly preserve π as the stationary distribution, we only need to consider the bounce events. When there is no refreshment, we can follow similar arguments as in [Fea+18, Section 2.2 and 3.2] to get the adjoint of the second part of the generator

$$\mathcal{A}_J^*[\pi(z, v)] = -\pi(z, v) \lambda(z, v) + \int \lambda(z, v') q(v | z, v') \pi(z, v') dv',$$

where

$$q(\cdot \mid z, v) := \delta_{\tilde{v}}(\cdot), \quad \tilde{v} := v - 2 \left[\frac{v \cdot \tilde{\nabla}_z \log \pi_S(z)}{\tilde{\nabla}_z \log \pi_S(z) \cdot \tilde{\nabla}_z \log \pi_S(z)} \right] \tilde{\nabla}_z \log \pi_S(z).$$

Therefore, it suffices to verify that $\pi(z, v)$ satisfies $\mathcal{A}^*[\pi(z, v)] = \mathcal{A}_D^*[\pi(z, v)] + \mathcal{A}_J^*[\pi(z, v)] = 0$. That is,

$$\mathcal{A}^*[\pi(z, v)] = -\pi(z, v)[v \cdot \nabla_z \log \pi_S(z) + \lambda(z, v)] + \int \lambda(z, v') q(v \mid z, v') \pi(z, v') dv'.$$

Then it is enough to verify

$$p(v \mid z)[\lambda(z, v) + v \cdot \nabla_z \log \pi_S(z)] - \lambda(z, \tilde{v}) p(\tilde{v} \mid z) = 0.$$

Note that $\tilde{v} \perp z$ which implies that $p(v \mid z) = p(\tilde{v} \mid z)$. Therefore, it suffices to verify

$$\lambda(z, v) - \lambda(z, \tilde{v}) = -v \cdot \nabla_z \log \pi_S(z).$$

Recall that in our PDMP, we have $\lambda(z, v) = \max\{0, [-v \cdot \nabla_z \log \pi_S(z)]\}$. Therefore, we only need to verify

$$-v \cdot \nabla_z \log \pi_S(z) = \tilde{v} \cdot \nabla_z \log \pi_S(z).$$

Using the definition of \tilde{v} and $\tilde{\nabla}_z \log \pi_S(z) = \nabla_z \log \pi_S(z) - [z \cdot \nabla_z \log \pi_S(z)] z$, together with the fact that $v \perp z$ and $\tilde{v} \perp z$, we have

$$-v \cdot \nabla_z \log \pi_S(z) = -v \cdot \tilde{\nabla}_z \log \pi_S(z) = \tilde{v} \cdot \tilde{\nabla}_z \log \pi_S(z) = \tilde{v} \cdot \nabla_z \log \pi_S(z),$$

which completes the proof. \square

A.4. Proof of Theorem 2.6.

Proof. Recall the definition of the transformation between $x \in \mathbb{R}^d$ and $z \in \mathbb{S}^d$:

$$x_i = R \frac{z_i}{1 - z_{d+1}}, \quad z_i = \frac{2Rx_i}{R^2 + \|x\|^2}, \quad \forall i = 1, \dots, d, \quad z_{d+1} = \frac{\|x\|^2 - R^2}{\|x\|^2 + R^2},$$

and the transformed target on \mathbb{S}^d is $\pi_S(z) \propto \pi(x)(R^2 + \|x\|^2)^d$. One version of $\nabla_z \log \pi_S(z)$ (there is no unique representation since $z \in \mathbb{R}^{d+1}$ but $x \in \mathbb{R}^d$) can be derived as

$$\begin{aligned} \frac{\partial \log \pi_S(z)}{\partial z_i} &= \frac{\partial \log \pi(x)}{\partial x_i} \frac{R^2 + \|x\|^2}{2R}, \quad i = 1, \dots, d. \\ \frac{\partial \log \pi_S(z)}{\partial z_{d+1}} &= \left[\frac{1}{d} \sum_{j=1}^d \frac{\partial \log \pi(x)}{\partial x_j} x_j + 1 \right] \frac{d}{2R^2} (R^2 + \|x\|^2). \end{aligned}$$

Recall that we define $\tilde{\nabla}_z \log \pi_S(z)$ as the projection of (any version of) $\nabla_z \log \pi_S(z)$ onto the (tangent plane of the) sphere:

$$\tilde{\nabla}_z \log \pi_S(z) = \nabla_z \log \pi_S(z) - [z \cdot \nabla_z \log \pi_S(z)] z.$$

Then the representation of $\tilde{\nabla}_z \log \pi_S(z)$ is unique.

Denote $(\cdot)_{d+1}$ as the $(d+1)$ -th coordinate. One can verify that

$$\limsup_{\{z: z_{d+1} \rightarrow 1\}} \left(\tilde{\nabla}_z \log \pi_S(z) \right)_{d+1} = \limsup_{\{x: \|x\| \rightarrow \infty\}} \sum_{i=1}^d \left(\frac{\partial \log \pi(x)}{\partial x_i} x_i \right) + 2d.$$

Therefore, the condition is equivalent to

$$\limsup_{\{z: z_{d+1} \rightarrow 1\}} \left(\tilde{\nabla}_z \log \pi_S(z) \right)_{d+1} < \frac{1}{2}.$$

We have assumed $\|v\| = 1$. Define the Lyapunov function

$$f(z, v) = 2 + v_{d+1},$$

which is bounded since $|v_{d+1}| \leq 1$. Note that moving along the greatest circle on sphere with constant speed $\|v\| = 1$ implies the equations

$$\begin{aligned} z(t) &= z(0) \cos(t) + v(0) \sin(t), \\ v(t) &= v(0) \cos(t) - z(0) \sin(t). \end{aligned}$$

For simplicity, we will write $z(0)$ and $v(0)$ as z and v in the rest of the proof. For two vectors a and b , we will use $a \cdot b$ to denote the inner product $a^T b$. The key property we will use is that $\frac{df}{dt} = \frac{dv_{d+1}}{dt} = -z_{d+1}$.

Now we can derive the (extended) generator of SBPS

$$\begin{aligned} \tilde{\mathcal{L}}f(z, v) &:= \lim_{t \rightarrow 0^+} \frac{1}{t} [f(z(t), v(t)) - f(z, v)] \\ &\quad + \int \lambda \psi(dw) [f(z, w) - f(z, v)] \\ &\quad + (-\nabla_z \log \pi_S(z) \cdot v)^+ [f(z, \tilde{v}) - f(z, v)] \\ &= -z_{d+1} - \lambda v_{d+1} + (-\nabla_z \log \pi_S(z) \cdot v)^+ (\tilde{v}_{d+1} - v_{d+1}), \end{aligned}$$

where we have used

$$\int \lambda \psi(dw) [f(z, w) - f(z, v)] = \int \lambda \psi(dw) [w_{d+1} - v_{d+1}] = -\lambda v_{d+1}.$$

Our goal is to establish a drift condition for the generator. Note that

$$\tilde{\mathcal{L}}f/f = \tilde{\mathcal{L}}f/(2 + v_{d+1}) \leq \max\{\tilde{\mathcal{L}}f, \tilde{\mathcal{L}}f/3\}$$

Therefore, we only need to focus on $\tilde{\mathcal{L}}f$ and prove it is negative outside a small set. It suffices to prove $\tilde{\mathcal{L}}f$ is negative in a small neighbourhood of the “north pole”.

Recall that

$$\tilde{v} := v - 2 \left[\frac{v \cdot \tilde{\nabla}_z \log \pi_S(z)}{\tilde{\nabla}_z \log \pi_S(z) \cdot \tilde{\nabla}_z \log \pi_S(z)} \right] \tilde{\nabla}_z \log \pi_S(z).$$

Also, it can be verified that

$$v \cdot \tilde{\nabla}_z \log \pi_S(z) = v \cdot \nabla_z \log \pi_S(z).$$

Therefore, we have

$$\tilde{\mathcal{L}}f(z, v) = -z_{d+1} - \lambda v_{d+1} + \left(-\tilde{\nabla}_z \log \pi_S(z) \cdot v \right)^+ \left[-2 \frac{v \cdot \tilde{\nabla}_z \log \pi_S(z)}{\|\tilde{\nabla}_z \log \pi_S(z)\|^2} \left(\tilde{\nabla}_z \log \pi_S(z) \right)_{d+1} \right].$$

Note that if $\left(\tilde{\nabla}_z \log \pi_S(z) \right)_{d+1} \leq 0$ then $\tilde{\mathcal{L}}f(z, v) \leq -z_{d+1} - \lambda v_{d+1}$. Otherwise, $\left(\tilde{\nabla}_z \log \pi_S(z) \right)_{d+1} > 0$, then we maximize the last term over v to get

$$\begin{aligned} & \left(-\tilde{\nabla}_z \log \pi_S(z) \cdot v \right)^+ \left[-2 \frac{v \cdot \tilde{\nabla}_z \log \pi_S(z)}{\|\tilde{\nabla}_z \log \pi_S(z)\|^2} \left(\tilde{\nabla}_z \log \pi_S(z) \right)_{d+1} \right] \\ & \leq \|\tilde{\nabla}_z \log \pi_S(z)\| \left[2 \frac{\|\tilde{\nabla}_z \log \pi_S(z)\|}{\|\tilde{\nabla}_z \log \pi_S(z)\|^2} \left(\tilde{\nabla}_z \log \pi_S(z) \right)_{d+1} \right] \\ & = 2 \left(\tilde{\nabla}_z \log \pi_S(z) \right)_{d+1} \end{aligned}$$

where the upper bound is achieved if

$$v = \frac{-\tilde{\nabla}_z \log \pi_S(z)}{\|\tilde{\nabla}_z \log \pi_S(z)\|}.$$

Overall, using $v_{d+1} \leq \sqrt{1 - z_{d+1}^2}$, we have already shown that

$$\sup_{\{z: z_{d+1}=z_*\}} \tilde{\mathcal{L}}f(z, v) \leq -z_* + \lambda \sqrt{1 - z_*^2} + 2 \sup_{\{z: z_{d+1}=z_*\}} \left(\tilde{\nabla}_z \log \pi_S(z) \right)_{d+1}^+$$

Finally, let $z_* \rightarrow 1$, the right hand side goes to

$$-1 + 2 \limsup_{\{z: z_{d+1} \rightarrow 1\}} \left(\tilde{\nabla}_z \log \pi_S(z) \right)_{d+1}^+$$

which is negative because of the condition in Theorem 5.6 that

$$\limsup_{\{z: z_{d+1} \rightarrow 1\}} \left(\tilde{\nabla}_z \log \pi_S(z) \right)_{d+1} < \frac{1}{2}.$$

Therefore, we have shown the (extended) generator is negative in a neighbourhood of the north pole, which implies a drift condition for the (extended) generator. Finally, by [DMT95, Theorem 5.2(c)], as the Lyapunov function is bounded, the Markov process is uniformly ergodic, which finishes the proof. \square

A.5. Proof of Corollary 2.7.

Proof. We present two versions of the proof. In this first version of the proof, we simply check the condition in Theorem 2.6. Let ν to be the DoF of the multivariate student's t target $\pi(x)$. We have

$$\log \pi(x) = -\frac{\nu + d}{2} \log \left(1 + \frac{1}{\nu} \|x\|^2 \right) + C$$

for some constant C . Then, one can get

$$\sum_{i=1}^d \frac{\partial \log \pi(x)}{\partial x_i} x_i = -\frac{\nu + d}{\nu} \frac{\|x\|^2}{1 + \|x\|^2/\nu}.$$

Taking $\|x\| \rightarrow \infty$ yields

$$-\frac{\nu + d}{\nu} \nu < \frac{1}{2} - 2d$$

which completes the proof since

$$\nu > d - \frac{1}{2}.$$

The alternative proof is by following the proof of Theorem 2.6. Let the degree of freedom for the multivariate student's t target $\pi(x)$ to be kd where $k > 1 - \frac{1}{2d}$. For simplicity of notations, we consider the case $R = \sqrt{d}$ without loss of generality. Since $\pi(x)$ is isotropic, we can verify that if $R = \sqrt{d}$, one version of $\nabla \log \pi_S(z)$ (as the representation is not unique) is

$$\nabla \log \pi_S(z) = \left(0, \dots, \frac{-dz_{d+1}(k-1)}{(1-z_{d+1})[(k-1)(1-z_{d+1})+2]} \right)$$

Then it is easy to verify using basic geometry of the sphere that if $k \geq 1$ and $z_{d+1} > 0$ then

$$\left(\tilde{\nabla}_z \log \pi_S(z) \right)_{d+1} \leq 0.$$

If $k < 1$ and $z_{d+1} > 0$ then

$$\frac{\left(\tilde{\nabla}_z \log \pi_S(z) \right)_{d+1}}{\|\tilde{\nabla}_z \log \pi_S(z)\|} = \sqrt{1 - z_{d+1}^2}$$

and

$$\|\tilde{\nabla}_z \log \pi_S(z)\| = \sqrt{1 - z_{1+d}^2} \frac{-dz_{d+1}(k-1)}{(1 - z_{d+1})[(k-1)(1 - z_{d+1}) + 2]}$$

Denoting $k = 1 - \epsilon$ and multiplying the two above two equations yields

$$\left(\tilde{\nabla}_z \log \pi_S(z)\right)_{d+1} = \frac{d\epsilon z_{d+1}(1 - z_{d+1}^2)}{(1 - z_{d+1})[2 - \epsilon(1 - z_{d+1})]} = \frac{d\epsilon z_{d+1}(1 + z_{d+1})}{2 - \epsilon(1 - z_{d+1})}$$

Letting $z_{d+1} \rightarrow 1$ yields

$$d\epsilon < d \frac{1}{2d} = \frac{1}{2}.$$

Therefore, the uniform ergodicity holds by Theorem 2.6. \square

A.6. On the conjecture in Remark 2.8. Our arguments include two parts. We first study a one-dimensional target distribution with density $\pi(t) \propto |t|^{-\alpha}$, $t \in [-1, 1]$ and $\alpha > 0$. We show that, for this target, the expected hitting time to the boundary (that is 1 or -1) of the BPS starting from $t = 0$ is finite (i.e., the BPS “escapes” the origin) if and only if $\alpha < 1$. Next, we show that, for target with the multivariate student’s t distribution with DoF ν , we can approximate the density on a greatest circle passing the north pole by a form of $\pi(t) \propto |t|^{-\alpha}$ if the chain is close to the north pole. Then $\alpha < 1$ corresponds to the condition in our conjecture in Remark 2.8, which is $\nu > d - 1$ in this case.

A.6.1. One-dimensional target. We consider the following one-dimensional target with density

$$f_0(t) \propto |t|^{-\alpha}, \quad \forall |t| < 1,$$

where $\alpha > 0$. Note that the density goes to infinity as $t \rightarrow 0$. In order to study the behavior of BPS, we consider the following “truncated” targets:

$$f_\epsilon(t) \propto (\epsilon + |t|)^{-\alpha}, \quad \forall t \in [-(1 - \epsilon), 1 - \epsilon]$$

and we will later let $\epsilon \rightarrow 0$ to recover $f_0(t)$.

Next, we consider T_ϵ to be the first bouncing time when starting state is from 0 with unit velocity and the target to be f_ϵ . Then we have

$$\mathbb{P}(T_\epsilon < 1 - \epsilon) = 1 - \exp\left(-\int_0^{1-\epsilon} (\log f_\epsilon)' dt\right)$$

Note that $f_\epsilon(1 - \epsilon) \propto 1$ and $f_\epsilon(0) \propto \epsilon^{-\alpha}$, both are up to the same constant. Therefore, we have

$$\int_0^{1-\epsilon} (\log f_\epsilon)' dt = \log(1) - \log(\epsilon^{-\alpha})$$

which implies

$$\mathbb{P}(T_\epsilon < 1 - \epsilon) = 1 - \epsilon^{-\alpha}.$$

Similarly, we can get the density of T_ϵ as

$$f_{T_\epsilon}(t) = -\epsilon^\alpha \frac{d}{dt}(\epsilon + |t|)^{-\alpha} = \alpha \epsilon^\alpha (\epsilon + |t|)^{-\alpha-1} = \frac{\alpha}{\epsilon} \left(\frac{|t|}{\epsilon} + 1 \right)^{-1-\alpha}, \quad \forall 0 < t < 1 - \epsilon.$$

Then, we define \tilde{T}_ϵ as the conditional bouncing time which is T_ϵ conditioned on $T_\epsilon < 1 - \epsilon$. Then we have the density of \tilde{T}_ϵ

$$f_{\tilde{T}_\epsilon}(t) = \frac{\alpha}{\epsilon(1 - \epsilon^\alpha)} \left(\frac{t}{\epsilon} + 1 \right)^{-1-\alpha}, \quad t \in [0, 1 - \epsilon].$$

Now we consider the “hitting time” to the boundary (that is, to $\pm(1 - \epsilon)$). We can denote the “hitting time” as

$$S^\epsilon = \sum_{i=1}^{G^\epsilon} (2\tilde{T}_{\epsilon,i}) + (1 - \epsilon),$$

where $\tilde{T}_{\epsilon,i}$ are i.i.d. from density $f_{\tilde{T}_\epsilon}$ and G^ϵ is a independent geometric random variable with parameter ϵ^α . Note that

$$\mathbb{E}[G^\epsilon] = \epsilon^{-\alpha}.$$

Therefore, to study $\lim_{\epsilon \rightarrow 0} \mathbb{E}[S^\epsilon] < \infty$, it suffices to study

$$\lim_{\epsilon \rightarrow 0} \mathbb{E} \left[\sum_{i=1}^{G^\epsilon} \tilde{T}_{\epsilon,i} \right] = \lim_{\epsilon \rightarrow 0} \epsilon^{-\alpha} \mathbb{E}[\tilde{T}_\epsilon].$$

Using the density of \tilde{T}_ϵ , we have

$$\begin{aligned}
\mathbb{E}[\tilde{T}_\epsilon] &= \frac{\alpha}{\epsilon(1-\epsilon^\alpha)} \int_0^{1-\epsilon} t \left(\frac{t}{\epsilon} + 1 \right)^{-1-\alpha} dt \\
&= \frac{\alpha}{\epsilon(1-\epsilon^\alpha)} \int_0^{1-\epsilon} \left[\epsilon \left(\frac{t}{\epsilon} + 1 \right) - \epsilon \right] \left(\frac{t}{\epsilon} + 1 \right)^{-1-\alpha} dt \\
&= \frac{\alpha}{\epsilon(1-\epsilon^\alpha)} \left[\int_0^{1-\epsilon} \epsilon \left(\frac{t}{\epsilon} + 1 \right)^{-\alpha} dt - \int_0^{1-\epsilon} \epsilon \left(\frac{t}{\epsilon} + 1 \right)^{-\alpha-1} dt \right] \\
&= \frac{\alpha}{\epsilon(1-\epsilon^\alpha)} \int_0^{1-\epsilon} \epsilon \left(\frac{t}{\epsilon} + 1 \right)^{-\alpha} dt - \epsilon \\
&= \frac{\alpha\epsilon}{1-\epsilon^\alpha} \int_0^{\frac{1-\epsilon}{\epsilon}} (u+1)^{-\alpha} du - \epsilon \\
&= \begin{cases} \frac{\epsilon}{1-\epsilon} \log\left(\frac{1-\epsilon}{\epsilon} + 1\right) - \epsilon, & \text{if } \alpha = 1, \\ \frac{\alpha\epsilon}{1-\epsilon^\alpha} \frac{(1+\frac{1-\epsilon}{\epsilon})^{1-\alpha} - 1}{1-\alpha} - \epsilon, & \text{otherwise.} \end{cases} \\
&= \begin{cases} \frac{\epsilon}{1-\epsilon} \log\left(\frac{1}{\epsilon}\right) - \epsilon, & \text{if } \alpha = 1, \\ \frac{\alpha}{1-\alpha} \frac{\epsilon^\alpha - \epsilon}{1-\epsilon^\alpha} - \epsilon, & \text{otherwise.} \end{cases}
\end{aligned}$$

Therefore, letting $\epsilon \rightarrow 0$, if $\alpha < 1$, then

$$\epsilon^{-\alpha} \mathbb{E}[\tilde{T}_\epsilon] \rightarrow \epsilon^{-\alpha} \frac{\alpha}{1-\alpha} \epsilon^\alpha = \frac{\alpha}{1-\alpha} < \infty.$$

On the other hand, if $\alpha = 1$, then

$$\epsilon^{-\alpha} \mathbb{E}[\tilde{T}_\epsilon] = \epsilon^{-1} \left[\frac{\epsilon}{1-\epsilon} \log\left(\frac{1}{\epsilon}\right) - \epsilon \right] = \frac{1}{1-\epsilon} \log\left(\frac{1}{\epsilon}\right) - 1 \rightarrow \infty.$$

Or if $\alpha > 1$, then

$$\epsilon^{-\alpha} \mathbb{E}[\tilde{T}_\epsilon] = \epsilon^{-\alpha} \left[\frac{\alpha}{\alpha-1} \frac{\epsilon - \epsilon^\alpha}{1-\epsilon^\alpha} - \epsilon \right] \rightarrow \frac{1}{\alpha-1} \epsilon^{1-\alpha} \rightarrow \infty.$$

Therefore, $\alpha < 1$ is required for the expected “escaping time” of the BPS to be finite.

A.6.2. Approximation round the north pole. We pick a greatest circle such that $z_2 = z_3 = \dots = z_d = 0$ and $z_1^2 + z_{d+1}^2 = 1$. Suppose the target distribution

$$\pi_\nu(x) \propto \left(1 + \frac{\|x\|^2}{\nu} \right)^{-\frac{\nu+d}{2}}, \quad x \in \mathbb{R}^d.$$

Then, for any $z \in \mathbb{S}^d$, we have

$$\log \pi_S(z) = \log \pi_\nu(x) + d \log(d + \|x\|^2) = C - dg_{\nu/d}(z_{d+1}),$$

where C is a constant and

$$g_k(z_{d+1}) := \frac{k+1}{2} \log \left(k - 1 + \frac{2}{1 - z_{d+1}} \right) + \log(1 - z_{d+1}).$$

Therefore, let $k := \nu/d$, we have

$$\pi_S(z) \propto \exp(-dg_k(z_{d+1})) = \left[\left(k - 1 + \frac{2}{1 - z_{d+1}} \right)^{\frac{k+1}{2}} \right]^{-d} (1 - z_{d+1})^{-d}.$$

Now consider the picked greatest circle, for any z such that $z_1^2 + z_{d+1}^2 = 1$, we have

$$\begin{aligned} \pi_S(z_1, z_{d+1} \mid z_{2:d} = 0) &\propto \left[\left(k - 1 + \frac{2}{1 - z_{d+1}} \right)^{\frac{k+1}{2}} \right]^{-d} (1 - z_{d+1})^{-d} \\ &= \left[\left(k - 1 + \frac{2}{1 - \sqrt{1 - z_1^2}} \right)^{\frac{k+1}{2}} \right]^{-d} \left(1 - \sqrt{1 - z_1^2} \right)^{-d}. \end{aligned}$$

If k is fixed, letting $z_1 \rightarrow 0$ and using the approximation $\sqrt{1 - z_1^2} \approx 1 - z_1^2/2$, we have

$$\left[\left(k - 1 + \frac{4}{z_1^2} \right)^{\frac{k+1}{2}} \right]^d \left(\frac{z_1^2}{2} \right)^{-d} \rightarrow \left[\left(\frac{4}{z_1^2} \right)^{\frac{k+1}{2}} \right]^{-d} \left(\frac{z_1^2}{2} \right)^{-d} \propto |z_1|^{(k+1)d-2d}$$

Therefore, if we write it as $|z_1|^{-\alpha}$ then we have

$$\alpha = (1 - k)d = (1 - \nu/d)d = d - \nu.$$

Therefore, $\alpha < 1$ corresponds to $\nu > d - 1$.

A.7. Proof of Lemma 3.1.

Proof. All the randomness for generating the proposal comes from the standard multivariate Gaussian random variable with distribution $\mathcal{N}(0, I_d)$ in the tangent space. We can denote it using the proposal variance h^2 and d independent standard Gaussian random variables $V_1, \dots, V_d \sim \mathcal{N}(0, 1)$. Then we can use $\sqrt{\sum_{j=1}^d V_j^2}$ to denote the Euclidean norm of the multivariate Gaussian random variable.

Suppose the current location of the chain is at z , and we are interested on the i -th coordinate of the proposal \hat{z} . If $z_i \notin \{-1, 1\}$, in the “tangent space” at z , there must be $d - 1$ directions orthogonal to the direction of the i -th coordinate of the sphere. This leaves only one direction in the “tangent space” at z which is not orthogonal to the direction of the i -th coordinate of the sphere. We denote the marginal of the multivariate Gaussian to this direction as U_i . Clearly, $U_i \sim \mathcal{N}(0, 1)$.

Then, using some facts from basic geometry, the random walk in the tangent space without projection back to sphere changes the “latitude” from z_{d+1} to $z_{d+1} +$

$\sqrt{1 - z_{d+1}^2} h U_{d+1}$ with distance to the origin equals to $\sqrt{1 + h^2 \sum_{j=1}^d V_j^2}$. Therefore, basic geometry tells us after projection back to sphere, the “latitude” of the proposal satisfies

$$\frac{\hat{z}_{d+1}}{1} = \frac{z_{d+1} + \sqrt{1 - z_{d+1}^2} h U_{d+1}}{\sqrt{1 + h^2 \sum_{j=1}^d V_j^2}}.$$

Similarly for other coordinates, we can get closed forms for any \hat{z}_i in terms of $\sum_{j=1}^d V_j^2$ and U_i for $i = 1, \dots, d+1$:

$$\hat{z}_i = \frac{1}{\sqrt{1 + h^2 \sum_{j=1}^d V_j^2}} \left(z_i + \sqrt{1 - z_i^2} h U_i \right) = \frac{1}{\sqrt{1 + h^2 d}} \left(z_i + \sqrt{1 - z_i^2} h U_i \right) (1 + \mathcal{O}_{\mathbb{P}}(d^{-1/2})).$$

Furthermore, we have

$$\begin{aligned} \hat{z}_i &= \frac{1}{\sqrt{1 + h^2 \sum_{j=1}^d V_j^2}} \left(z_i + \sqrt{1 - z_i^2} h U_i \right) \\ &= \frac{\sqrt{1 + h^2 U_i^2}}{\sqrt{1 + h^2 \sum_{j=1}^d V_j^2}} \left(\frac{z_i}{\sqrt{1 + h^2 U_i^2}} + \frac{\sqrt{1 - z_i^2} h U_i}{\sqrt{1 + h^2 U_i^2}} \right) \end{aligned}$$

Intuitively, the term $\frac{z_i}{\sqrt{1 + h^2 U_i^2}} + \frac{\sqrt{1 - z_i^2} h U_i}{\sqrt{1 + h^2 U_i^2}}$ comes from the change of i -th coordinate caused by U_i . The other term $\frac{\sqrt{1 + h^2 U_i^2}}{\sqrt{1 + h^2 \sum_{j=1}^d V_j^2}}$ comes from the change of the i -th coordinate by the other $d - 1$ orthogonal directions through the “curvature” of the sphere when projecting back to the sphere.

Note that $\{U_i, i = 1, \dots, d+1\}$ are dependent, all of which can be written as linear combinations of $\{V_i\}$. If $h = \mathcal{O}(d^{-1/2})$, observing that $\sum_{j=1}^d V_j^2 - U_i^2$ is chi-squared distributed with degree of freedom $d - 1$, we can write

$$\begin{aligned} \hat{z}_i &= \frac{\sqrt{1 + h^2 U_i^2}}{\sqrt{1 + h^2 \left(\sum_{j=1}^d V_j^2 - U_i^2 \right) + h^2 U_i^2}} \left(\frac{z_i}{\sqrt{1 + h^2 U_i^2}} + \frac{\sqrt{1 - z_i^2} h U_i}{\sqrt{1 + h^2 U_i^2}} \right) \\ &= \frac{\sqrt{1 + h^2 U_i^2} (1 + \mathcal{O}_{\mathbb{P}}(h^4))}{\sqrt{\left(1 + h^2 \left(\sum_{j=1}^d V_j^2 - U_i^2 \right) \right) (1 + h^2 U_i^2)}} \left(\frac{z_i}{\sqrt{1 + h^2 U_i^2}} + \frac{\sqrt{1 - z_i^2} h U_i}{\sqrt{1 + h^2 U_i^2}} \right) \\ &= \frac{1}{\sqrt{1 + h^2 (d - 1)}} \left[\left(1 - \frac{1}{2} h^2 U_i^2 \right) z_i - \sqrt{1 - z_i^2} h U_i \right] + \mathcal{O}_{\mathbb{P}}(h^3). \end{aligned}$$

Therefore, in the stationary phase, if $z_{d+1} = \mathcal{O}(d^{-1/2})$, then we have

$$\hat{z}_{d+1} = \frac{1}{\sqrt{1+h^2(d-1)}} (z_{d+1} - hU_{d+1}) + o_{\mathbb{P}}(h^2) + \mathcal{O}_{\mathbb{P}}(hz_{d+1}^2).$$

In the transient phase, if $z_{d+1}^2 = 1 - o(h^2)$, we have

$$\hat{z}_{d+1} = \frac{1}{\sqrt{1+h^2(d-1)}} \left(1 - \frac{1}{2}h^2U_{d+1}^2\right) z_{d+1} + o_{\mathbb{P}}(h^2).$$

□

A.8. Proof of Theorem 4.2.

Proof. Throughout the proof, we assume $h = o(d^{-1/2})$ so that $dh^2 \rightarrow 0$. For bounded random variables, convergence in probability implies convergence in L_1 . Therefore, it suffices to show $\left(1 \wedge \frac{\pi_{\mu,\Sigma}(\hat{X})(R^2 + \|\hat{X}\|^2)^d}{\pi_{\mu,\Sigma}(X)(R^2 + \|X\|^2)^d}\right) \xrightarrow{\mathbb{P}} 1$. Furthermore, for any $\epsilon > 0$

$$\mathbb{P} \left(\left| 1 \wedge \frac{\pi_{\mu,\Sigma}(\hat{X})(R^2 + \|\hat{X}\|^2)^d}{\pi_{\mu,\Sigma}(X)(R^2 + \|X\|^2)^d} - 1 \right| > \epsilon \right) \leq \mathbb{P} \left(\left| \frac{\pi_{\mu,\Sigma}(\hat{X})(R^2 + \|\hat{X}\|^2)^d}{\pi_{\mu,\Sigma}(X)(R^2 + \|X\|^2)^d} - 1 \right| > \epsilon \right)$$

Therefore, it suffices to show $\frac{\pi_{\mu,\Sigma}(\hat{X})(R^2 + \|\hat{X}\|^2)^d}{\pi_{\mu,\Sigma}(X)(R^2 + \|X\|^2)^d} \xrightarrow{\mathbb{P}} 1$, or equivalently

$$\log \frac{\pi_{\mu,\Sigma}(\hat{X})(R^2 + \|\hat{X}\|^2)^d}{\pi_{\mu,\Sigma}(X)(R^2 + \|X\|^2)^d} \xrightarrow{\mathbb{P}} 0.$$

Defining $\delta_i := \lambda_i^{-1} - 1$, we can write $\pi_{\mu,\Sigma}(x)$ as

$$\log \pi_{\mu,\Sigma}(x) = \log \pi_{0,I_d}(x) - \frac{1}{2} \sum_i \delta_i x_i^2 + \sum_i \mu_i (1 + \delta_i) x_i - \frac{1}{2} \sum_i \log(\lambda_i),$$

where π_{0,I_d} is just the standard multivariate Gaussian density. Furthermore, using $R = d^{1/2}$ and

$$\log \frac{(d + \|\hat{X}\|^2)^d}{(d + \|X\|^2)^d} = d \log \frac{1 - z_{d+1}}{1 - \hat{z}_{d+1}},$$

we have

$$\begin{aligned} \log \frac{\pi_{\mu,\Sigma}(\hat{X})(d + \|\hat{X}\|^2)^d}{\pi_{\mu,\Sigma}(X)(d + \|X\|^2)^d} &= \log \frac{\pi_{\mu,\Sigma}(\hat{X})}{\pi_{\mu,\Sigma}(X)} + d \log \frac{1 - z_{d+1}}{1 - \hat{z}_{d+1}} \\ &= \log \frac{\pi_{0,I_d}(\hat{X})}{\pi_{0,I_d}(X)} + d \log \frac{1 - z_{d+1}}{1 - \hat{z}_{d+1}} - \frac{1}{2} \sum_i \delta_i (\hat{X}_i^2 - X_i^2) + \sum_i \mu_i (1 + \delta_i) (\hat{X}_i - X_i). \end{aligned}$$

Therefore, it suffices to show that if h satisfies the condition of Theorem 4.2 then we have all of the three results:

$$\log \frac{\pi_{0,I_d}(\hat{X})}{\pi_{0,I_d}(X)} + d \log \frac{1 - z_{d+1}}{1 - \hat{z}_{d+1}} \xrightarrow{\mathbb{P}} 0, \quad (14)$$

$$\sum_i \delta_i(\hat{X}_i^2 - X_i^2) \xrightarrow{\mathbb{P}} 0, \quad (15)$$

$$\sum_i \mu_i(1 + \delta_i)(\hat{X}_i - X_i) \xrightarrow{\mathbb{P}} 0. \quad (16)$$

The rest of the proof is just to show Eqs. (14) to (16) using Taylor expansions and Lemma 3.1.

A.8.1. *Proof of Eq. (14).* Writing $X = \mu + \Sigma^{1/2} \tilde{N}$ where \tilde{N} is a standard multivariate Gaussian vector, because of the conditions in Theorem 4.2 that there exist constants $C < \infty$ and $c > 0$ such that $c \leq \lambda_i \leq C$ and $|\mu_i| \leq C$, we have $\mu^T \Sigma^{1/2} \tilde{N} = \mathcal{O}_{\mathbb{P}}(d^{1/2})$. Then using the fact $\tilde{N}^T \Sigma \tilde{N} = \sum_i \lambda_i + \mathcal{O}_{\mathbb{P}}(d^{1/2})$, we have

$$\begin{aligned} \|X\|^2 &= \|X - \mu\|^2 + \sum_i \mu_i^2 + 2\mu^T \Sigma^{1/2} \tilde{N} \\ &= \tilde{N}^T \Sigma \tilde{N} + \sum_i \mu_i^2 + 2\mu^T \Sigma^{1/2} \tilde{N} \\ &= \left(d - \sum_i (1 - \lambda_i) + \mathcal{O}_{\mathbb{P}}(d^{1/2}) \right) + \sum_i \mu_i^2 + \mathcal{O}_{\mathbb{P}}(d^{1/2}). \end{aligned}$$

Then we have $\|X\|^2 = d + \sum_i \mu_i^2 - \sum_i (1 - \lambda_i) + \mathcal{O}_{\mathbb{P}}(d^{1/2})$ and

$$z_{d+1} = \frac{\|X\|^2 - d}{\|X\|^2 + d} = \frac{\sum_i \mu_i^2 - \sum_i (1 - \lambda_i)}{2d + \sum_i \mu_i^2 - \sum_i (1 - \lambda_i)} + \mathcal{O}_{\mathbb{P}}(d^{-1/2}). \quad (17)$$

By Eq. (9), $|\sum_i \mu_i^2 - \sum_i (1 - \lambda_i)| = \mathcal{O}(d^\alpha)$, we have $\|X\|^2 = d + \mathcal{O}(d^\alpha) + \mathcal{O}_{\mathbb{P}}(d^{1/2})$ and $z_{d+1} = \mathcal{O}(d^{\alpha-1}) + \mathcal{O}_{\mathbb{P}}(d^{-1/2})$, where the $\mathcal{O}(d^{\alpha-1})$ term represents $\frac{\sum_i \mu_i^2 - \sum_i (1 - \lambda_i)}{2d + \sum_i \mu_i^2 - \sum_i (1 - \lambda_i)}$ which is bounded away from 1. Note that $h = o(d^{-1/2})$ so we have $\hat{z}_{d+1} = z_{d+1} + \mathcal{O}_{\mathbb{P}}(h)$

by Eq. (6) in Lemma 3.1. Then we have

$$\begin{aligned}
& \log \frac{\pi_{0,I_d}(\hat{X})}{\pi_{0,I_d}(X)} + d \log \frac{1 - z_{d+1}}{1 - \hat{z}_{d+1}} \\
&= d \left(\frac{1}{1 - z_{d+1}} - \frac{1}{1 - \hat{z}_{d+1}} \right) + \log \frac{1 - z_{d+1}}{1 - \hat{z}_{d+1}} \\
&= d \frac{z_{d+1} - \hat{z}_{d+1}}{(1 - z_{d+1})(1 - \hat{z}_{d+1})} - \frac{z_{d+1} - \hat{z}_{d+1}}{1 - \hat{z}_{d+1}} + \mathcal{O}_{\mathbb{P}}(dh^2) \\
&= d \frac{(z_{d+1} - \hat{z}_{d+1})z_{d+1}}{(1 - z_{d+1})(1 - \hat{z}_{d+1})} + \mathcal{O}_{\mathbb{P}}(dh^2) \\
&= d \frac{\mathcal{O}_{\mathbb{P}}(h)[\mathcal{O}_{\mathbb{P}}(d^{-1/2}) + \mathcal{O}(d^{\alpha-1})]}{1 - \mathcal{O}_{\mathbb{P}}(d^{-1/2}) - \mathcal{O}(d^{\alpha-1}) - \mathcal{O}_{\mathbb{P}}(h)} + \mathcal{O}_{\mathbb{P}}(dh^2) = o_{\mathbb{P}}(1),
\end{aligned}$$

where the last equality is because $h = o(d^{-\alpha})$, $h = o(d^{-1/2})$, and the term $\mathcal{O}(d^{\alpha-1})$ is $\frac{\sum_i \mu_i^2 - \sum_i (1 - \lambda_i)}{2d + \sum_i \mu_i^2 - \sum_i (1 - \lambda_i)}$ which is bounded away from 1.

A.8.2. *Proof of Eq. (15).* First of all, we have

$$\hat{X}_i = \frac{d^{1/2}}{1 - \hat{z}_{d+1}} \hat{z}_i, \quad X_i = \frac{d^{1/2}}{1 - z_{d+1}} z_i.$$

Using Taylor expansion and $\hat{z}_i = z_i + \mathcal{O}_{\mathbb{P}}(h)$, we have

$$\begin{aligned}
\sum_i \delta_i \left(\hat{X}_i^2 - X_i^2 \right) &= d \sum_i \delta_i \frac{\hat{z}_i^2 (1 - z_{d+1})^2 - z_i^2 (1 - z_{d+1})^2}{(1 - z_{d+1})^2 (1 - \hat{z}_{d+1})^2} \\
&= d \sum_i \delta_i z_i^2 \left[2(\hat{z}_{d+1} - z_{d+1}) + 3(\hat{z}_{d+1}^2 - z_{d+1}^2) + \mathcal{O}_{\mathbb{P}}(h^3) \right] \\
&\quad + d \sum_i \delta_i (\hat{z}_i^2 - z_i^2) (1 + \mathcal{O}_{\mathbb{P}}(d^{-1/2})).
\end{aligned}$$

We further approximate z_i and \hat{z}_i as follows. First, we can replace \hat{z}_i by z_i using Eq. (6) in Lemma 3.1:

$$\hat{z}_i = a_d z_i + a_d \sqrt{1 - z_i^2} h U_i - \frac{1}{2} a_d z_i h^2 U_i^2 + \mathcal{O}_{\mathbb{P}}(h^3), \quad (18)$$

where $a_d = \frac{1}{\sqrt{1 + h^2(d-1)}}$ and $U_i \sim \mathcal{N}(0, 1)$. Then for given z , we can get

$$\hat{z}_i^2 - z_i^2 = (a_d^2 - 1) z_i^2 + 2a_d^2 z_i \sqrt{1 - z_i^2} h U_i + a_d^2 h^2 U_i^2 + \mathcal{O}_{\mathbb{P}}(z_i h^3 + z_i^2 h^2). \quad (19)$$

Then, we can replace z_i using z_{d+1} and X_i since

$$z_i = (1 - z_{d+1}) d^{-1/2} X_i. \quad (20)$$

Finally, by Eq. (17), for z_{d+1} we have

$$z_{d+1} = \frac{\sum_i \mu_i^2 - \sum_i (1 - \lambda_i)}{2d + \sum_i \mu_i^2 - \sum_i (1 - \lambda_i)} + \mathcal{O}_{\mathbb{P}}(d^{-1/2}). \quad (21)$$

Overall, we have

$$\begin{aligned} \sum_i \delta_i \left(\hat{X}_i^2 - X_i^2 \right) &= d \sum_i \delta_i z_i^2 \left[2(\hat{z}_{d+1} - z_{d+1}) + 3(\hat{z}_{d+1}^2 - z_{d+1}^2) + \mathcal{O}_{\mathbb{P}}(h^3) \right] \\ &\quad + d \sum_i \delta_i (\hat{z}_i^2 - z_i^2) (1 + \mathcal{O}_{\mathbb{P}}(d^{-1/2})) \\ &= \mathcal{O}_{\mathbb{P}}(dh) \left(\frac{1}{d} \sum_i \delta_i X_i^2 \right) + d \sum_i \delta_i (\hat{z}_i^2 - z_i^2) (1 + \mathcal{O}_{\mathbb{P}}(d^{-1/2})) + o_{\mathbb{P}}(1). \end{aligned} \quad (22)$$

We first focus on the term $d \sum_i \delta_i (\hat{z}_i^2 - z_i^2)$. For given X , using Eq. (18), replacing z_i using Eq. (20), simplifying z_{d+1} with Eq. (21), we have

$$d \sum_i \delta_i (\hat{z}_i^2 - z_i^2) = d \sum_i \delta_i [(a_d^2 - 1)X_i^2/d + d^{-1/2}hX_iU_i + a_d^2h^2U_i^2 + \mathcal{O}_{\mathbb{P}}(z_ih^3 + z_i^2h^2)]$$

Recall that $U_i \sim \mathcal{N}(0, 1)$ but for $i \neq j$, U_i and U_j are in general not independent since they are obtained by marginalizing the same multivariate Gaussian to two non-orthogonal directions. However, by basic geometry on the angle between the two marginalization directions corresponding to U_i and U_j , respectively, we know $\mathbb{E}[U_i U_j \mid X] = \mathcal{O}(z_i z_j) = \mathcal{O}(d^{-1} X_i X_j) + \mathcal{O}(d^{-3/2})$. That is, although U_i and U_j are independent if and only if either $z_i = 0$ or $z_j = 0$, their correlation is quite small.

Therefore, we have

$$\begin{aligned}
d \sum_i \delta_i (\hat{z}_i^2 - z_i^2) &= d \sum_i \delta_i (a_d^2 - 1) X_i^2 / d + d \sum_i \delta_i (d^{-1/2} h) X_i U_i + \mathcal{O}(dh^2) \sum_i \delta_i U_i^2 + o_{\mathbb{P}}(1) \\
&= d(a_d^2 - 1) \left(\frac{1}{d} \sum_i \delta_i X_i^2 \right) + \mathcal{O}(dh) \left(\frac{1}{d^{1/2}} \sum_i \delta_i X_i U_i \right) + \mathcal{O}(d^2 h^2) \left(\frac{1}{d} \sum_i \delta_i U_i^2 \right) + o_{\mathbb{P}}(1) \\
&= d(a_d^2 - 1) \left(\frac{1}{d} \sum_i \delta_i X_i^2 \right) + \mathcal{O}(dh) \mathcal{O}_{\mathbb{P}} \left(\sqrt{\frac{2}{d^2} \sum_{i \neq j} \delta_i \delta_j X_i^2 X_j^2 + \frac{1}{d} \sum_i \delta_i^2 X_i^2} \right) \\
&\quad + \mathcal{O}(d^2 h^2) \mathcal{O}_{\mathbb{P}} \left(\frac{1}{d} \sum_i \delta_i \right) + o_{\mathbb{P}}(1) \\
&= d(a_d^2 - 1) \left(\frac{1}{d} \sum_i \delta_i X_i^2 \right) + \mathcal{O}(dh) \left[\mathcal{O}_{\mathbb{P}} \left(\sqrt{\frac{1}{d} \sum_i \delta_i^2 X_i^2} \right) + \mathcal{O}_{\mathbb{P}} \left(\frac{1}{d} \sum_i \delta_i X_i^2 \right) \right] \\
&\quad + \mathcal{O}(d^2 h^2) \mathcal{O}_{\mathbb{P}} \left(\frac{1}{d} \sum_i \delta_i \right) + o_{\mathbb{P}}(1).
\end{aligned}$$

Substituting to Eq. (22), using $1 - a_d^2 = \mathcal{O}(h^2 d)$ and $h = o(d^{-1/2})$, we have

$$\sum_i \delta_i (\hat{X}_i^2 - X_i^2) = \mathcal{O}_{\mathbb{P}}(d^2 h^2 + dh) \left(\frac{1}{d} \sum_i \delta_i X_i^2 + \frac{1}{d} \sum_i \delta_i \right) + \mathcal{O}_{\mathbb{P}}(dh) \sqrt{\frac{1}{d} \sum_i \delta_i^2 X_i^2} + o_{\mathbb{P}}(1). \tag{23}$$

Now note that both $\frac{1}{d} \sum_i \delta_i X_i^2$ and $\frac{1}{d} \sum_i \delta_i^2 X_i^2$ concentrate to their means. Using $X_i \sim \mathcal{N}(\mu_i, \lambda_i)$, we have

$$\frac{1}{d} \sum_i \delta_i X_i^2 = \frac{1}{d} \sum_i \delta_i (\mu_i^2 + \lambda_i) + \mathcal{O}_{\mathbb{P}}(d^{-1/2}), \quad \frac{1}{d} \sum_i \delta_i^2 X_i^2 = \frac{1}{d} \sum_i \delta_i^2 (\mu_i^2 + \lambda_i) + \mathcal{O}_{\mathbb{P}}(d^{-1/2})$$

Therefore, substituting to Eq. (23), in order to guarantee $\sum_i \delta_i (\hat{X}_i^2 - X_i^2) \xrightarrow{\mathbb{P}} 0$, a sufficient condition for h in terms of $\{\mu_i\}$ and $\{\lambda_i\}$ is

$$(d^2 h^2 + dh) \cdot \left(\frac{1}{d} \sum_i \delta_i (\lambda_i + \mu_i^2) + \frac{1}{d} \sum_i \delta_i \right) + (dh) \cdot \sqrt{\frac{1}{d} \sum_i \delta_i^2 (\lambda_i + \mu_i^2)} = o(1).$$

Therefore, it is sufficient to assume

$$h = o \left(d^{-1} / \sqrt{\max \left\{ \left| \frac{1}{d} \sum_i \frac{\delta_i}{1 + \delta_i} \right|, \left| \frac{1}{d} \sum_i \delta_i \mu_i^2 \right|, \left| \frac{1}{d} \sum_i \frac{\delta_i^2}{1 + \delta_i} \right|, \left| \frac{1}{d} \sum_i \delta_i^2 \mu_i^2 \right|, \left| \frac{1}{d} \sum_i \delta_i \right| \right\} \wedge d^{-1/2}} \right). \quad (24)$$

A.8.3. *Proof of Eq. (16).* We use a similar approach as the previous part. Using Taylor expansion and Eq. (18) to replace \hat{z}_i , we have

$$\begin{aligned} \hat{X}_i - X_i &= \frac{d^{1/2}}{1 - \hat{z}_{d+1}} \hat{z}_i - \frac{d^{1/2}}{1 - z_{d+1}} z_i \\ &= \frac{d^{1/2}}{1 - z_{d+1}} \left(a_d z_i + a_d \sqrt{1 - z_i^2} h U_i + \mathcal{O}_{\mathbb{P}}(h^2) \right) (1 + \mathcal{O}(\hat{z}_{d+1} - z_{d+1}) + \mathcal{O}_{\mathbb{P}}(h^2)) - \frac{d^{1/2}}{1 - z_{d+1}} z_i. \end{aligned}$$

Substituting to Eq. (16), and using Eq. (20) to replace z_i by X_i , we can get

$$\sum_i \mu_i (1 + \delta_i) (\hat{X}_i - X_i) = (a_d - 1) \sum_i [\mu_i (1 + \delta_i) X_i] + a_d h \sum_i \left[\sqrt{d - X_i^2} \mu_i (1 + \delta_i) U_i \right] + o_{\mathbb{P}}(1). \quad (25)$$

Now we first focus on the term $(a_d - 1) \sum_i [\mu_i (1 + \delta_i) X_i]$ in Eq. (25). Using the fact that $a_d - 1 = \mathcal{O}(h^2 d)$ and $X_i \sim \mathcal{N}(\mu_i, \lambda_i)$ are independent random variables, we have

$$(a_d - 1) \sum_i [\mu_i (1 + \delta_i) X_i] = \mathcal{O}(h^2 d^2) \left[\frac{1}{d} \sum_i \mu_i^2 (1 + \delta_i) + \frac{1}{d} \mathcal{O}_{\mathbb{P}} \left(\sqrt{\sum_i \mu_i^2 (1 + \delta_i)^2 \lambda_i} \right) \right].$$

Therefore, $(a_d - 1) \sum_i [\mu_i (1 + \delta_i) X_i] \xrightarrow{\mathbb{P}} 0$ if $(h^2 d^2) \cdot \frac{1}{d} \sum_i \mu_i^2 (1 + \delta_i) = o(1)$. Next, we focus on the term $a_d h \sum_i \left[\sqrt{d - X_i^2} \mu_i (1 + \delta_i) U_i \right]$ in Eq. (25). Using $U_i \sim \mathcal{N}(0, 1)$ conditional on X and variance decomposition formula, we have

$$\begin{aligned} &\text{var} \left[a_d h \sum_i \left(\sqrt{d - X_i^2} \mu_i (1 + \delta_i) U_i \right) \right] \\ &= \mathbb{E} \left[a_d^2 h^2 \sum_i (d - X_i^2) \mu_i^2 (1 + \delta_i)^2 \right] + \mathcal{O}(d^{-1}) \left(\sum_i a_d h \sqrt{d} \mu_i (1 + \delta_i) \right)^2 \\ &= \mathcal{O}(d^2 h^2) \left[\frac{1}{d} \sum_i \left(1 - \frac{\mu_i^2 + \lambda_i}{d} \right) \mu_i^2 (1 + \delta_i)^2 + \left(\frac{1}{d} \sum_i \mu_i (1 + \delta_i) \right)^2 \right]. \end{aligned}$$

Therefore, $a_d h \sum_i \left(\sqrt{d - X_i^2} \mu_i (1 + \delta_i) U_i \right) \xrightarrow{\mathbb{P}} 0$ if both $(d^2 h^2) \cdot \frac{1}{d} \sum_i \mu_i^2 (1 + \delta_i)^2 = o(1)$ and $(dh) \left| \frac{1}{d} \sum_i \mu_i (1 + \delta_i) \right| = o(1)$. Overall, in order to make $\sum_i \mu_i (1 + \delta_i) (\hat{X}_i - X_i)$ to converge to 0 in probability, we need Eq. (25) to be $o_{\mathbb{P}}(1)$. Then, a sufficient condition for h in terms of $\{\mu_i\}$ and $\{\lambda_i\}$ is

$$d^2 h^2 \max \left\{ \frac{1}{d} \sum_i \mu_i^2 (1 + \delta_i), \frac{1}{d} \sum_i \mu_i^2 (1 + \delta_i)^2 \right\} \rightarrow 0, \quad dh \left| \frac{1}{d} \sum_i \mu_i (1 + \delta_i) \right| \rightarrow 0.$$

Therefore, it is sufficient if

$$h = o \left(d^{-1} / \sqrt{\max \left\{ \left| \frac{1}{d} \sum_i \frac{\delta_i}{1 + \delta_i} \right|, \left| \frac{1}{d} \sum_i \delta_i \mu_i^2 \right|, \left| \frac{1}{d} \sum_i \delta_i^2 \mu_i^2 \right|, \left| \frac{1}{d} \sum_i \mu_i^2 \right| \right\} \wedge d^{-1/2}} \right). \quad (26)$$

Overall, combining Eq. (24) and Eq. (26), since we only need the order of h , Eq. (24) can be relaxed to

$$h = o \left(d^{-1} / \sqrt{\frac{1}{d} \sum_i |1 - \lambda_i| \wedge d^{-1/2}} \right)$$

and Eq. (26) can be relaxed to

$$h = o \left(d^{-1} / \sqrt{\max \left\{ \frac{1}{d} \sum_i |1 - \lambda_i|, \frac{1}{d} \sum_i \mu_i^2 \right\} \wedge d^{-1/2}} \right).$$

Combining the above two with $h = o(d^{-\alpha})$ completes the proof. \square

A.9. Proof of Lemma 5.2.

Proof. We use z and \hat{z} to denote the corresponding coordinates of X and \hat{X} on the unit sphere. We first “upgrade” Eq. (6) in Lemma 3.1 to a convergence in L_1 statement. Define

$$\bar{z}_i := \frac{1}{\sqrt{1 + h^2(d-1)}} \left[\left(1 - \frac{1}{2} h^2 U^2 \right) z_i - \sqrt{1 - z_i^2} h U \right].$$

Using Eq. (6) and the facts that \hat{z}_i is bounded and \bar{z}_i has a finite exponential moment, applying Cauchy–Schwarz inequality and Markov inequality, we have

$$\begin{aligned} \mathbb{E}[|\hat{z}_i - \bar{z}_i|] &\leq \mathbb{E}[|\hat{z}_i - \bar{z}_i \mathbf{1}_{|\bar{z}_i| \leq C \log(d)}|] + \mathbb{E}[|\bar{z}_i \mathbf{1}_{|\bar{z}_i| > C \log(d)}|] \\ &= C \log(d) \mathcal{O}(h^3) + \sqrt{\mathbb{E}[\bar{z}_i^2]} \sqrt{\mathbb{P}(\exp(|\bar{z}_i|) > d^C)} \\ &= \mathcal{O}(\log(d) h^3) + \mathcal{O}(d^{-C/2}) = \mathcal{O}(\log(d) h^3), \end{aligned}$$

where C is chosen as a large enough constant so that $d^{-C/2} = o(\log(d)h^3)$. Therefore, Eq. (6) in Lemma 3.1 can be rewritten as a convergence in L_1 statement:

$$\mathbb{E}_{\hat{z}_i|z_i} \left[\left| \hat{z}_i - \left(\frac{1}{\sqrt{1+h^2(d-1)}} \left[\left(1 - \frac{1}{2}h^2U^2 \right) z_i - \sqrt{1-z_i^2}hU \right] \right) \right| \right] = \mathcal{O}(\log(d)h^3). \quad (27)$$

Next, we want to rule out some subsets of “bad states”, including those states with the “latitude” z_{d+1} too close to 1. That is, we define a sequence of “typical sets” $\{F_d\}$ with $\pi(F_d) \rightarrow 1$ such that when $x \in F_d$, the corresponding z_{d+1} is bounded away from 1. We define

$$\begin{aligned} F_d := & \left\{ x \in \mathbb{R}^d : \left| \frac{1}{d} \sum_{i=1}^d [(\log f(x_i))']^2 - \mathbb{E}_f [((\log f)')^2] \right| < d^{-1/2} \log(d) \right\} \\ & \cap \left\{ x \in \mathbb{R}^d : \left| \frac{1}{d} \sum_{i=1}^d [(\log f(x_i))''] - \mathbb{E}_f [((\log f)'')] \right| < d^{-1/2} \log(d) \right\} \\ & \cap \left\{ x \in \mathbb{R}^d : \left| \frac{1}{d} \sum_{i=1}^d x_i (\log f(x_i))' - \mathbb{E}_f [X(\log f)'] \right| < d^{-1/2} \log(d) \right\} \\ & \cap \left\{ x \in \mathbb{R}^d : \left| \frac{1}{d} \sum_{i=1}^d x_i^2 - \mathbb{E}_f (X^2) \right| < d^{-1/2} \log(d) \right\} \end{aligned}$$

Note that by the assumption $\lim_{x \rightarrow \pm\infty} x f'(x) = 0$, we have

$$\mathbb{E}_f [X(\log f)'] = \int \left[\frac{x}{f(x)} f'(x) \right] f(x) dx = \int x f'(x) dx = 0 - \int f(x) dx = -1.$$

Therefore our assumptions on π imply

$$\pi(F_d^c) = \mathbb{P}_\pi(X \notin F_d) = \mathcal{O} \left(\left(\frac{d^{1/2}}{\log(d)d^{1/2}} \right)^4 + \left(\frac{d^{1/2}}{\log(d)d^{1/2}} \right)^3 \right) = o(1).$$

Using the definition of $\{F_d\}$, we can assume $X \in F_d$ and only consider the expectation over \hat{X} given X . By the definition of $\{F_d\}$, we know z_{d+1} is bounded away from 1.

Next, we want to rule out the subset of “bad proposals” where the proposal “latitude” \hat{z}_{d+1} is too close to 1. Under stationarity, we know $R^{\frac{1+z_{d+1}}{1-z_{d+1}}} = \lambda d^{\frac{1+z_{d+1}}{1-z_{d+1}}} = d + \mathcal{O}_{\mathbb{P}}(d^{1/2})$, which implies $z_{d+1} = \frac{1-\lambda}{1+\lambda} + \mathcal{O}_{\mathbb{P}}(d^{-1/2})$ and $\frac{1}{1-z_{d+1}} = \frac{1+\lambda}{2\lambda} + \mathcal{O}_{\mathbb{P}}(d^{-1/2})$. Furthermore, for given $X \in F_d$, since we know

$$\hat{z}_{d+1} = z_{d+1} + \mathcal{O}_{\mathbb{P}}(h),$$

uniformly on $X \in F_d$, for all large enough d , we have

$$z_{d+1} + h \log(d) = \frac{1 - \lambda}{1 + \lambda} + \mathcal{O}(\log(d)d^{-1/2}) + h \log(d) < 1 - \epsilon,$$

where $\frac{\lambda}{1+\lambda} < \epsilon < 1$ is a fixed constant. Furthermore, we have

$$\sup_{X \in F_d} \mathbb{P}(\hat{z}_{d+1} > 1 - \epsilon) \leq \sup_{X \in F_d} \mathbb{P}(\hat{z}_{d+1} > z_{d+1} + h \log(d)) = o(d^{-1/2}).$$

Therefore, we only need consider the cases such that \hat{z}_{d+1} is no smaller than $1 - \epsilon$ since

$$\begin{aligned} & \sup_{X \in F_d} \mathbb{E}_{\hat{X}|X} \left[\left| 1 \wedge \frac{\pi(\hat{X})(R^2 + \|\hat{X}\|^2)^d}{\pi(X)(R^2 + \|X\|^2)^d} - 1 \wedge \exp(W_{\hat{X}|X}) \right| \right] \\ & \leq \sup_{X \in F_d} \mathbb{E}_{\hat{X}|X} \left[\left| 1 \wedge \left(\frac{\pi(\hat{X})(R^2 + \|\hat{X}\|^2)^d}{\pi(X)(R^2 + \|X\|^2)^d} \mathbf{1}_{\{\hat{z}_{d+1} \leq 1 - \epsilon\}} \right) - 1 \wedge \exp(W_{\hat{X}|X}) \right| \right] + \sup_{X \in F_d} \mathbb{P}(\hat{z}_{d+1} > 1 - \epsilon) \\ & \leq \sup_{X \in F_d} \mathbb{E}_{\hat{X}|X} \left[\left| \log \frac{\pi(\hat{X})(R^2 + \|\hat{X}\|^2)^d}{\pi(X)(R^2 + \|X\|^2)^d} \mathbf{1}_{\{\hat{z}_{d+1} \leq 1 - \epsilon\}} - W_{\hat{X}|X} \right| \right] + o(d^{-1/2}), \end{aligned}$$

where the last step is because $1 \wedge e^x$ is a 1-Lipschitz function.

In the rest of the proof, all we will use for approximating \hat{z}_{d+1} is Eq. (27). Since $\frac{\lambda}{1+\lambda} < \epsilon < 1$, Eq. (27) is also true if we replace \hat{z}_{d+1} by $\hat{z}_{d+1} \mathbf{1}_{\{\hat{z}_{d+1} \leq 1 - \epsilon\}}$. That is, for truncated \hat{z}_{d+1} :

$$\sup_{X \in F_d} \mathbb{E}_{\hat{z}_{d+1}|z_{d+1}} \left[\left| \hat{z}_{d+1} \mathbf{1}_{\{\hat{z}_{d+1} \leq 1 - \epsilon\}} - \bar{z}_{d+1} \right| \right] = \mathcal{O}(\log(d)h^3). \quad (28)$$

Therefore, in the rest of the proof, we simply work on the cases such that $\hat{z}_{d+1} \leq 1 - \epsilon$ and sometimes omit the term $\mathbf{1}_{\{\hat{z}_{d+1} \leq 1 - \epsilon\}}$ for simplicity. The goal is then to consider $X \in F_d$ and establish a Gaussian approximation result for

$$\left(\sum_{i=1}^d [\log f(\hat{X}_i) - \log f(X_i)] + d[\log(1 - z_{d+1}) - \log(1 - \hat{z}_{d+1})] \right) \mathbf{1}_{\{\hat{z}_{d+1} < 1 - \epsilon\}}.$$

Note that by Eq. (27), we know $\mathbb{E}[|\hat{z}_i - z_i|^3] = \mathcal{O}(h^3)$, $\mathbb{E}[|\hat{z}_i - z_i|(\hat{z}_{d+1} - z_{d+1})^2] = \mathcal{O}(h^3)$, $\mathbb{E}[|\hat{z}_{d+1} - z_{d+1}|(\hat{z}_i - z_i)^2] = \mathcal{O}(h^3)$. Furthermore, we only need to consider $\frac{1}{1 - \hat{z}_{d+1}}$ is bounded as \hat{z}_{d+1} is bounded away from 1. Then, using

$$\begin{aligned} \hat{X}_i - X_i &= \frac{R}{1 - \hat{z}_{d+1}} \hat{z}_i - \frac{R}{1 - z_{d+1}} z_i \\ &= \frac{R}{(1 - z_{d+1})(1 - \hat{z}_{d+1})} (\hat{z}_{d+1} - z_{d+1}) z_i + \left(\frac{R(\hat{z}_{d+1} - z_{d+1})}{(1 - z_{d+1})(1 - \hat{z}_{d+1})} + \frac{R}{1 - z_{d+1}} \right) (\hat{z}_i - z_i), \end{aligned} \quad (29)$$

together with Taylor expansion and mean value theorem, uniformly on $\forall X \in F_d$, we have

$$\mathbb{E}_{\hat{X}|X} \left[\left| \sum_{i=1}^d \log \frac{f(\hat{X}_i)}{f(X_i)} - d \log \frac{1 - \hat{z}_{d+1}}{1 - z_{d+1}} - (\text{Term I}) - (\text{Term II}) \right| \cdot \mathbf{1}_{\{\hat{z}_{d+1} \leq 1-\epsilon\}} \right] = \mathcal{O}(dh^3),$$

where

$$\begin{aligned} \text{Term I} &:= \sum_i \left[(\log f(X_i))'(\hat{X}_i - X_i) \right] + \frac{d}{1 - z_{d+1}}(\hat{z}_{d+1} - z_{d+1}), \\ \text{Term II} &:= \frac{1}{2} \left\{ \sum_i \left[(\log f(X_i))''(\hat{X}_i - X_i)^2 \right] + \frac{d}{(1 - z_{d+1})^2}(\hat{z}_{d+1} - z_{d+1})^2 \right\}. \end{aligned}$$

We will see that, similar to the CLT arguments used for analyzing RWM [RGG97; YRR20] for general targets, the mean of the CLT result is determined by the sum of the mean of Term I and the mean of Term II whereas the variance of the CLT result is determined by the variance of Term I only. In the rest of the proof, we first approximate Term I and II separately, then we combine them in the end.

A.9.1. Term I. Using Eq. (29) and Eq. (27), with the definition of F_d , we can get the following approximation of $\hat{X}_i - X_i$:

$$\sup_{X \in F_d} \mathbb{E}_{\hat{X}|X} \left[\left| \hat{X}_i - X_i - \frac{1 + \lambda}{2\lambda}(\hat{z}_{d+1} - z_{d+1})X_i + \frac{R}{1 - z_{d+1}}(\hat{z}_i - z_i) \right| \cdot \mathbf{1}_{\{\hat{z}_{d+1} \leq 1-\epsilon\}} \right] = \mathcal{O}(d^{1/2}h^2).$$

Next, let $\hat{z} - z = (\hat{z}_1 - z_1, \dots, \hat{z}_{d+1} - z_{d+1})^T$, we can approximate the “Term I” by

$$\sup_{X \in F_d} \mathbb{E}_{\hat{X}|X} \left[\left| (\text{Term I}) - \frac{R}{1 - z_{d+1}} \cdot (\text{Inner Product Term}) \right| \cdot \mathbf{1}_{\{\hat{z}_{d+1} \leq 1-\epsilon\}} \right] = o(d^{-1/2}),$$

where the “Inner Product Term” represents

$$\left((\log f(X_1))', \dots, (\log f(X_d))', \sum_{i=1}^d \left(\frac{1 + \lambda}{2\lambda}(\log f(X_i))'z_i + \frac{1}{R} \right) \right) \cdot (\hat{z} - z).$$

The key observation is that: we can see the inner product term as the “projection” of $\hat{z} - z$ to the particular “direction” defined by

$$\tilde{v} := \left((\log f(X_1))', \dots, (\log f(X_d))', \sum_{i=1}^d \left(\frac{1 + \lambda}{2\lambda}(\log f(X_i))'z_i + \frac{1}{R} \right) \right).$$

This observation allows us to just study the distribution of Term I through projections of the current locations and the proposal to this particular direction. Note that the approximation results of Eq. (27) and its proof hold not only for all coordinates, but also hold for projections to any directions due to the symmetry of the sphere.

The “projection” of z onto \tilde{v} is

$$\begin{aligned}\tilde{z} &:= \frac{\tilde{v} \cdot z}{\|\tilde{v}\|} = \frac{\left[\sum_{i=1}^d ((\log f(X_i))' z_i) \right] + z_{d+1} \left[\sum_{i=1}^d \left(\frac{1+\lambda}{2\lambda} (\log f(X_i))' z_i + \frac{1}{R} \right) \right]}{\sqrt{\sum_{i=1}^d ((\log f(X_i))')^2 + \left[\sum_{i=1}^d \left(\frac{1+\lambda}{2\lambda} (\log f(X_i))' z_i + \frac{1}{R} \right) \right]^2}} \\ &= \frac{\left(\frac{2\lambda}{1+\lambda} + z_{d+1} \right) \left[\sum_{i=1}^d \left(\frac{1+\lambda}{2\lambda} (\log f(X_i))' z_i + \frac{1}{R} \right) \right] - \frac{2\lambda}{1+\lambda} \frac{d}{R}}{\sqrt{\sum_{i=1}^d ((\log f(X_i))')^2 + \left[\sum_{i=1}^d \left(\frac{1+\lambda}{2\lambda} (\log f(X_i))' z_i + \frac{1}{R} \right) \right]^2}} \in [-1, 1]\end{aligned}$$

Then we can write

$$\begin{aligned}\|\tilde{v}\|^2 - |\tilde{v} \cdot z|^2 &= \sum_{i=1}^d ((\log f(X_i))')^2 + \left[\sum_{i=1}^d \left(\frac{1+\lambda}{2\lambda} (\log f(X_i))' z_i + \frac{1}{R} \right) \right]^2 \\ &\quad - \left(\frac{2\lambda}{1+\lambda} + z_{d+1} \right)^2 \left[\sum_{i=1}^d \left(\frac{1+\lambda}{2\lambda} (\log f(X_i))' z_i + \frac{1}{R} \right) \right]^2 - \left(\frac{2\lambda}{1+\lambda} \right)^2 \frac{d^2}{R^2} \\ &\quad + \frac{2\lambda}{1+\lambda} \frac{2d \left(\frac{2\lambda}{1+\lambda} + z_{d+1} \right)}{R} \left[\sum_{i=1}^d \left(\frac{1+\lambda}{2\lambda} (\log f(X_i))' z_i + \frac{1}{R} \right) \right].\end{aligned}$$

Note that by the definition of F_d , we know $\sum_{i=1}^d (\log f(X_i))' X_i + d = o(d)$ and $\frac{2\lambda}{1+\lambda} + z_{d+1} = 1 + \mathcal{O}(d^{-1/3})$. Then, we have

$$\sup_{X \in F_d} \mathbb{E}_{\hat{X}|X} \left[\left| \|\tilde{v}\|^2 - |\tilde{v} \cdot z|^2 - (\text{Term III}) \right| \cdot \mathbf{1}_{\{\hat{z}_{d+1} \leq 1-\epsilon\}} \right] = o(d^{1/2}),$$

where the “Term III” is defined by

$$\text{Term III} := \sum_{i=1}^d ((\log f(X_i))')^2 + \frac{2\lambda}{1+\lambda} \frac{2d}{R} \sum_{i=1}^d \left(\frac{1+\lambda}{2\lambda} (\log f(X_i))' z_i \right) + \left[\frac{4\lambda}{1+\lambda} - \left(\frac{2\lambda}{1+\lambda} \right)^2 \right] \frac{d^2}{R^2}.$$

Let \tilde{z}' be the “projection” of \hat{z} onto \tilde{v} . Then, the inner product term can be written as $\tilde{v} \cdot (\hat{z} - z) = \|\tilde{v}\|(\tilde{z}' - \tilde{z})$. Next, we can approximate the “projection” of \hat{z} onto \tilde{v} using the equivalent result of Eq. (27) for \tilde{z}

$$\sup_{X \in F_d} \mathbb{E}_{\hat{X}|X} \left[\left| \tilde{z}' - a_d \left(\tilde{z} - \sqrt{1 - \tilde{z}^2} h \tilde{U} \right) \right| \right] = \mathcal{O}(h^2),$$

where \tilde{U} is a standard Gaussian and $a_d := \frac{1}{\sqrt{1+(d-1)h^2}}$. Therefore, we have

$$\sup_{X \in F_d} \mathbb{E}_{\hat{X}|X} \left[\left| \|\tilde{v}\|(\tilde{z}' - \tilde{z}) - W_1 \right| \cdot \mathbf{1}_{\{\hat{z}_{d+1} \leq 1-\epsilon\}} \right] = o(d^{-1/2}),$$

where $W_1 \sim \mathcal{N}(\mu_1, \sigma_1^2)$ with $\mu_1 := (a_d - 1) \|\tilde{v}\| \tilde{z}$ and $\sigma_1^2 := (1 - \tilde{z}^2) \|\tilde{v}\|^2 a_d^2 h^2$. Substituting $1 - \tilde{z}^2 = \frac{\|\tilde{v}\|^2 - \|\tilde{v} \cdot z\|^2}{\|\tilde{v}\|^2}$, using the definition of F_d , we can compute the mean and variance of W_1 as

$$\begin{aligned} \mu_1 &= (a_d - 1) \frac{1 + \lambda}{2\lambda} \left[\sum_i (\log f(X_i))' X_i + \frac{1 - \lambda}{1 + \lambda} d \right] + o(d^{-1/2}) \\ &= (a_d - 1) \frac{1 + \lambda}{2\lambda} \left[d\mathbb{E}[(\log f(X_1))' X_1] + \frac{1 - \lambda}{1 + \lambda} d \right] + \mathcal{O}(d^{-1/2} \log(d)), \\ \sigma_1^2 &= \frac{(1 + \lambda)^2}{4\lambda} da_d^2 h^2 \left[\sum_i ((\log f(X_i))')^2 + \frac{4}{1 + \lambda} \sum_i (\log f(X_i))' X_i + \frac{4d}{(1 + \lambda)^2} \right] + o(d^{-1/2}) \\ &= \frac{(1 + \lambda)^2}{4\lambda} da_d^2 h^2 \left[d\mathbb{E} \left[((\log f(X_1))')^2 \right] + \frac{4d}{1 + \lambda} \mathbb{E}[(\log f(X_1))' X_1] + \frac{4d}{(1 + \lambda)^2} \right] + \mathcal{O}(d^{-1/2} \log(d)). \end{aligned}$$

A.9.2. Term II. Next, we approximate Term II in the Taylor expansion. Clearly, the variance of Term II can be ignored since it is of the order $o(d^{-1})$. We only need to focus on the expectation. We start from computing

$$\sup_{X \in F_d} \mathbb{E}_{\hat{X}|X} \left[(\log f(X_i))'' (\hat{X}_i - X_i)^2 \cdot \mathbf{1}_{\{\hat{z}_{d+1} \leq 1 - \epsilon\}} \right].$$

Note that

$$\sup_{X \in F_d} \mathbb{E}_{\hat{X}|X} \left[\left| (\hat{X}_i - X_i)^2 - (\text{Term IV}) \right| \cdot \mathbf{1}_{\{\hat{z}_{d+1} \leq 1 - \epsilon\}} \right] = o(d^{1/2} h^2),$$

where the “Term IV” is defined as

$$\left(\frac{1 + \lambda}{2\lambda} \right)^2 (\hat{z}_{d+1} - z_{d+1})^2 X_i^2 + \frac{R^2}{(1 - z_{d+1})^2} (\hat{z}_i - z_i)^2 + \frac{1 + \lambda}{2\lambda} \frac{2RX_i}{1 - z_{d+1}} (\hat{z}_{d+1} - z_{d+1})(\hat{z}_i - z_i).$$

Taking expectation over \hat{X} given X and using

$$\begin{aligned} \mathbb{E}_{\hat{X}|X}[\hat{z}_i - z_i] &= (a_d - 1) z_i + o(d^{-1}) \\ \mathbb{E}_{\hat{X}|X}[(\hat{z}_i - z_i)^2] &= a_d^2 h^2 + [(a_d - 1)^2 - a_d^2 h^2] z_i^2 + o(d^{-1}), \end{aligned}$$

substituting to the “Term IV”, then uniformly over $X \in F_d$, we have

$$\begin{aligned}\mathbb{E}_{\hat{X}|X}[(\hat{X}_i - X_i)^2] &= \left(\frac{1+\lambda}{2\lambda}\right)^2 X_i^2 [a_d^2 h^2 (1 - z_{d+1}^2) + (1 - a_d)^2 z_{d+1}^2] \\ &\quad + \frac{R^2}{(1 - z_{d+1})^2} [a_d^2 h^2 (1 - z_i^2) + (1 - a_d)^2 z_i^2] \\ &\quad + \frac{1+\lambda}{2\lambda} \frac{2RX_i}{1 - z_{d+1}} (1 - a_d)^2 z_i z_{d+1} + o(d^{-1}) + o(d^{1/2} h^2).\end{aligned}$$

This implies that, uniformly over $X \in F_d$, we have

$$\begin{aligned}\sum_i \mathbb{E}_{\hat{X}|X}[(\hat{X}_i - X_i)^2] &= \left(\frac{1+\lambda}{2\lambda}\right)^2 \frac{d}{\lambda} [a_d^2 h^2 (1 - z_{d+1}^2) + (1 - a_d)^2 z_{d+1}^2] \\ &\quad + \frac{R^2}{(1 - z_{d+1})^2} d a_d^2 h^2 - d a_d^2 h^2 + (1 - a_d)^2 d + \frac{1+\lambda}{2\lambda} \frac{d}{\lambda} (1 - a_d)^2 z_{d+1} + \mathcal{O}(d^{-1/2}) \\ &= \frac{R^2}{(1 - z_{d+1})^2} d a_d^2 h^2 + \mathcal{O}(d^{-1/2}) = (1 - a_d^2) d \frac{(1+\lambda)^2}{4\lambda} + \mathcal{O}(d^{-1/2}).\end{aligned}$$

Therefore, uniformly on F_d , we have

$$\begin{aligned}&\sum_{i=1}^d \mathbb{E}_{\hat{X}|X} \left[(\log f(X_i))'' (\hat{X}_i - X_i)^2 \right] + \frac{d}{(1 - z_{d+1})^2} \mathbb{E}_{\hat{X}|X} [(\hat{z}_{d+1} - z_{d+1})^2] \\ &= \frac{R^2}{(1 - z_{d+1})^2} a_d^2 h^2 \left[\sum_{i=1}^d (\log f(X_i))'' - \left[1 - \left(\frac{1+\lambda}{2\lambda} \right)^2 (1 - z_{d+1}^2) \right] \sum_{i=1}^d ((\log f(X_i))'' z_i^2) \right] \\ &\quad + \frac{R^2}{(1 - z_{d+1})^2} (1 - a_d)^2 \left[1 + \left(\frac{1+\lambda}{2\lambda} \right)^2 z_{d+1}^2 + \frac{1+\lambda}{\lambda} z_{d+1} \right] \sum_{i=1}^d ((\log f(X_i))'' z_i^2) \\ &\quad + \frac{1 + z_{d+1}}{1 - z_{d+1}} d a_d^2(h) h^2 + \frac{d(1 - a_d)^2 z_{d+1}^2}{(1 - z_{d+1})^2} + \mathcal{O}(d^{-1/2}).\end{aligned}$$

Finally, using the definition of F_d , we can have

$$\begin{aligned}&2 \cdot \text{Term II} + \mathcal{O}(d^{-1/2} \log(d)) \\ &= \frac{(1+\lambda)^2}{4\lambda} d a_d^2 h^2 \sum_i \mathbb{E} [(\log f(X_i))''] - a_d^2 h^2 \left(1 - \frac{1}{\lambda} \right) \sum_i \mathbb{E} [(\log f(X_i))'' X_i^2] \\ &\quad + \frac{(1+\lambda)^2}{4\lambda} (1 - a_d)^2 \sum_i \mathbb{E} [(\log f(X_i))'' X_i^2] + \frac{1}{\lambda} d a_d^2 h^2 + \frac{(1-\lambda)^2}{4\lambda^2} (1 - a_d)^2 d.\end{aligned}$$

A.9.3. *Combining Term I and Term II.* Finally, we combine Term I and Term II. Using the assumption $\lim_{x \rightarrow \pm\infty} x f'(x) = 0$ which implies $\lim_{x \rightarrow \pm\infty} f'(x) = 0$, one can show

$$\mathbb{E}_f[(\log f)'' + ((\log f)')^2] = \int \left[\frac{f(x)f''(x) - (f'(x))^2}{f(x)^2} + \left(\frac{1}{f(x)} f'(x) \right)^2 \right] f(x) dx = \int f''(x) dx = 0,$$

$$\mathbb{E}_f[X(\log f)'] = \int \left[\frac{x}{f(x)} f'(x) \right] f(x) dx = \int x f'(x) dx = 0 - \int f(x) dx = -1.$$

Using the above results and $(d-1)a_d^2 h^2 = 1 - a_d^2$, we have

$$\mu_1 = -(1 - a_d) \frac{1 + \lambda}{2\lambda} d \mathbb{E}_f[X(\log f)'] - (1 - a_d) \frac{1 - \lambda}{2\lambda} d + \mathcal{O}(d^{-1/2} \log(d)),$$

$$\mathbb{E}[\text{Term II}] = (1 - a_d) \frac{(1 + \lambda)^2}{4\lambda} d \mathbb{E}_f[(\log f)'] + \mathcal{O}(d^{-1/2} \log(d)),$$

$$\frac{\sigma_1^2}{2} = (1 - a_d) \frac{(1 + \lambda)^2}{4\lambda} d \mathbb{E}_f[((\log f)')^2] + (1 - a_d) \frac{1 + \lambda}{\lambda} d \mathbb{E}_f[X(\log f)'] + (1 - a_d) \frac{d}{\lambda} + \mathcal{O}(d^{-1/2} \log(d)).$$

Therefore, the mean and variance of the Gaussian distribution satisfy

$$\begin{aligned} \mu &= \mu_1 + \mathbb{E}[\text{Term II}] + \mathcal{O}(d^{-1/2} \log(d)) = d(1 - a_d) \frac{(1 + \lambda)^2}{4\lambda} \left\{ \frac{4\lambda}{(1 + \lambda)^2} + \mathbb{E} \left[\frac{\partial^2 \log \pi}{\partial x^2} \right] \right\}, \\ \frac{\sigma^2}{2} &= \frac{\sigma_1^2}{2} + \mathcal{O}(d^{-1/2} \log(d)) = d(1 - a_d) \frac{(1 + \lambda)^2}{4\lambda} \left\{ \mathbb{E} \left[\left(\frac{\partial \log \pi}{\partial x} \right)^2 \right] - \frac{4\lambda}{(1 + \lambda)^2} \right\}. \end{aligned}$$

Using $1 - a_d = \frac{\ell^2}{2d} \frac{4\lambda}{(1 + \lambda)^2}$, we have

$$\mu = \frac{\ell^2}{2} \left\{ \frac{4\lambda}{(1 + \lambda)^2} - \mathbb{E}_f \left[((\log f)')^2 \right] \right\}, \quad \sigma^2 = \ell^2 \left\{ \mathbb{E}_f \left[((\log f)')^2 \right] - \frac{4\lambda}{(1 + \lambda)^2} \right\}.$$

Therefore, we have shown a Gaussian random variable $W_{\hat{X}|X} \sim \mathcal{N}(\mu, \sigma^2)$ which satisfies

$$\sup_{X \in F_d} \mathbb{E}_{\hat{X}|X} \left[\left((\text{Term I} + \text{Term II}) \cdot \mathbf{1}_{\{\hat{z}_{d+1} \leq 1 - \epsilon\}} - W_{\hat{X}|X} \right)^2 \right] = \mathcal{O}(d^{-1/2} \log(d)).$$

Combining everything together, we have shown

$$\begin{aligned} &\sup_{X \in F_d} \mathbb{E}_{\hat{X}|X} \left[\left| \log \frac{\pi(\hat{X})(R^2 + \|\hat{X}\|^2)^d}{\pi(X)(R^2 + \|X\|^2)^d} \mathbf{1}_{\{\hat{z}_{d+1} \leq 1 - \epsilon\}} - W_{\hat{X}|X} \right| \right] \\ &= \mathcal{O}(\sqrt{d^{-1/2} \log(d)}) = o(d^{-1/4} \log(d)), \end{aligned}$$

which completes the proof. \square

A.10. Proof of Theorem 5.6.

Proof. By the i.i.d. assumption, it suffices to consider the first coordinate as

$$\text{ESJD} = d \cdot \mathbb{E}_{X \sim \pi} \mathbb{E}_{\hat{X} | X} \left[(\hat{X}_1 - X_1)^2 \left(1 \wedge \frac{\pi(\hat{X})(R^2 + \|\hat{X}\|^2)^d}{\pi(X)(R^2 + \|X\|^2)^d} \right) \right].$$

We first follow a similar approach as the proof of Lemma 5.2. We define a sequence of “typical sets” $\{F_d\}$ such that $\pi(F_d) \rightarrow 1$. Define the sequence of sets $\{F_d\}$ by

$$\begin{aligned} F_d := & \left\{ x \in \mathbb{R}^d : \left| \frac{1}{d-1} \sum_{i=2}^d [(\log f(x_i))']^2 - \mathbb{E}_f [((\log f)')^2] \right| < d^{-1/8} \right\} \\ & \cap \left\{ x \in \mathbb{R}^d : \left| \frac{1}{d-1} \sum_{i=2}^d [(\log f(x_i))''] - \mathbb{E}_f [((\log f)'')] \right| < d^{-1/8} \right\} \\ & \cap \left\{ x \in \mathbb{R}^d : \left| \frac{1}{d-1} \sum_{i=2}^d x_i (\log f(x_i))' - \mathbb{E}_f [X(\log f)'] \right| < d^{-1/8} \right\} \\ & \cap \left\{ x \in \mathbb{R}^d : \left| \frac{1}{d} \sum_{i=1}^d x_i^2 - \mathbb{E}_f (X^2) \right| < d^{-1/6} \log(d) \right\} \\ & \cap \{x \in \mathbb{R}^d : |x_1| < d^{1/5}\}. \end{aligned} \tag{30}$$

Following the arguments in Appendix A.9, there exists a constant $0 < \epsilon < 1$ such that $\sup_{X \in F_d} \mathbb{P}(\hat{z}_{d+1} > 1 - \epsilon) = o(1)$. We define

$$\bar{F}_d := \{x \in \mathbb{R}^d : z_{d+1} \leq 1 - \epsilon\}.$$

We will rule out the “bad” proposals such that $\hat{X} \in \bar{F}_d^c$. By Cauchy–Schwarz inequality

$$\begin{aligned} & d \cdot \mathbb{E}_{X \sim \pi} \mathbb{E}_{\hat{X} | X} \left[(\hat{X}_1 - X_1)^2 \mathbf{1}_{\{X \notin F_d\} \cup \{\hat{X} \notin \bar{F}_d\}} \right] \\ & \leq d \sqrt{\mathbb{E}[(\hat{X}_1 - X_1)^4]} \sqrt{\mathbb{P}(\{X \notin F_d\} \cup \{\hat{X} \notin \bar{F}_d\})} = o(d^2 h^2) = o(1). \end{aligned}$$

Therefore, we have

$$\begin{aligned} \text{ESJD} / d &= \mathbb{E} \left\{ (\hat{X}_1 - X_1)^2 \mathbf{1}_{\{X \in F_d, \hat{X} \in \bar{F}_d\}} \left(1 \wedge \exp \left[\log \frac{\pi(\hat{X})}{\pi(X)} + \log \frac{(R^2 + \|\hat{X}\|^2)^d}{(R^2 + \|X\|^2)^d} \right] \right) \right\} + o(d^{-1}) \\ &\leq \sup_{x \in F_d} \mathbb{E}_{\hat{X} | x} \left\{ (\hat{X}_1 - x_1)^2 \left(1 \wedge \exp \left[\log \frac{\pi(\hat{X})}{\pi(x)} + \log \frac{(R^2 + \|\hat{X}\|^2)^d}{(R^2 + \|x\|^2)^d} \right] \right) \mathbf{1}_{\{\hat{X} \in \bar{F}_d\}} \right\} + o(d^{-1}) \end{aligned} \tag{31}$$

In order to remove the dependence on \hat{X}_1 from $\|\hat{X}\|^2$, we construct a coupling $\tilde{X} \stackrel{d}{=} \hat{X}$ such that only $\hat{X}_{2:d} = \tilde{X}_{2:d}$ and \tilde{X}_1 is identical distributed as \hat{X}_1 . Furthermore, \tilde{X}_1 is independent with \hat{X}_1 conditional on $\hat{X}_{2:d}$:

$$\tilde{X} := (\tilde{X}_1, \dots, \tilde{X}_d), \quad \tilde{X}_{2:d} = \hat{X}_{2:d}, \quad \left(\tilde{X}_1 \perp\!\!\!\perp \hat{X}_1 \mid \hat{X}_{2:d} \right), \quad \tilde{X}_1 \stackrel{d}{=} \hat{X}_1.$$

Using a similar argument, we can replace $\mathbf{1}_{\{\hat{X} \in \bar{F}_d\}}$ by $\mathbf{1}_{\{\hat{X} \in \bar{F}_d, \tilde{X} \in \bar{F}_d\}}$ in the first term of the r.h.s. of Eq. (31), which gives

$$\sup_{x \in \bar{F}_d} \mathbb{E}_{(\hat{X}, \tilde{X})|x} \left\{ (\hat{X}_1 - x_1)^2 \mathbf{1}_{\{\hat{X} \in \bar{F}_d, \tilde{X} \in \bar{F}_d\}} \cdot \left[1 \wedge \exp \left(\log \frac{f(\hat{X}_1)}{f(x_1)} + \log \frac{(R^2 + \|\hat{X}\|^2)^d}{(R^2 + \|\tilde{X}\|^2)^d} + \sum_{i=2}^d \log \frac{f(\hat{X}_i)}{f(x_i)} + \log \frac{(R^2 + \|\tilde{X}\|^2)^d}{(R^2 + \|x\|^2)^d} \right) \right] \right\}. \quad (32)$$

Using the fact that $1 \wedge \exp(\cdot)$ is 1-Lipschitz, for two random variables A and B , if $\sup_{x \in \bar{F}_d} \mathbb{E}[(\hat{X}_1 - x_1)^2 | A - B| \mathbf{1}_{\{\hat{X} \in \bar{F}_d, \tilde{X} \in \bar{F}_d\}}] = o(d^{-1})$, then

$$\begin{aligned} & \sup_{x \in \bar{F}_d} \mathbb{E} \left\{ (\hat{X}_1 - x_1)^2 \mathbf{1}_{\{\hat{X} \in \bar{F}_d, \tilde{X} \in \bar{F}_d\}} | [1 \wedge \exp(A)] - [1 \wedge \exp(B)] | \right\} \\ & \leq \sup_{x \in \bar{F}_d} \mathbb{E} \left\{ (\hat{X}_1 - x_1)^2 | A - B | \mathbf{1}_{\{\hat{X} \in \bar{F}_d, \tilde{X} \in \bar{F}_d\}} \right\} = o(d^{-1}). \end{aligned}$$

Alternatively, if $\sup_{x \in \bar{F}_d} \mathbb{E}[(A - B)^2 \mathbf{1}_{\{\hat{X} \in \bar{F}_d, \tilde{X} \in \bar{F}_d\}}] = o(1)$, then by Cauchy–Schwarz inequality

$$\begin{aligned} & \sup_{x \in \bar{F}_d} \mathbb{E} \left\{ (\hat{X}_1 - x_1)^2 | A - B | \mathbf{1}_{\{\hat{X} \in \bar{F}_d, \tilde{X} \in \bar{F}_d\}} \right\} \\ & \leq \sup_{x \in \bar{F}_d} \sqrt{\mathbb{E}[(\hat{X}_1 - x_1)^4]} \sqrt{\mathbb{E}[(A - B)^2 \mathbf{1}_{\{\hat{X} \in \bar{F}_d, \tilde{X} \in \bar{F}_d\}}]} = o(dh^2) = o(d^{-1}). \end{aligned}$$

We next use the above approximations several times to approximate Eq. (32). We first approximate $\log \frac{(R^2 + \|\hat{X}\|^2)^d}{(R^2 + \|\tilde{X}\|^2)^d}$ by $\frac{\hat{X}_1^2 - \mathbb{E}[\tilde{X}_1^2]}{2}$, since by Taylor expansion and mean value theorem, using the fact $R^2 = d$, one can show

$$\sup_{x \in \bar{F}_d} \mathbb{E} \left[(\hat{X}_1 - x_1)^2 \left| \log \frac{(R^2 + \|\hat{X}\|^2)^d}{(R^2 + \|\tilde{X}\|^2)^d} - \frac{\hat{X}_1^2 - \tilde{X}_1^2}{2} \right| \mathbf{1}_{\{\hat{X} \in \bar{F}_d, \tilde{X} \in \bar{F}_d\}} \right] = \mathcal{O}(d^{-1/2} dh^2),$$

and

$$\sup_{x \in \bar{F}_d} \mathbb{E} \left[(\hat{X}_1 - x_1)^2 \left| \frac{\hat{X}_1^2 - \mathbb{E}[\tilde{X}_1^2]}{2} \right| \mathbf{1}_{\{\hat{X} \in \bar{F}_d, \tilde{X} \in \bar{F}_d\}} \right] = \mathcal{O}(d^{-1/2} dh^2).$$

Next, we consider the conditional expectation over \tilde{X} of the term $\sum_{i=2}^d \log \left(\frac{f(\tilde{X}_i)}{f(x_i)} \right)$. Since $\sup_{x \in F_d} \mathbb{E}[\sum_{i=2}^d (\tilde{X}_i - x_i)^3 \mathbf{1}_{\{\tilde{X} \in \bar{F}_d\}}] = o(d^{-1})$, we can approximate $\sum_{i=2}^d \log \left(\frac{f(\tilde{X}_i)}{f(x_i)} \right)$ by the first two terms of its Taylor expansion. Using Taylor expansion and mean value theorem, we have

$$\begin{aligned} & \sup_{x \in F_d} \mathbb{E}_{\tilde{X}|x} \left[\left(\sum_{i=2}^d \log \left(\frac{f(\tilde{X}_i)}{f(x_i)} \right) - (\text{Term I} + \text{Term II}) \right)^2 \mathbf{1}_{\{\tilde{X} \in \bar{F}_d\}} \right] \\ &= \mathcal{O} \left(\sup_{x \in F_d} \mathbb{E}_{\tilde{X}|x} \left[\left| \sum_{i=2}^d (\tilde{X}_i - x_i)^3 \right|^2 \mathbf{1}_{\{\tilde{X} \in \bar{F}_d\}} \right] \right) = o(d^{-1}), \end{aligned} \quad (33)$$

where

$$\text{Term I} + \text{Term II} := \sum_{i=2}^d \left[(\log f(x_i))' (\tilde{X}_i - x_i) + \frac{1}{2} (\log f(x_i))'' (\tilde{X}_i - x_i)^2 \right].$$

Furthermore, following the Gaussian approximation arguments in the proof of Lemma 5.2, we have the following result:

$$\sup_{x \in F_d} \mathbb{E}_{\tilde{X}|x} \left[\left((\text{Term I} + \text{Term II}) + \log \frac{(R^2 + \|\tilde{X}\|^2)^d}{(R^2 + \|x\|^2)^d} - W_{\tilde{X}|x} \right)^2 \mathbf{1}_{\{\tilde{X} \in \bar{F}_d\}} \right] = o(1)$$

where $W_{\tilde{X}|x} \sim \mathcal{N}(\mu, \sigma^2)$ with

$$\mu = \frac{\ell^2}{2} \left\{ 1 - \mathbb{E}_f \left[((\log f)')^2 \right] \right\}, \quad \sigma^2 = \ell^2 \left\{ \mathbb{E}_f \left[((\log f)')^2 \right] - 1 \right\}.$$

Therefore, after the above approximations, we have simplified Eq. (32) to

$$\sup_{x \in F_d} \mathbb{E}_{(\hat{X}_1, \tilde{X})|x} \left\{ (\hat{X}_1 - x_1)^2 \mathbf{1}_{\{\hat{X} \in \bar{F}_d\}} \left[1 \wedge \exp \left(\log \frac{f(\hat{X}_1)}{f(x_1)} + \frac{\hat{X}_1^2 - \mathbb{E}[\tilde{X}_1^2]}{2} + W_{\tilde{X}|x} \right) \right] \right\}. \quad (34)$$

Note that the randomness of $\log \frac{f(\hat{X}_1)}{f(x_1)} + \frac{\hat{X}_1^2 - \mathbb{E}[\tilde{X}_1^2]}{2}$ only comes from \hat{X}_1 , and the randomness of $W_{\tilde{X}|x}$ comes from \tilde{X} . However, $W_{\tilde{X}|x}$ is not independent with \hat{X}_1 , because of the weak dependence of \hat{X}_1 with $\tilde{X}_{2:d} = \hat{X}_{2:d}$. Indeed, it can be argued that $W_{\tilde{X}|x}$ is asymptotically independent with \hat{X}_1 . However, we wish $W_{\tilde{X}|x}$ being independent with \hat{X}_1 in order to make further progress.

In Appendix A.10.1, we will construct another random variable \tilde{W} , which is identically distributed with $W_{\tilde{X}|x}$, but independent with \hat{X}_1 . Furthermore, \tilde{W} is “physically

close" to $W_{\hat{X}|x}$ such that

$$\sup_{x \in F_d} \mathbb{E} \left[\left(\tilde{W} - W_{\hat{X}|x} \right)^2 \right] = o(1). \quad (35)$$

Note that the existence of \tilde{W} is very intuitive: if $W_{\hat{X}|x}$ is asymptotically independent with \hat{X}_1 , then there should have an identically distributed random variable \tilde{W} , which is independent with \hat{X}_1 and dependent with $W_{\hat{X}|x}$. Furthermore, $W_{\hat{X}|x}$ becomes "physically closer and closer" to \tilde{W} .

Using Eq. (35) and the Lipschitz property of $1 \wedge \exp(\cdot)$, we can simplify Eq. (34) to

$$\begin{aligned} & \sup_{x \in F_d} \mathbb{E}_{(\hat{X}_1, \tilde{X})|x} \left\{ (\hat{X}_1 - x_1)^2 \mathbf{1}_{\{\hat{X} \in \bar{F}_d\}} \left[1 \wedge \exp \left(\log \frac{f(\hat{X}_1)}{f(x_1)} + \frac{\hat{X}_1^2 - \mathbb{E}[\tilde{X}_1^2]}{2} + W_{\hat{X}|x} \right) \right] \right\} \\ & \rightarrow \sup_{x \in F_d} \mathbb{E}_{(\hat{X}, \tilde{X})|x} \left\{ (\hat{X}_1 - x_1)^2 \mathbf{1}_{\{\hat{X} \in \bar{F}_d\}} \left[1 \wedge \exp \left(\log \frac{f(\hat{X}_1)}{f(x_1)} + \frac{\hat{X}_1^2 - \mathbb{E}[\tilde{X}_1^2]}{2} + \tilde{W} \right) \right] \right\} \\ & \rightarrow \sup_{x \in F_d} \mathbb{E}_{(\tilde{W}, \tilde{X})|x} \left\{ (\hat{X}_1 - x_1)^2 \left[1 \wedge \exp \left(\log \frac{f(\hat{X}_1)}{f(x_1)} + \frac{\hat{X}_1^2 - \mathbb{E}[\tilde{X}_1^2]}{2} + \tilde{W} \right) \right] \right\} \\ & = \sup_{x \in F_d} \mathbb{E}_{\hat{X}_1|x} \left\{ (\hat{X}_1 - x_1)^2 \mathbb{E}_{\tilde{W}|\hat{X}_1, x} \left[1 \wedge \exp \left(\log \frac{f(\hat{X}_1)}{f(x_1)} + \frac{\hat{X}_1^2 - \mathbb{E}[\tilde{X}_1^2]}{2} + \tilde{W} \right) \right] \right\}. \end{aligned} \quad (36)$$

Lemma A.1. [RGG97, Proposition 2.4] If $W \sim \mathcal{N}(\mu, \sigma^2)$ then

$$\mathbb{E}_W[1 \wedge \exp(W)] = \Phi(\mu/\sigma) + \exp(\mu + \sigma^2/2)\Phi(-\sigma - \mu/\sigma)$$

where $\Phi(\cdot)$ is the standard normal cumulative distribution function.

By Lemma A.1, the inside expectation of Eq. (36) is

$$\begin{aligned} M(\hat{X}_1) &:= \mathbb{E}_{\tilde{W}|\hat{X}_1, x} \left[1 \wedge \exp \left(\log \frac{f(\hat{X}_1)}{f(x_1)} + \frac{\hat{X}_1^2 - \mathbb{E}[\tilde{X}_1^2]}{2} + \tilde{W} \right) \right] \\ &= \Phi \left(-\frac{\sigma}{2} + \frac{\log \left(\frac{f(\hat{X}_1)}{f(x_1)} \right) + \frac{\hat{X}_1^2 - \mathbb{E}[\tilde{X}_1^2]}{2}}{\sigma} \right) \\ &\quad + \exp \left(\log \left(\frac{f(\hat{X}_1)}{f(x_1)} \right) + \frac{\hat{X}_1^2 - \mathbb{E}[\tilde{X}_1^2]}{2} \right) \cdot \Phi \left(-\frac{\sigma}{2} - \frac{\log \left(\frac{f(\hat{X}_1)}{f(x_1)} \right) + \frac{\hat{X}_1^2 - \mathbb{E}[\tilde{X}_1^2]}{2}}{\sigma} \right). \end{aligned}$$

Note that $\mathbb{E}[\tilde{X}_1^2] = x_1^2 + \mathcal{O}(d^{-1})$. Then it can be easily verified that

$$M(x_1) \rightarrow 2\Phi\left(-\frac{\sigma}{2}\right).$$

Therefore, substituting $M(\hat{X}_1)$ to Eq. (36) and by Taylor expansion, as $d \rightarrow \infty$, we have

$$\begin{aligned} \text{ESJD} &\rightarrow d \cdot \left\{ \mathbb{E}[(\hat{X}_1 - x_1)^2] \cdot 2\Phi\left(-\frac{\sigma}{2}\right) \right\} \\ &\rightarrow 2\ell^2 \cdot \Phi\left(-\frac{\ell}{2} \sqrt{\mathbb{E}_f[(\log f)']^2} - 1\right), \end{aligned}$$

which completes the proof. Therefore, it suffices to show the construction of \tilde{W} .

A.10.1. Construction of \tilde{W} . For simplicity of notations, we will write $W_{\tilde{X}|x}$ as W . Recall the following definitions in Appendix A.7: all the randomness comes from a standard Gaussian $\mathcal{N}(0, I_d)$. We can write it as d independent standard $\mathcal{N}(0, 1)$ as V_1, \dots, V_d . We have also defined U_1, \dots, U_{d+1} which are marginal Gaussian random variables with $U_i \sim \mathcal{N}(0, 1)$. Recall that U_1, \dots, U_{d+1} are usually not independent. However, in the stationary phase when $R = d^{1/2}$, $\{U_i\}$ are “almost independent” since their correlations are very small. Particularly, if $z_i \rightarrow 0$ then U_i is asymptotically independent with all $\{U_j : j \neq i\}$.

Recall that in Appendix A.7, we have derived that the proposed \hat{z}_i can be written as

$$\hat{z}_i = \frac{\sqrt{1 + h^2 U_i^2}}{\sqrt{1 + h^2 \left(\sum_{j=1}^d V_j^2\right)}} \left(\frac{z_i}{\sqrt{1 + h^2 U_i^2}} + \frac{\sqrt{1 - z_i^2} h U_i}{\sqrt{1 + h^2 U_i^2}} \right), \quad i = 1, \dots, d+1.$$

Also, $\hat{X}_i = d^{1/2} \frac{\hat{z}_i}{1 - \hat{z}_{d+1}}$ as $R = d^{1/2}$. To emphasize the sources of randomness, we write

$$\hat{z}_i = \mathcal{F}_{\hat{z}_i} \left(\sum_{j=1}^d V_j^2, U_i \right), \quad i = 1, \dots, d+1,$$

to denote that the randomness of \hat{z}_i comes from $\sum_j V_j^2$ and U_i . Similarly, we can write \hat{X}_i as

$$\hat{X}_i = \mathcal{F}_{\hat{X}_i} \left(\sum_{j=1}^d V_j^2, U_i, U_{d+1} \right), \quad i = 1, \dots, d$$

to denote the randomness of \hat{X}_i comes from $\sum_j V_j^2$, U_i , and U_{d+1} .

Now recall that W is a function of \tilde{X} , where \tilde{X}_1 is conditional independent with \hat{X}_1 , and $\tilde{X}_i = \hat{X}_i$ for all $i = 2, \dots, d$. We can therefore write W as a random function of $\hat{X}_{2:d}$. Therefore, we can write the following:

$$W = \mathcal{F}_W \left(\sum_{j=1}^d V_j^2, U_{2:d+1} \right), \quad \hat{X}_1 = \mathcal{F}_{\hat{X}_1} \left(\sum_{j=1}^d V_j^2, U_1, U_{d+1} \right).$$

Now, it is clear that the dependence of W on \hat{X}_1 has three sources:

- (1) Shared source of randomness, $\sum_{j=1}^d V_j^2$, which is a chi-squared random variable with degree of freedom d ;
- (2) The weak dependence between $U_{2:d}$ and U_1 . Note that $U_1, U_{2:d}$ are correlated and joint Gaussian distributed. When $z_1 \rightarrow 0$, then U_1 becomes (asymptotically) independent with $U_{2:d}$.
- (3) Shared source of randomness U_{d+1} , which becomes (asymptotically) independent with $U_{1:d}$ when $z_{d+1} \rightarrow 0$.

In order to replace W by an identical distributed \tilde{W} , that is also independent with \hat{X}_1 , we do three coupling arguments as follows:

- (1) First coupling argument: we first replace $\sum_{j=1}^d V_j^2$ by a constant d to define

$$W' := \mathcal{F}_W(d, U_{2:d+1})$$

Following the proof of Lemma 5.2, it's very easy to check that W' has the same distribution as W . The key is to show W' and W are “physically close” so that

$$\sup_{x \in F_d} \mathbb{E}[(W' - W)^2] = o(1).$$

Actually, we can show a better rate that

$$\sup_{x \in F_d} \mathbb{E}[(W' - W)^2] = \mathcal{O}(d^{-1}).$$

The proof is delayed to Appendix A.10.2.

- (2) Second coupling argument: we remove the dependence of $U_{2:d+1}$ on U_1 . Note that $U_{2:d+1}$ are “almost independent” with U_1 . We “orthogonalize” these Gaussian random variables $U_{2:d+1}$ by the following decomposition:

$$U_i = c_i^{\parallel} U_1 + c_i^{\perp} U_i^{\perp}, \quad i = 2, \dots, d+1$$

where c_i^{\parallel} is the component that U_i is “parallel” with U_1 , and c_i^{\perp} is the “orthogonal” (that is, independent) component. Now we replace the U_1 in the decomposition by an independent copy \tilde{U}_1 . That is, we define

$$U'_i := c_i^{\parallel} \tilde{U}_1 + c_i^{\perp} U_i^{\perp}, \quad i = 2, \dots, d+1,$$

where \tilde{U}_1 is independent standard Gaussian random variable. Note that U'_i is highly correlated with U_i since the component $c_i^\perp U_i^\perp$ remains. If $z_1 = 0$, for example, we recover $U'_i = U_i$. Next, we define

$$W'' := \mathcal{F}_W(d, U'_{2:d+1}).$$

It is clear that W'' is identically distributed as W' . When $z_1 = 0$, we recover $|W'' - W'| = 0$. Intuitively, W'' is “physically close” to W' , when z_1 is small. Actually, our definition of F_d guarantees that for all $x \in F_d$ we have $x_1 = \mathcal{O}(d^{1/5})$ which implies $z_1 = \mathcal{O}(d^{1/5-1/2})$ is indeed small. Then, our goal is to show

$$\sup_{x \in F_d} \mathbb{E}[(W'' - W')^2] = o(1).$$

Actually, we can prove slightly better rate, which is

$$\sup_{x \in F_d} \mathbb{E}[(W' - W'')^2] = \mathcal{O}(z_1^2) = \mathcal{O}(d^{-3/5}).$$

The proof is delayed to Appendix [A.10.3](#).

- (3) Third coupling argument: finally, we construct \tilde{W} based on W'' . Recall that $W'' = \mathcal{F}_W(d, U'_{2:d+1})$. In order to construct \tilde{W} which is independent with \hat{X}_1 , it suffices to replace the source of U'_{d+1} by an independent copy \tilde{U}_{d+1} . We first “orthogonalize” $U'_{2:d}$ using the same way as the previous coupling argument:

$$U'_i = \tilde{c}_i^\parallel U'_{d+1} + \tilde{c}_i^\perp U_i'^\perp, \quad i = 2, \dots, d.$$

and then replace the component U'_{d+1} by an independent copy \tilde{U}_{d+1} to define $\tilde{U}_{2:d}$ by

$$\tilde{U}_i := \tilde{c}_i^\parallel \tilde{U}_{d+1} + \tilde{c}_i^\perp U_i'^\perp, \quad i = 2, \dots, d.$$

Finally, we define

$$\tilde{W} := \mathcal{F}_W(d, \tilde{U}_{2:d+1}).$$

It is clear that \tilde{W} is identically distributed as W'' and it is now independent with \hat{X}_1 . Then the goal is to show

$$\sup_{x \in F_d} \mathbb{E}[(\tilde{W} - W'')^2] = o(1).$$

It can be seen that the “orthogonalization” part of the coupling argument is the same as the second coupling. We then expect this part causes a distance of order $\mathcal{O}_{\mathbb{P}}(z_{d+1})$, which is indeed the case. By the definition of F_d , for all $x \in F_d$ we have $\|x_i\|^2 - d = o(d^{6/7})$ so $z_{d+1} = o(d^{6/7-1}) = o(d^{-1/7})$. The other

part of the coupling argument is to replace the direct dependence on U'_{d+1} by \tilde{U}_{d+1} , which we can prove a distance of order $\mathcal{O}(d^{-1/8})$. Overall, we can show

$$\sup_{x \in F_d} \mathbb{E}[(\tilde{W} - W'')^2] = \mathcal{O}(d^{-1/4}) + \mathcal{O}(z_{d+1}^2) = \mathcal{O}(d^{-1/4}) + o(d^{-2/7}).$$

The proof is delayed to Appendix A.10.4.

Overall, we have shown the construction of \tilde{W} , which has the same distribution as W and is independent with \hat{X}_1 . Most importantly, we have shown

$$\begin{aligned} \sup_{x \in F_d} \mathbb{E}[(\tilde{W} - W)^2] &\leq \sup_{x \in F_d} \mathbb{E}[(|\tilde{W} - W''| + |W'' - W'| + |W' - W|)^2] \\ &= \mathcal{O}(d^{-1/4}) + o(d^{-2/7}) + \mathcal{O}(d^{-3/5}) + \mathcal{O}(d^{-1}) = o(1). \end{aligned}$$

A.10.2. *The first coupling argument.* We first define the replacement of \hat{z}_i by

$$z'_i := \frac{\sqrt{1 + h^2 U_i^2}}{\sqrt{1 + h^2 d}} \left(\frac{z_i}{\sqrt{1 + h^2 U_i^2}} + \frac{\sqrt{1 - z_i^2} h U_i}{\sqrt{1 + h^2 U_i^2}} \right), \quad i = 1, \dots, d+1,$$

in which we only replace $\sum_j V_j^2$ in \hat{z}_i by a constant d . It is clear that \hat{z}_i and z'_i are highly correlated, we can write

$$\hat{z}_i = (1 + \mathcal{O}_{\mathbb{P}}(h^2 d^{1/2})) \frac{\sqrt{1 + h^2 U_i^2}}{\sqrt{1 + h^2 d}} \left(\frac{z_i}{\sqrt{1 + h^2 U_i^2}} + \frac{\sqrt{1 - z_i^2} h U_i}{\sqrt{1 + h^2 U_i^2}} \right). \quad (37)$$

Following the proof of Lemma 5.2, it is obvious that W' has the same distribution as W , which means the mean of $W - W'$ is zero. Therefore, we only need to focus how fast the variance of $W - W'$ goes to zero.

Recall that in the proof of W using Lemma 5.2, the variance of W is dominated by the variance of the following inner product term

$$\frac{R}{1 - z_{d+1}} \underbrace{\left(0, (\log f(x_2))', \dots, (\log f(x_d))', \sum_{i=2}^d \left((\log f(x_i))' z_i + \frac{1}{R} \right) \right)}_{\text{inner product}} \cdot (\hat{z} - z)$$

When we prove the variance of $W - W'$, by replacing $\hat{z} - z$ to the difference of $\hat{z} - z$ and $z' - z$, which is $\hat{z} - z'$, following the same arguments as the proof of Lemma 5.2, the variance of $W - W'$ is then determined by the variance of

$$\frac{R}{1 - z_{d+1}} \left(0, (\log f(x_2))', \dots, (\log f(x_d))', \sum_{i=2}^d \left((\log f(x_i))' z_i + \frac{1}{R} \right) \right) \cdot (\hat{z} - z')$$

where $\hat{z} - z' = (\hat{z}_1 - z'_1, \dots, \hat{z}_{d+1} - z'_{d+1})^T$. Substituting the definition of \hat{z} and z' , using $\mathcal{O}(h^2 d^{1/2}) = \mathcal{O}(d^{-3/2})$, we get the order of variance as $\mathcal{O} \left(\left(\sum_{i=1}^d (\log f(x_i))' x_i \right)^2 \right) \mathcal{O}(d^{-3})$.

By the definition of F_d , we know $\sum_{i=1}^d (\log f(x_i))' x_i = \mathcal{O}(d)$. Therefore, we have

$$\sup_{x \in F_d} \mathbb{E}[(W - W')^2] = \mathcal{O}(d^2) \mathcal{O}(d^{-3}) = \mathcal{O}(d^{-1}).$$

A.10.3. *The second coupling argument.* By the construction of W'' , it is clear that W'' has the same distribution as W' . Define the replacement of z'_i by

$$z''_i := \frac{\sqrt{1 + h^2(U'_i)^2}}{\sqrt{1 + h^2 d}} \left(\frac{z_i}{\sqrt{1 + h^2(U'_i)^2}} + \frac{\sqrt{1 - z_i^2} h U'_i}{\sqrt{1 + h^2(U'_i)^2}} \right), \quad i = 1, \dots, d+1,$$

Then we can again follow the proof of Lemma 5.2 and focus on the variance of $W' - W''$ (since the mean of $W' - W''$ is clearly zero). Then the variance of $W' - W''$ is determined by the variance of

$$\frac{R}{1 - z_{d+1}} \left(0, (\log f(x_2))', \dots, (\log f(x_d))', \sum_{i=2}^d \left((\log f(x_i))' z_i + \frac{1}{R} \right) \right) \cdot (z'' - z')$$

where $z'' - z' = (z''_1 - z'_1, \dots, z''_{d+1} - z'_{d+1})^T$. Using the fact that

$$U_i - U'_i = c_i^{\parallel} (U_1 - \tilde{U}_1), \quad i = 2, \dots, d+1,$$

we can get that the variance of $W' - W''$ is bounded by

$$\left\{ d \sum_{i=2}^d ((\log f(x_i))')^2 + \left[\sum_{i=2}^d ((\log f(x_i))' x_i + 1) \right]^2 \right\} \left\{ 2h^2 \sum_{i=2}^d (c_i^{\parallel})^2 + o(h^2) \right\}$$

Note that, by the definition of F_d , we have

$$d \sum_{i=2}^d ((\log f(x_i))')^2 = \mathcal{O}(d^2), \quad \left[\sum_{i=2}^d ((\log f(x_i))' x_i + 1) \right]^2 = o(d^2).$$

Using some basic geometry to analyze the “angle” between U_i and U_1 , we know $c_i^{\parallel} = \mathcal{O}(z_i z_1)$. Therefore, using $h^2 = \mathcal{O}(d^{-2})$, we have

$$\sup_{x \in F_d} \mathbb{E}[(W' - W'')^2] = \mathcal{O} \left(\sum_{i=2}^d (c_i^{\parallel})^2 \right) = \mathcal{O} \left(\sum_{i=2}^d z_i^2 z_1 \right) = \mathcal{O}(z_1^2).$$

Finally, for all $x \in F_d$, we have $x_1 = \mathcal{O}(d^{1/5})$ which implies that $z_1 = \mathcal{O}(d^{1/5-1/2}) = \mathcal{O}(d^{-3/10})$.

A.10.4. *The third coupling argument.* By the construction of \tilde{W} , it is clear that the distribution of \tilde{W} is the same as the distribution of W'' . Therefore, the mean of $\tilde{W} - W''$ is zero.

We define the replacement of z_i'' by

$$\tilde{z}_i := \frac{\sqrt{1 + h^2 \tilde{U}_i^2}}{\sqrt{1 + h^2 d}} \left(\frac{z_i}{\sqrt{1 + h^2 \tilde{U}_i^2}} + \frac{\sqrt{1 - z_i^2 h \tilde{U}_i}}{\sqrt{1 + h^2 \tilde{U}_i^2}} \right), \quad i = 1, \dots, d+1.$$

Again, following the proof of Lemma 5.2, the variance of $\tilde{W} - W''$ is determined by the variance of

$$\begin{aligned} & \frac{R}{1 - z_{d+1}} \left(0, (\log f(x_2))', \dots, (\log f(x_d))', \sum_{i=2}^d \left((\log f(x_i))' z_i + \frac{1}{R} \right) \right) \cdot (\tilde{z} - z'') \\ &= \underbrace{\frac{R}{1 - z_{d+1}} (0, (\log f(x_2))', \dots, (\log f(x_d))', 0) \cdot (\tilde{z} - z'')}_{\text{the first term}} \\ & \quad + \underbrace{\frac{R}{1 - z_{d+1}} \left(0, \dots, 0, \sum_{i=2}^d \left((\log f(x_i))' z_i + \frac{1}{R} \right) \right) \cdot (\tilde{z} - z'')}_{\text{the second term}} \end{aligned}$$

where $\tilde{z} - z'' = (\tilde{z}_1 - z_1'', \dots, \tilde{z}_{d+1} - z_{d+1}'')$. Note that we have decomposed the inner product to the sum of two terms. We compute the variances of the two terms separately.

Similar to the previous coupling argument, the variance of the first term is bounded by

$$\left[d \sum_{i=2}^d ((\log f(x_i))')^2 \right] \left[2h^2 \sum_{i=2}^d (\tilde{c}_i^{\parallel})^2 + o(h^2) \right] = \mathcal{O}(z_{d+1}^2).$$

The second term can be written as

$$\sum_{i=2}^d [(\log f(x_i))' x_i + 1] (1 + \mathcal{O}_{\mathbb{P}}(z_{d+1})) (\tilde{z}_{d+1} - z_{d+1}'').$$

By the definition of F_d , we know

$$\sum_{i=2}^d [(\log f(x_i))' x_i + 1] = d\mathcal{O}(d^{-1/8}), \quad z_{d+1} = o(d^{-1/7})$$

Furthermore, by the definition of \tilde{z}_{d+1} and z''_{d+1} , both have finite exponential moments. Moreover, we have

$$\mathbb{E} \left[\left| \tilde{z}_{d+1} - z''_{d+1} - \sqrt{1 - z_{d+1}^2} h(\tilde{U}_{d+1} - U'_{d+1}) \right| \right] = \mathcal{O}(d^{-2}).$$

Therefore, we have the second term

$$\begin{aligned} & \sum_{i=2}^d [(\log f(x_i))' x_i + 1] (1 + \mathcal{O}_{\mathbb{P}}(z_{d+1})) (\tilde{z}_{d+1} - z''_{d+1}) \\ &= d\mathcal{O}(d^{-1/8})(1 + o(d^{-1/7}))h\mathcal{O}_{\mathbb{P}}(1) = \mathcal{O}_{\mathbb{P}}(d^{-1/8}), \end{aligned}$$

and its variance is of order $\mathcal{O}(d^{-1/4})$. Overall, adding the variance of the second term to the variance of the first term yields

$$\sup_{x \in F_d} \mathbb{E}[(\tilde{W} - W'')^2] = \mathcal{O}(z_{d+1}^2) + \mathcal{O}(d^{-1/4}) = o(d^{-2/7}) + \mathcal{O}(d^{-1/4}).$$

This completes the proof. □

A.11. Proof of Theorem 5.9.

Proof. We follow the framework of [RGG97] using the generator approach [EK86]. Define the (discrete time) generator of x by

$$(G_d V)(x) := d\mathbb{E}_{\hat{X}} \left\{ [V(\hat{X}) - V(x)] \left(1 \wedge \frac{\pi(\hat{X})(R^2 + \|\hat{X}\|^2)^d}{\pi(x)(R^2 + \|x\|^2)^d} \right) \right\}$$

for any function V for which this definition makes sense. In the Skorokhod topology, it doesn't cause any problem to treat G_d as a continuous time generator. We shall restrict attention to test functions such that $V(x) = V(x_1)$. We show uniform convergence of G_d to G , the generator of the limiting (one-dimensional) Langevin diffusion, for a suitable large class of real-valued functions V , where, for some fixed function $h(\ell)$,

$$(GV)(x_1) := h(\ell) \left\{ \frac{1}{2} V''(x_1) + \frac{1}{2} [(\log f)'(x_1)] V'(x_1) \right\}.$$

Since f'/f is Lipschitz, by [EK86, Thm 2.1 in Ch.8], a core for the generator has domain C_c^∞ , which is the class of continuous functions with compact support such that all orders of derivatives exist. This enable us to restrict attentions to functions $V \in C_c^\infty$ such that $V(x) = V(x_1)$.

Define the sequence of sets $\{F_d\}$ by

$$\begin{aligned}
F_d := & \left\{ x \in \mathbb{R}^d : \left| \frac{1}{d-1} \sum_{i=2}^d [(\log f(x_i))']^2 - \mathbb{E}_f [((\log f)')^2] \right| < d^{-1/8} \right\} \\
& \cap \left\{ x \in \mathbb{R}^d : \left| \frac{1}{d-1} \sum_{i=2}^d [(\log f(x_i))''] - \mathbb{E}_f [((\log f)'')] \right| < d^{-1/8} \right\} \\
& \cap \left\{ x \in \mathbb{R}^d : \left| \frac{1}{d-1} \sum_{i=2}^d x_i (\log f(x_i))' - \mathbb{E}_f [X(\log f)'] \right| < d^{-1/8} \right\} \\
& \cap \left\{ x \in \mathbb{R}^d : \left| \frac{1}{d} \sum_{i=1}^d x_i^2 - \mathbb{E}_f (X^2) \right| < d^{-1/6} \log(d) \right\} \\
& \cap \{x \in \mathbb{R}^d : |x_1| < d^{1/5}\}
\end{aligned} \tag{38}$$

Then, for fixed t , by the union bound, Markov inequality, and the assumptions Eq. (13), we have

$$\begin{aligned}
& \mathbb{P}(X^d(\lfloor ds \rfloor) \notin F_d, \exists 0 \leq s \leq t) \leq td \mathbb{P}_\pi(X \notin F_d) \\
& = \mathcal{O} \left(td \left(\frac{d^{1/8}}{(d-1)^{1/2}} \right)^4 + td \left(\frac{d^{1/6}}{\log(d)d^{1/2}} \right)^3 + td \left(\frac{1}{d^{1/5}} \right)^6 \right) = \mathcal{O}(t(\log(d))^{-3}).
\end{aligned}$$

Therefore, for any fixed t , if $d \rightarrow \infty$, the probability of all $\{X^d(\lfloor ds \rfloor), 0 \leq s \leq t\}$ are in F_d goes to 1. It then suffices to consider only $x \in F_d$.

Next, we decompose the expectation over $\hat{X} = (\hat{X}_1, \dots, \hat{X}_d)$ into expectations over \hat{X}_1 and $\hat{X}_{2:d} := (\hat{X}_2, \dots, \hat{X}_d)$. Recall that $\hat{X}_1 = \hat{X}'_1$, $\hat{X}_{2:d} = \hat{X}''_{2:d}$, and \hat{X}' is independent with \hat{X}'' . Therefore, \hat{X}_1 is independent with $\hat{X}_{2:d}$. Then, we have

$$\begin{aligned}
(G_d V)(x) &= d \mathbb{E}_{\hat{X}_1} \left\{ [V(\hat{X}_1) - V(x_1)] \mathbb{E}_{\hat{X}_{2:d}} \left[1 \wedge \frac{\pi(\hat{X})(R^2 + \|\hat{X}\|^2)^d}{\pi(x)(R^2 + \|x\|^2)^d} \right] \right\} \\
&= d \mathbb{E}_{\hat{X}_1} \left\{ [V(\hat{X}_1) - V(x_1)] \mathbb{E}_{\hat{X}_1'' | \hat{X}_{2:d}} \mathbb{E}_{\hat{X}_{2:d}} \left[1 \wedge \frac{\pi(\hat{X})(R^2 + \|\hat{X}\|^2)^d}{\pi(x)(R^2 + \|x\|^2)^d} \right] \right\} \\
&= d \mathbb{E}_{\hat{X}_1} \left\{ [V(\hat{X}_1) - V(x_1)] \mathbb{E}_{\hat{X}''} \left[1 \wedge \frac{\pi(\hat{X})(R^2 + \|\hat{X}\|^2)^d}{\pi(x)(R^2 + \|x\|^2)^d} \right] \right\}.
\end{aligned}$$

Now we focus on the inner expectation

$$\begin{aligned} & \mathbb{E}_{\hat{X}''} \left[1 \wedge \frac{\pi(\hat{X})(R^2 + \|\hat{X}\|^2)^d}{\pi(x)(R^2 + \|x\|^2)^d} \right] \\ &= \mathbb{E}_{\hat{X}''} \left[1 \wedge \exp \left\{ d \log \left(\frac{R^2 + \|\hat{X}\|^2}{R^2 + \|\hat{X}''\|^2} \right) + \sum_{i=1}^d \log \left(\frac{f(\hat{X}_i)}{f(x_i)} \right) + d \log \left(\frac{R^2 + \|\hat{X}''\|^2}{R^2 + \|x\|^2} \right) \right\} \right]. \end{aligned}$$

Following the proof of Theorem 5.6, for any $x \in F_d$, we can replace $\sum_{i=2}^d \log \left(\frac{f(\hat{X}_i)}{f(x_i)} \right) + d \log \left(\frac{R^2 + \|\hat{X}''\|^2}{R^2 + \|x\|^2} \right)$ by $W \sim \mathcal{N}(\mu, \sigma^2)$ is a Gaussian random variable with

$$\mu = \frac{\ell^2}{2} \left\{ 1 - \mathbb{E}_f \left[((\log f)')^2 \right] \right\}, \quad \sigma^2 = \ell^2 \left\{ \mathbb{E}_f \left[((\log f)')^2 \right] - 1 \right\}.$$

To keep the dependence on \hat{X}_1 , we denote $r(\hat{X}_1) := d \mathbb{E}_{\hat{X}''} \left[\log \left(\frac{R^2 + \|\hat{X}\|^2}{R^2 + \|\hat{X}''\|^2} \right) \right]$. Using Taylor expansion we can verify that $r(x_1) = \mathcal{O}(d^{-1})$ and $r'(x_1) = x_1 + o(d^{-1/2})$. Therefore, it suggests that we can approximate

$$d \log \left(\frac{R^2 + \|\hat{X}\|^2}{R^2 + \|\hat{X}''\|^2} \right) + \sum_{i=1}^d \log \left(\frac{f(\hat{X}_i)}{f(x_i)} \right) + d \log \left(\frac{R^2 + \|\hat{X}''\|^2}{R^2 + \|x\|^2} \right)$$

by $\log \left(\frac{f(\hat{X}_1)}{f(x_1)} \right) + r(\hat{X}_1) + W$. Hence, we define

$$(\tilde{G}_d V)(x) := d \mathbb{E}_{\hat{X}_1} \left\{ [V(\hat{X}_1) - V(x_1)] \cdot \mathbb{E}_{\hat{X}''} \left[1 \wedge \exp \left\{ \log \left(\frac{f(\hat{X}_1)}{f(x_1)} \right) + r(\hat{X}_1) + W \right\} \right] \right\}. \quad (39)$$

Since $V \in C_c^\infty$, we have for some $Z_1 \in (x_1, \hat{X}_1)$ or (\hat{X}_1, x_1) that

$$V(\hat{X}_1) - V(x_1) = V'(x_1)(\hat{X}_1 - x_1) + \frac{1}{2} V''(Z_1)(\hat{X}_1 - x_1)^2.$$

This implies that $\mathbb{E}_{\hat{X}_1} [V(\hat{X}_1) - V(x_1)] = \mathcal{O}(x_1 d^{-1}) = o(d^{-1/2})$ and $\mathbb{E} \left[|V(\hat{X}_1) - V(x_1)| \right] = \mathcal{O}(d^{-1/2})$, since $x_1 = \mathcal{O}(d^{1/5})$ for $x \in F_d$. Using the fact that the function $1 \wedge \exp(x)$ is Lipschitz [RGG97, Proposition 2.2], we can have

$$\begin{aligned} \sup_{x \in F_d} \left| (G_d V)(x) - (\tilde{G}_d V)(x) \right| &= d \sup_{x \in F_d} \mathbb{E}_{\hat{X}_1} [V(\hat{X}_1) - V(x_1)] \mathcal{O}(d^{-1/2}) \\ &\quad + d \sup_{x \in F_d} \mathbb{E}_{\hat{X}_1} \left[|V(\hat{X}_1) - V(x_1)| (o(d^{-1/2})) \right] = o(1). \end{aligned}$$

Therefore, we can now concentrate on $(\tilde{G}_d V)(x)$ defined in Eq. (39) for $x \in F_d$.

Note that conditional on \hat{X}_1 , the term inside the inner expectation of Eq. (39) is Gaussian distributed, since $\log\left(\frac{f(\hat{X}_1)}{f(x_1)}\right) + r(\hat{X}_1) + W \sim \mathcal{N}(\mu', \sigma^2)$ where $\mu' := \mu + \log\left(\frac{f(\hat{X}_1)}{f(x_1)}\right) + r(\hat{X}_1)$. Therefore, by Lemma A.1, we have

$$\begin{aligned} M(\hat{X}_1) &:= \mathbb{E}_{\hat{X}''} \left[1 \wedge \exp \left\{ \log \left(\frac{f(\hat{X}_1)}{f(x_1)} \right) + r(\hat{X}_1) + W \right\} \right] \\ &= \Phi \left(-\frac{\sigma}{2} + \frac{\log \left(\frac{f(\hat{X}_1)}{f(x_1)} \right) + r(\hat{X}_1)}{\sigma} \right) \\ &\quad + \exp \left(\log \left(\frac{f(\hat{X}_1)}{f(x_1)} \right) + r(\hat{X}_1) \right) \cdot \Phi \left(-\frac{\sigma}{2} - \frac{\log \left(\frac{f(\hat{X}_1)}{f(x_1)} \right) + r(\hat{X}_1)}{\sigma} \right). \end{aligned}$$

Since $r(x_1) = \mathcal{O}(d^{-1})$ and $r'(x_1) = x_1 + o(d^{-1/2})$, it can be verified that

$$M(x_1) \rightarrow 2\Phi\left(-\frac{\sigma}{2}\right), \quad M'(x_1) \rightarrow \Phi\left(-\frac{\sigma}{2}\right) [(\log f(x_1))' + x_1 + o(d^{-1/2})]. \quad (40)$$

Furthermore, one can verify $M''(x_1)$ is bounded since $\Phi(\cdot)$, $\Phi'(\cdot)$, and $\Phi''(\cdot)$ are all bounded functions.

Therefore, by mean value theorem, there exists constants K_1 and K_2 such that

$$\begin{aligned} &d[V(\hat{X}_1) - V(x_1)]M(\hat{X}_1) \\ &= d \left[V'(x_1)(\hat{X}_1 - x_1) + \frac{1}{2}V''(x_1)(\hat{X}_1 - x_1)^2 + K_1(\hat{X}_1 - x_1)^3 \right] \\ &\quad \cdot \left[M(x_1) + M'(x_1)(\hat{X}_1 - x_1) + K_2(\hat{X}_1 - x_1)^2 \right] \\ &= dV'(x_1)M(x_1)(\hat{X}_1 - x_1) \\ &\quad + d \left[\frac{1}{2}V''(x_1)M(x_1) + V'(x_1)M'(x_1) \right] (\hat{X}_1 - x_1)^2 + \mathcal{O}(|d(\hat{X}_1 - x_1)^3|). \end{aligned}$$

Taking expectations over \hat{X}_1 , using Eq. (40), as $d \rightarrow \infty$, we have

$$\begin{aligned}
(\tilde{G}_d V)(x) &= \mathbb{E}_{\hat{X}_1} \left[d[V(\hat{X}_1) - V(x_1)]M(\hat{X}_1) \right] \\
&\rightarrow dV'(x_1)M(x_1)\mathbb{E}[\hat{X}_1 - x_1] + d \left[\frac{1}{2}V''(x_1)M(x_1) + V'(x_1)M'(x_1) \right] \mathbb{E}[(\hat{X}_1 - x_1)^2] \\
&\rightarrow -\frac{\ell^2}{2}x_1V'(x_1)M(x_1) + \ell^2 \left[\frac{1}{2}V''(x_1)M(x_1) + V'(x_1)M'(x_1) \right] \\
&\rightarrow \Phi \left(-\frac{\sigma}{2} \right) \left[-\ell^2x_1V'(x_1) + \ell^2V''(x_1) + \ell^2V'(x_1)[(\log f(x_1))' + x_1 + o(d^{-1/2})] \right] \\
&\rightarrow 2\ell^2\Phi \left(-\frac{\sigma}{2} \right) \left[\frac{1}{2}V''(x_1) + \frac{1}{2}[(\log f)'(x_1)]V'(x_1) \right] \\
&\rightarrow 2\ell^2\Phi \left(-\frac{\ell\sqrt{\mathbb{E}_f[(\log f)']^2} - 1}{2} \right) \left[\frac{1}{2}V''(x_1) + \frac{1}{2}[(\log f)'(x_1)]V'(x_1) \right].
\end{aligned}$$

This completes the proof. \square

A.12. Comments on Remark 3.4. To illustrate the issue that for heavy tail targets, the SPS might stuck if starting from the “south pole”, we consider multivariate student’s t targets. For these targets, one can easily derive that the “equator” is always a stationary point of the density (which is maximum if $\nu < d$ and minimum if $\nu > d$).

We first consider the case that $k = \nu/d < 1$ is a small constant, from Lemma 3.1 and Fig. 9, one can see that in the *transient phase*, the acceptance rate goes to 0 exponentially fast as $d \rightarrow \infty$. For example, when $k = 0.01$ if $z = -1$ and $\hat{z} = 0$, then the acceptance rate is roughly $\exp(-1.7d) \approx 1/5^d$.

Next we consider an approximation for the cases $\nu = \mathcal{O}(1)$ and $d \rightarrow \infty$. Consider current location $x = 0$ which corresponding to the south pole and the “typical” proposal \tilde{x} satisfying $\|\tilde{x}\|^d \approx d$. For multivariate student’s t target with DoF $\nu = \mathcal{O}(1)$, we have

$$\log \frac{\pi(\tilde{x})}{\pi(x)} \approx -\frac{\nu + d}{2} \log(1 + \frac{d}{\nu - 2}) = \mathcal{O}(d \log(d))$$

and $\log \frac{(R^2 + \|\tilde{x}\|^2)^d}{(R^2 + \|x\|^2)^d} = \mathcal{O}(d)$. Therefore, the acceptance probability for a “typical” proposal starting from the south pole is

$$\min \left\{ 1, \frac{\pi(\tilde{x})}{\pi(x)} \frac{(R^2 + \|\tilde{x}\|^2)^d}{(R^2 + \|x\|^2)^d} \right\} \approx 1/(d^d),$$

which implies for multivariate student’s t targets with DoF $\nu = \mathcal{O}(1)$, the SPS chain initialized at the south pole can stuck when the proposal variance is large.

A.13. Proof of the Jacobian determinant Eq. (1). The Jacobian determinant of the stereographic projection is well-known. For example, see [GMP17, Lemma 3.2.1]. One way to derive it is to calculate the Jacobian by comparing the ratio of volumes. Let $x = \text{SP}(z)$ and $y = \text{SP}(w)$, one can get

$$\begin{aligned} \|z - w\|^2 &= \sum_{i=1}^d \|z_i - w_i\|^2 + \|z_{d+1} - w_{d+1}\|^2 \\ &= \sum_{i=1}^d 4 \left(\frac{Rx_i}{R^2 + \|x\|^2} - \frac{Ry_i}{R^2 + \|y\|^2} \right)^2 + 4 \left(\frac{R^2}{R^2 + \|x\|^2} - \frac{R^2}{R^2 + \|y\|^2} \right)^2 \\ &= \frac{4R^2}{(R^2 + \|x\|^2)(R^2 + \|y\|^2)} \|x - y\|^2. \end{aligned}$$

Then we know the Euclidean distance from \mathbb{R}^d to \mathbb{S}^d is scaled by $\frac{2R}{\sqrt{(R^2 + \|x\|^2)(R^2 + \|y\|^2)}}$. Therefore, comparing ratio of volume elements on \mathbb{R}^d and \mathbb{S}^d , the Jacobian determinant is proportional to $(R^2 + \|x\|^2)^d$.

B. ADDITIONAL SIMULATIONS

We have included some numerical examples in Section 6. In this section, we give additional simulations for SPS and SBPS.

B.1. The function $g_k(\cdot)$ used in Section 3.2. We plot the function g_k in Fig. 9 for different values of k .

B.2. SPS: burn-in starting from the south pole. We have shown the traceplots and ACFs for starting from the north pole in Fig. 5. In this example, Fig. 10 shows traceplots and ACFs of SPS (the first column) starting from the south pole and RWM (the second column) starting from the target mode. We plot the traceplots and ACFs of the 1-st coordinate and negative log-target density, as well as traceplots of the first two coordinates. The target is standard Gaussian in $d = 100$ dimensions. The proposal variance for RWM is tuned such that the acceptance rate is about 0.234, which is known to be the optimal acceptance rate [RGG97]. For SPS, the acceptance rate is roughly 0.78, which is the lowest acceptance rate possible.

According to Fig. 10, the SPS mixes almost immediately. Indeed, the transient phase of SPS in $d = 100$ dimensions is less than 10 iterations. Comparing with SPS, even starting from the target mode, the first 100 iterations are the transient phase of RWM. In the stationary phase, with an acceptance rate of 0.78, SPS generates almost uncorrelated samples according to the ACFs. Comparing with SPS, the samples from RWM with optimal acceptance rate 0.234 are highly correlated in high dimensions.

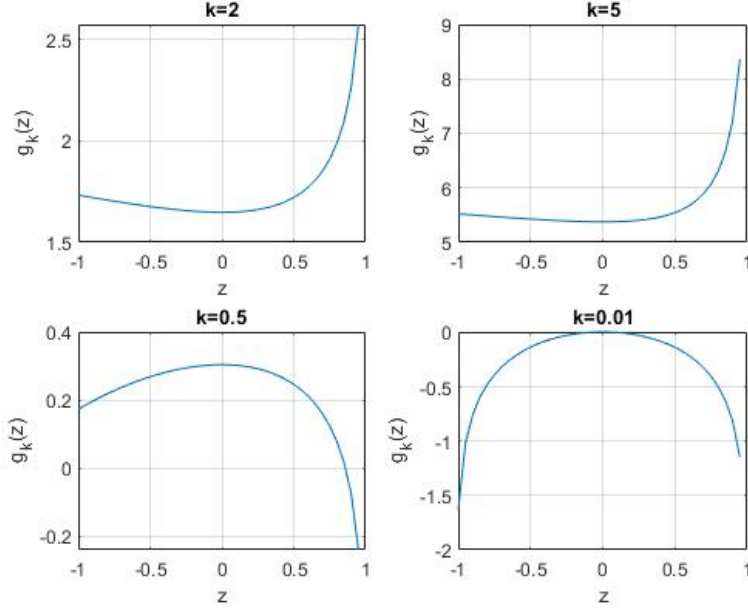


FIGURE 9. The function $g_k(z)$ used in Section 3.2 for different values of k .

B.3. SPS versus GSPS. In this example, we study SPS when the covariance matrix of the target distribution does not equal to the identity matrix. We choose $R = \sqrt{d}$ and the target is multivariate student's t with covariance matrix Σ that satisfies the sum of eigenvalues of Σ is d , i.e., $\lambda_1 + \dots + \lambda_d = d$. We compare the decay of the performance of SPS with the performance of GSPS which uses the covariance matrix Σ . In the simulations, we consider the cases that a sequence of covariance matrices $\Sigma_1, \Sigma_2, \dots, \Sigma_{50}$ are all block-diagonal and we add different numbers of diagonal sub-blocks which equal to a particular 2×2 matrix. For example, for the case of one sub-block, denoted by Σ_1 :

$$\Sigma_1 := \begin{pmatrix} 1 & 0.8 & 0 & \cdots & 0 \\ 0.8 & 1 & 0 & \cdots & 0 \\ 0 & 0 & 1 & \cdots & 0 \\ \vdots & \vdots & \cdots & \ddots & \vdots \\ 0 & 0 & 0 & \cdots & 1 \end{pmatrix}$$

One can easily verify the eigenvalues are

$$\Lambda_1 = (0.2, 1.8, 1, 1, \dots, 1)^T$$

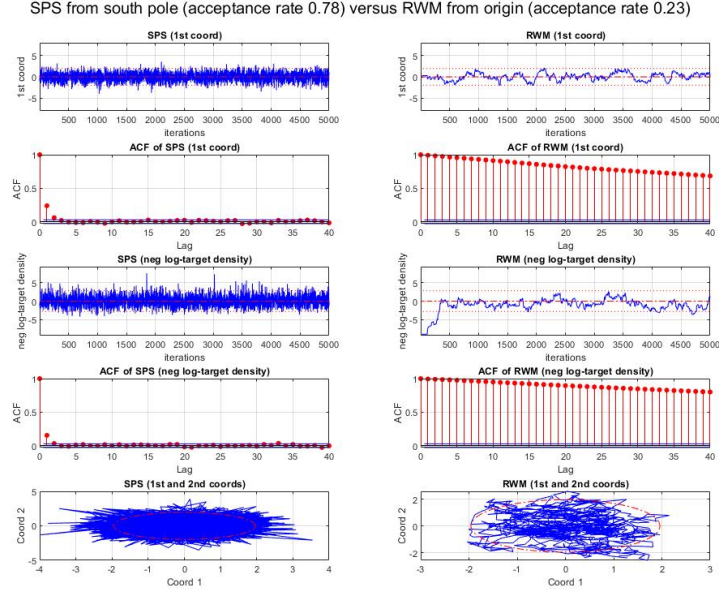


FIGURE 10. Traceplots and ACFs of the 1-st coordinate, negative log-target density, and the first two coordinates, for standard Gaussian target in dimension 100: SPS from south pole (the first column) vs RWM from origin (the second column).

and the first two coordinates has rotation with angle $3\pi/4$, since

$$\begin{pmatrix} 1 & 0.8 \\ 0.8 & 1 \end{pmatrix} = \begin{pmatrix} \cos \frac{3\pi}{4} & -\sin \frac{3\pi}{4} \\ \sin \frac{3\pi}{4} & \cos \frac{3\pi}{4} \end{pmatrix} \begin{pmatrix} 0.2 & 0 \\ 0 & 1.8 \end{pmatrix} \begin{pmatrix} \cos \frac{3\pi}{4} & -\sin \frac{3\pi}{4} \\ \sin \frac{3\pi}{4} & \cos \frac{3\pi}{4} \end{pmatrix}^T$$

Thus, we have the corresponding rotation matrix used by GSPS:

$$Q_1 := \begin{pmatrix} \cos \frac{3\pi}{4} & -\sin \frac{3\pi}{4} & 0 & \cdots & 0 \\ \sin \frac{3\pi}{4} & \cos \frac{3\pi}{4} & 0 & \cdots & 0 \\ 0 & 0 & 1 & \cdots & 0 \\ \vdots & \vdots & \cdots & \ddots & \vdots \\ 0 & 0 & 0 & \cdots & 1. \end{pmatrix}$$

Similarly, we can replace the diagonal terms by 2 sub-blocks to define Σ_2 and the corresponding rotation matrix:

$$\Sigma_2 := \begin{pmatrix} 1 & 0.8 & 0 & 0 & 0 & \cdots & 0 \\ 0.8 & 1 & 0 & 0 & 0 & \cdots & 0 \\ 0 & 0 & 1 & 0.8 & 0 & \cdots & 0 \\ 0 & 0 & 0.8 & 1 & 0 & \cdots & 0 \\ 0 & 0 & 0 & 0 & 1 & \cdots & 0 \\ \vdots & \vdots & \cdots & \ddots & \vdots & & \\ 0 & 0 & 0 & 0 & 0 & \cdots & 1 \end{pmatrix}, \quad Q_2 := \begin{pmatrix} \cos \frac{3\pi}{4} & -\sin \frac{3\pi}{4} & 0 & 0 & 0 & \cdots & 0 \\ \sin \frac{3\pi}{4} & \cos \frac{3\pi}{4} & 0 & 0 & 0 & \cdots & 0 \\ 0 & 0 & \cos \frac{3\pi}{4} & -\sin \frac{3\pi}{4} & 0 & \cdots & 0 \\ 0 & 0 & \sin \frac{3\pi}{4} & \cos \frac{3\pi}{4} & 0 & \cdots & 0 \\ 0 & 0 & 0 & 0 & 1 & \cdots & 0 \\ \vdots & \vdots & \cdots & \ddots & \vdots & & \\ 0 & 0 & 0 & 0 & 0 & \cdots & 1 \end{pmatrix}.$$

We can define $\Sigma_3, \dots, \Sigma_{50}$ and the corresponding rotation matrices used for GSPS in the same way.

We run simulations for SPS for certain targets without using the true covariance matrices and we tune the acceptance rate of SPS to be 0.234 (or the closest possible). For comparison with the GSPS, we assume GSPS use the correct covariance matrices of the targets, but the proposal variances h^2 are chosen to be *the same* as those used for SPS. We then consider the performance of GSPS as the *benchmark*, since GSPS provides the optimal performance for SPS by using the information of the true target covariance matrix with the same proposal variance. We consider ACFs of two cases: the “latitude” and the 1-st coordinate. In Fig. 11, the first and third columns show the ACFs of the latitude and first coordinate of SPS for $d = 100$ dimensional multivariate student’s t targets with different covariance matrices indexed by the number of sub-blocks (the proposal variances are tuned to target the 0.234 acceptance rate). For the same proposal variances, the second and fourth columns show the performance of the GSPS (the “benchmark”) using the true target covariance matrices. From Fig. 11, one can see that the SPS performs well when the number of sub-blocks is small. For the first and second rows, the acceptance rates of SPS cannot be as low as 0.234 and they equal to 0.48 and 0.30, respectively. The ACF decreases slower as the lag when the number of sub-blocks increases. From the “benchmark” in the second and fourth column, we know the proposal variance h^2 becomes smaller. However, even in the case of Σ_{50} (the last row), the ACF still decreases much faster than RWM Fig. 5 for Gaussian targets. Note that in this examples, all the targets are heavy-tailed targets and we know RWM is not even geometrically ergodic so the performance of RWM would be much worse than in Fig. 5. Overall, we can conclude that SPS is much better than RWM even when the covariance matrix is Σ_{50} and the performance can be significantly improved by GSPS even without changing the proposal variance. This suggest that adaptively tuning the parameters of GSPS (in the adaptive MCMC framework) is very promising.

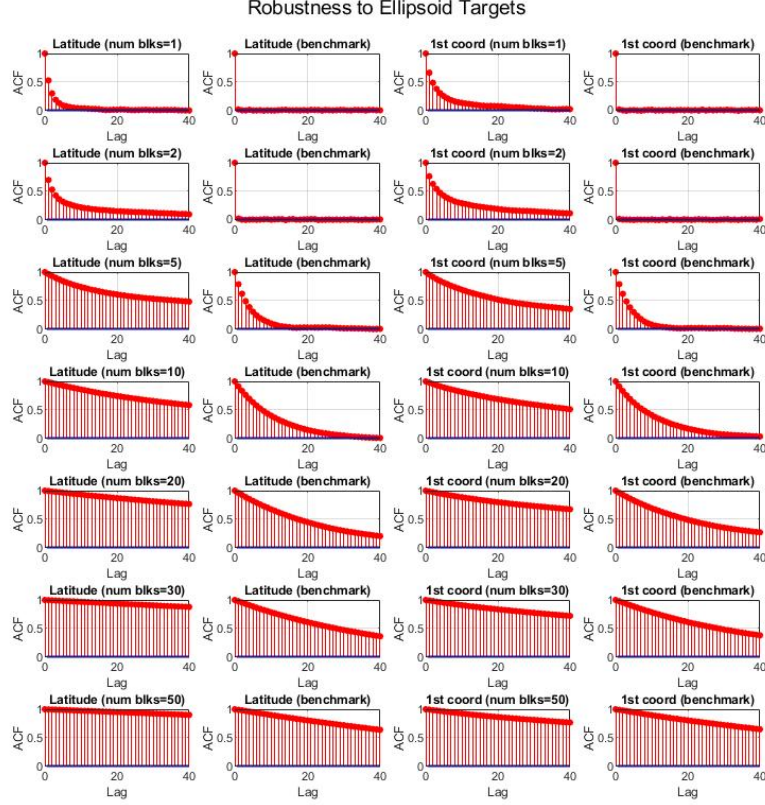


FIGURE 11. SPS versus GPS: ACFs of latitude (first two columns) and 1-st coordinate (last two columns) for SPS (first and third columns) and GPS (second and fourth columns). The proposal variances of SPS are chosen to target the 0.234 acceptance rate (for the first and second rows, the acceptance rates are 0.48 and 0.30, respectively). The proposal variances of GPS are chosen to be the same as those for SPS to provide the “benchmark” performance. Target is 100-dim ellipsoid targets using 2×2 blocks; GPS (benchmark) uses the true covariance matrices.

B.4. The definition of Effective Sample Size (ESS) for SBPS. We study the PDMP algorithms using the notion of Effective Sample Size (ESS) per switch. We first recall the definition of ESS in [BFR19, supplemental material]. Consider a function

$g : \mathbb{R}^d \rightarrow \mathbb{R}$, for a continuous process $Y(t)$, by CLT

$$\frac{1}{\sqrt{t}} \int_0^t [g(Y(s)) - \pi(h)] ds \rightarrow \sigma_g^2$$

where σ_h^2 is called *asymptotic variance*.

The asymptotic variance can be estimated using batches of length T/B

$$\hat{\sigma}_g^2 = \frac{1}{B-1} \sum_{i=1}^B (X_i - \bar{X})^2,$$

where $\bar{X} = \frac{1}{B} \sum_i X_i$ and

$$X_i := \sqrt{\frac{B}{T}} \int_{(i-1)T/B}^{iT/B} g(Y(s)) ds.$$

We also estimate the mean and variance under π by

$$\widehat{\pi(g)} := \frac{1}{T} \int_0^T g(Y(s)) ds, \quad \widehat{\text{var}_\pi(g)} := \frac{1}{T} \int_0^T g(Y(s))^2 ds - \left(\widehat{\pi(g)} \right)^2.$$

Then the ESS is estimated by

$$\widehat{\text{ESS}} := \frac{T \widehat{\text{var}_\pi(g)}}{\hat{\sigma}_g^2}$$

The ESS per switch is estimated by

$$\text{ESS per Switch} = \frac{\widehat{\text{ESS}}}{\text{Number of Events Simulated}}$$

We consider three cases for g , one is the first coordinate, the second one is the *negative log-target density*:

$$g(t) = \sqrt{d} \left(\frac{\|Y(t)\|^2}{d} - 1 \right) \sim \mathcal{N}(0, 2),$$

where the distribution holds for standard Gaussian target. The third one is the square of the first coordinate.

Remark B.1. If in a simulation of event, there's only one evaluation of the full likelihood, then ESS per switch is the same as ESS per epoch. \triangleleft

B.5. SBPS: traceplots and ACFs. In Fig. 7, we have studied SBPS by the traceplots and ACFs for the multivariate student's t target with DoF = $d = 100$ for low refresh rate. In this example, we study other settings. Fig. 12 shows the traceplots and ACFs for multivariate student's t target with large refresh rate), Fig. 13 and Fig. 14 are those for standard Gaussian target (with $d = 100$) using small and large refresh rates, respectively. We consider three cases: the 1-st coordinate, the negative log-density, and the squared 1-st coordinate, respectively. Since SBPS is a continuous time process, for the traceplot and ACF, we further discretize every unit time into 5 samples. $N = 1000$ events are simulated. Low refresh rate corresponds to 0.2 and high refresh rate corresponds to 2.

From Fig. 13, there are several similar interesting observations as in Fig. 7. The ACFs for all three cases have certain periodic behavior, and can take negative values for the first two cases. As a result of negative ACFs, the ESS per Switch is larger than 1 in the first two cases. For high refresh rate cases such as in Fig. 12 and Fig. 14, the periodic behavior and negativity of ACFs disappear and the corresponding ESS per Switch is smaller than 1, (note that the performance for SBPS is always significantly better than the traditional BPS in the simulations). This suggests that larger proportion of bounce events are helpful since bounce events use the information of the gradients of log-target density. As the refreshment events for SBPS are very efficient in the transient phase, the refresh rate can be chosen to be very low. This is not the case for BPS and the refreshments in the transient phase for BPS is inefficient in high dimensions.

B.6. SBPS: ESS per switch for multivariate student's t target. We have studied the efficiency curves of SBPS and BPS in terms of ESS per Switch versus the refresh rate for Gaussian target in Fig. 8. In this example, we consider the case of multivariate student's t target with DoF equals d . The first subplot of Fig. 15 contains the proportion of refreshments in all the N events for varying refresh rates. Note that there is no bounce events for the SBPS so all the events for SBPS are refreshments. In the other three subplots of Fig. 15, we plot the logarithm of ESS per Switch as a function of the refresh rate for three cases, the 1-st coordinate, the negative log-density, and the squared 1-st coordinate. For each efficiency curve, $N = 1000$ events are simulated, random initial value for SBPS and BPS starts from stationarity. As SBPS and BPS are continuous-time processes, each unit time is discretized into 5 samples.

According to Fig. 15, the ESS per Switch of SBPS is much larger than the ESS per Switch of BPS for all cases (actually the gap is larger than the cases for Gaussian target, and the gap becomes larger in higher dimensions). For all the three cases, the ESS per Switch of SBPS can be larger than 1 if the refresh rate is relatively low, this is also better than the cases for Gaussian target. For BPS, however, even starting from stationarity, the ESS per Switch is always much smaller than 1.

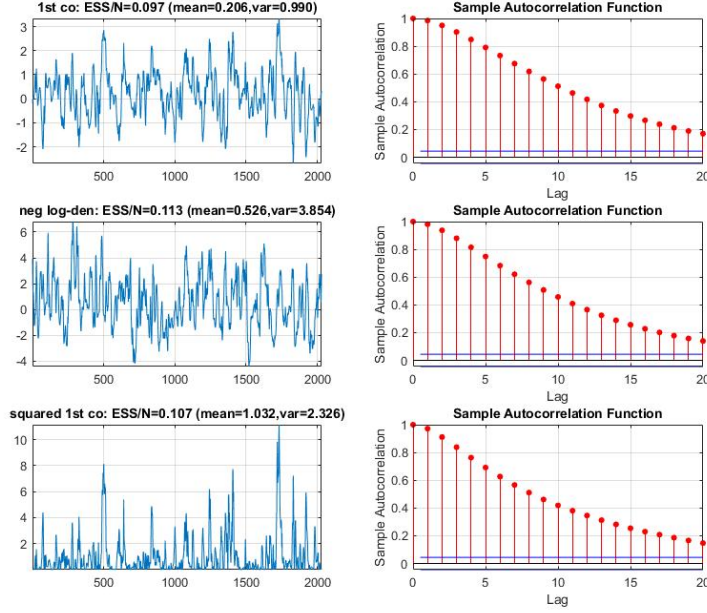
Trace Plots and ACFs: Refresh Rate=2.0 (random initial, $d=100$, $N=1000$, $\text{DoF}/d=1.0$, discretize=0.2)

FIGURE 12. Trace plots and ACFs for the 1-st coordinate, the negative log-density, and the squared 1-st coordinate. Target distribution is multivariate student's t with $\text{DoF} = d = 100$. Every unit time is discretized into 5 samples. $N = 1000$ events are simulated. High refresh rate = 2.

B.7. SBPS: robustness to target variance. Previously, in Fig. 13 and Fig. 14, we have studied the traceplots and ACFs of SBPS for standard Gaussian target with $d = 100$ using small and large refresh rates, respectively. In this example, we repeat the same numerical experiments except that, instead of considering standard Gaussian targets, we consider Gaussian targets with larger or smaller variances. Since we still choose $R = \sqrt{d}$, this is equivalent to study the robustness of SBPS to the choice of the radius of the sphere. Other than the target variances, numerical experiment settings are the same as in Fig. 13 and Fig. 14.

We consider two cases, Gaussian target $\mathcal{N}(0, 1.5I_d)$ (see Fig. 16 for small refresh rate and Fig. 17 for large refresh rate) and Gaussian target $\mathcal{N}(0, 0.7I_d)$ (see Fig. 18 for small refresh rate and Fig. 19 for large refresh rate). Comparing with the cases when the variance is 1 in Fig. 13 and Fig. 14, we can see that the traceplots and ACFs for first coordinate and squared first coordinate are not affected too much. For the negative log-target density, the traceplots and ACFs behave quite differently. When the target covariance matrix is $1.5I_d$, more bounce events occur when the SBPS

Trace Plots and ACFs: Refresh Rate=0.2 (random initial, $d=100$, $N=1000$, $\text{DoF}/d=\text{Inf}$, $\text{discretize}=0.2$)

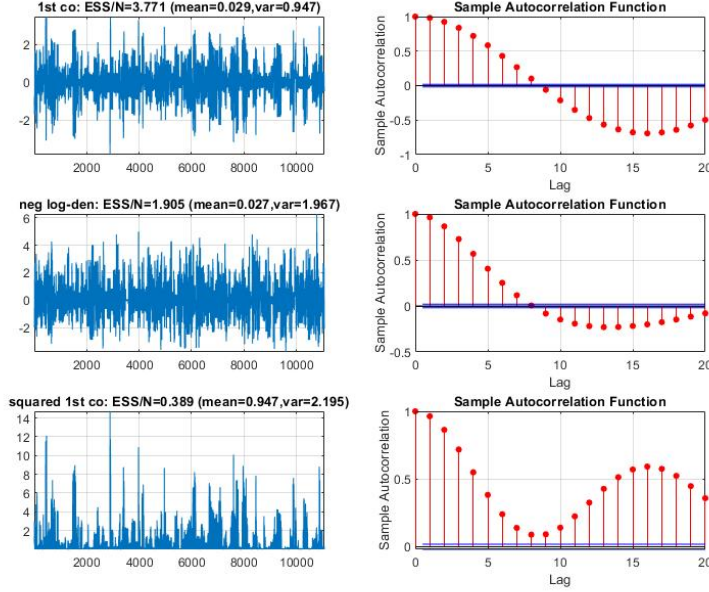


FIGURE 13. Trace plots and ACFs for the 1-st coordinate, the negative log-density, and the squared 1-st coordinate. Target distribution is standard Gaussian with $d = 100$. Every unit time is discretized into 5 samples. $N = 1000$ events are simulated. Low refresh rate = 0.2.

is moving to the equator. As a result, the SBPS stays almost all the time in the “northern hemisphere”. When the target covariance matrix is $0.7I_d$, the situation is exactly the opposite: the SBPS stays almost all the time in the “southern hemisphere”. The traceplots and ACFs in all the four figures show that the performance of SBPS is quite robust to the target variance.

Trace Plots and ACFs: Refresh Rate=2.0 (random initial, $d=100$, $N=1000$, $\text{DoF}/d=\text{Inf}$, discretize=0.2)

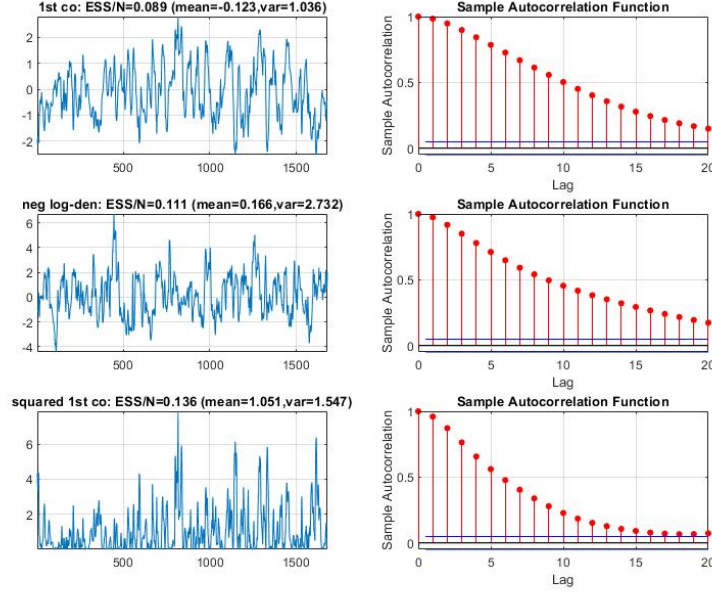


FIGURE 14. Trace plots and ACFs for the 1-st coordinate, the negative log-density, and the squared 1-st coordinate. Target distribution is standard Gaussian with $d = 100$. Every unit time is discretized into 5 samples. $N = 1000$ events are simulated. High refresh rate = 2.

Efficiency Curves: ESS/N vs refresh rate (Student-T(d) target)

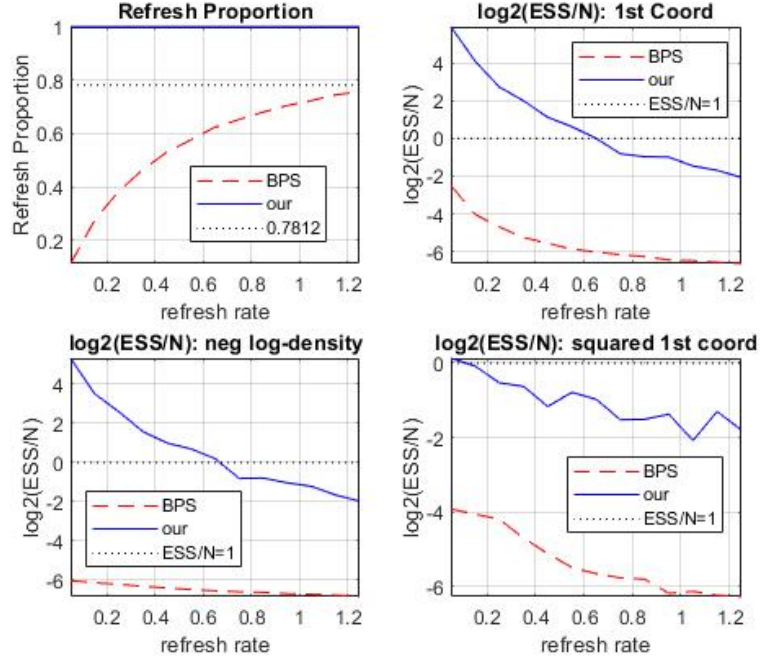


FIGURE 15. Efficiency: ESS per Switch for SBPS and BPS for varying refresh rate. $N = 1000$ events are simulated, Random initial values for SBPS and BPS starts from stationarity. Each unit time is discretized to 5 samples. Target distribution: Multivariate student's t with DoF = $d = 100$. The first subplot is the proportion of refreshment events in all N events. The other three subplots are ESS for the 1-st coordinate, the negative log-density, and the squared 1-st coordinate, respectively.

Trace Plots and ACFs: Gaussian(0.0,1.5) (refresh=0.2 , d=100, N=1000, discretize=0.2)

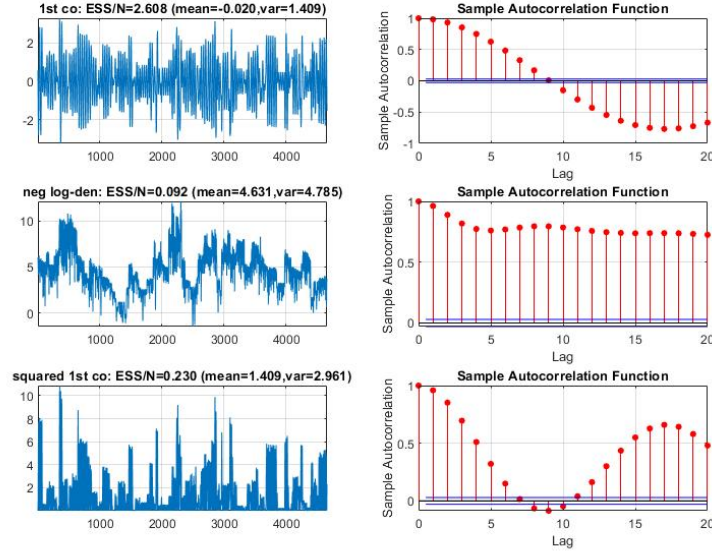


FIGURE 16. Trace plots and ACFs for the 1-st coordinate, the negative log-density, and the squared 1-st coordinate. Target distribution is $\mathcal{N}(0, 1.5I_d)$ with $d = 100$ and we choose $R = d^{1/2}$. Every unit time is discretized into 5 samples. $N = 1000$ events are simulated. Low refresh rate = 0.2.

Trace Plots and ACFs: Gaussian(0.0,1.5) (refresh=2.0 , d=100, N=1000, discretize=0.2)

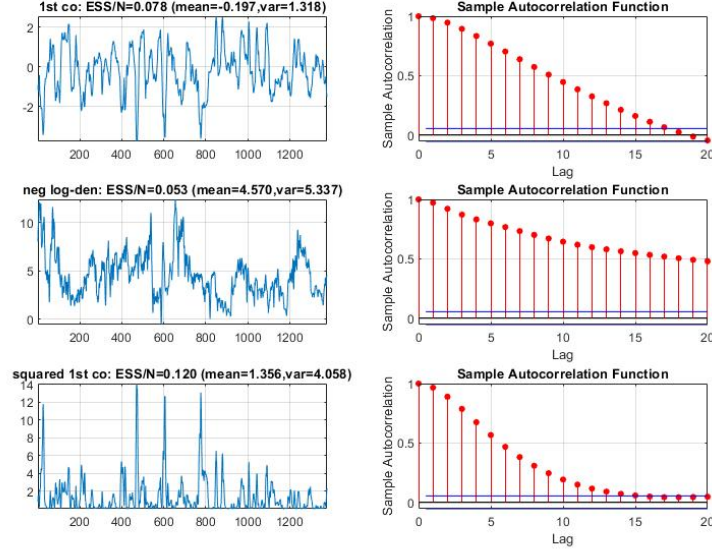


FIGURE 17. Trace plots and ACFs for the 1-st coordinate, the negative log-density, and the squared 1-st coordinate. Target distribution is $\mathcal{N}(0, 1.5I_d)$ with $d = 100$ and we choose $R = d^{1/2}$. Every unit time is discretized into 5 samples. $N = 1000$ events are simulated. High refresh rate = 2.

Trace Plots and ACFs: Gaussian(0.0,0.7) (refresh=0.2 , d=100, N=1000, discretize=0.2)

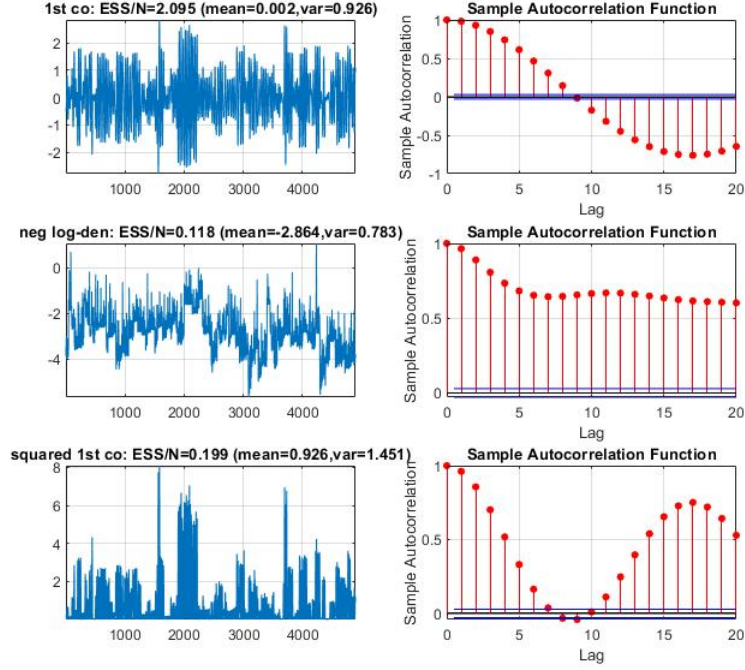


FIGURE 18. Trace plots and ACFs for the 1-st coordinate, the negative log-density, and the squared 1-st coordinate. Target distribution is $\mathcal{N}(0, 0.7I_d)$ with $d = 100$ and we choose $R = d^{1/2}$. Every unit time is discretized into 5 samples. $N = 1000$ events are simulated. Low refresh rate = 0.2.

Trace Plots and ACFs: Gaussian(0.0,0.7) (refresh=2.0 , d=100, N=1000, discretize=0.2)

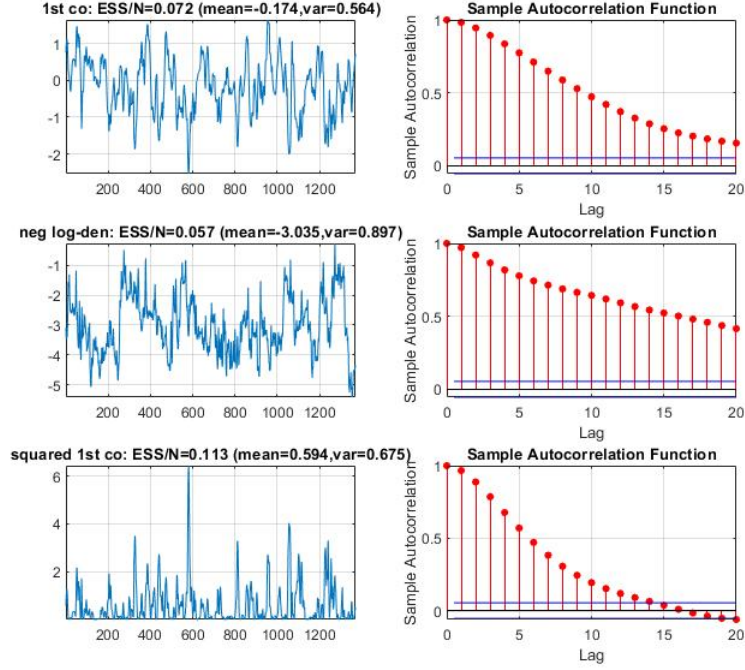


FIGURE 19. Trace plots and ACFs for the 1-st coordinate, the negative log-density, and the squared 1-st coordinate. Target distribution is $\mathcal{N}(0, 0.7I_d)$ with $d = 100$ and we choose $R = d^{1/2}$. Every unit time is discretized into 5 samples. $N = 1000$ events are simulated. High refresh rate = 2.

REFERENCES

- [ADW21] C. Andrieu, P. Dobson, and A. Q. Wang. “Subgeometric hypocoercivity for piecewise-deterministic Markov process Monte Carlo methods”. *Electronic Journal of Probability* 26 (2021), pp. 1–26.
- [And+21] C. Andrieu, A. Durmus, N. Nüsken, and J. Roussel. “Hypocoercivity of piecewise deterministic Markov process-Monte Carlo”. *The Annals of Applied Probability* 31.5 (2021), pp. 2478–2517.
- [BCVD18] A. Bouchard-Côté, S. J. Vollmer, and A. Doucet. “The bouncy particle sampler: A nonreversible rejection-free Markov chain Monte Carlo method”. *Journal of the American Statistical Association* 113.522 (2018), pp. 855–867.
- [BFR19] J. Bierkens, P. Fearnhead, and G. Roberts. “The zig-zag process and super-efficient sampling for Bayesian analysis of big data”. *The Annals of Statistics* 47.3 (2019), pp. 1288–1320.
- [BKR18] J. Bierkens, K. Kamatani, and G. O. Roberts. “High-dimensional scaling limits of piecewise deterministic sampling algorithms”. *arXiv:1807.11358* (2018).
- [BKW09] E. P. Bernard, W. Krauth, and D. B. Wilson. “Event-chain Monte Carlo algorithms for hard-sphere systems”. *Physical Review E* 80.5 (2009), p. 056704.
- [Cot+13] S. L. Cotter, G. O. Roberts, A. M. Stuart, and D. White. “MCMC methods for functions: modifying old algorithms to make them faster”. *Statistical Science* 28.3 (2013), pp. 424–446.
- [Cox61] H. S. M. Coxeter. “Introduction to geometry” (1961).
- [CRR05] O. F. Christensen, G. O. Roberts, and J. S. Rosenthal. “Scaling limits for the transient phase of local Metropolis–Hastings algorithms”. *Journal of the Royal Statistical Society: Series B (Statistical Methodology)* 67.2 (2005), pp. 253–268.
- [DBCD19] G. Deligiannidis, A. Bouchard-Côté, and A. Doucet. “Exponential ergodicity of the bouncy particle sampler”. *The Annals of Statistics* 47.3 (2019), pp. 1268–1287.
- [Del+21] G. Deligiannidis, D. Paulin, A. Bouchard-Côté, and A. Doucet. “Randomized Hamiltonian Monte Carlo as scaling limit of the bouncy particle sampler and dimension-free convergence rates”. *The Annals of Applied Probability* 31.6 (2021), pp. 2612–2662.
- [DGM20] A. Durmus, A. Guillin, and P. Monmarché. “Geometric ergodicity of the bouncy particle sampler”. *The Annals of Applied Probability* 30.5 (2020), pp. 2069–2098.

- [DMT95] D. Down, S. P. Meyn, and R. L. Tweedie. “Exponential and uniform ergodicity of Markov processes”. *The Annals of Probability* 23.4 (1995), pp. 1671–1691.
- [EK86] S. N. Ethier and T. G. Kurtz. *Markov processes: Characterization and Convergence*. Wiley Series in Probability and Mathematical Statistics: Probability and Mathematical Statistics. Characterization and convergence. Wiley, New York, 1986. ISBN: 0-471-08186-8.
- [Fea+18] P. Fearnhead, J. Bierkens, M. Pollock, G. O. Roberts, et al. “Piecewise deterministic Markov processes for continuous-time Monte Carlo”. *Statistical Science* 33.3 (2018), pp. 386–412.
- [GC11] M. Girolami and B. Calderhead. “Riemann manifold langevin and hamiltonian monte carlo methods”. *Journal of the Royal Statistical Society: Series B (Statistical Methodology)* 73.2 (2011), pp. 123–214.
- [GMP17] F. W. Gehring, G. J. Martin, and B. P. Palka. *An introduction to the theory of higher-dimensional quasiconformal mappings*. Vol. 216. American Mathematical Soc., 2017.
- [JG12] L. T. Johnson and C. J. Geyer. “Variable transformation to obtain geometric ergodicity in the random-walk Metropolis algorithm”. *The Annals of Statistics* (2012), pp. 3050–3076.
- [JH00] S. F. Jarner and E. Hansen. “Geometric ergodicity of Metropolis algorithms”. *Stochastic processes and their applications* 85.2 (2000), pp. 341–361.
- [JR07] S. F. Jarner and G. O. Roberts. “Convergence of Heavy-tailed Monte Carlo Markov Chain Algorithms”. *Scandinavian Journal of Statistics* 34.4 (2007), pp. 781–815.
- [Kam18] K. Kamatani. “Efficient strategy for the Markov chain Monte Carlo in high-dimension with heavy-tailed target probability distribution”. *Bernoulli* 24.4B (2018), pp. 3711–3750.
- [Lie+21] H. C. Lie, D. Rudolf, B. Sprungk, and T. J. Sullivan. “Dimension-independent Markov chain Monte Carlo on the sphere”. *arXiv:2112.12185* (2021).
- [Lig10] T. M. Liggett. *Continuous time Markov processes: an introduction*. Vol. 113. American Mathematical Soc., 2010.
- [MMB18] A. Mijatović, V. Mramor, and G. U. Bravo. “Projections of spherical Brownian motion”. *Electronic Communications in Probability* 23 (2018), pp. 1–12.
- [MS18] O. Mangoubi and A. Smith. “Rapid mixing of geodesic walks on manifolds with positive curvature”. *The Annals of Applied Probability* 28.4 (2018), pp. 2501–2543.

- [MT12] S. P. Meyn and R. L. Tweedie. *Markov chains and stochastic stability*. Springer Science & Business Media, 2012.
- [MT96] K. L. Mengersen and R. L. Tweedie. “Rates of convergence of the Hastings and Metropolis algorithms”. *The Annals of Statistics* 24.1 (1996), pp. 101–121.
- [Oll09] Y. Ollivier. “Ricci curvature of Markov chains on metric spaces”. *Journal of Functional Analysis* 256.3 (2009), pp. 810–864.
- [PHL20] E. Pompe, C. Holmes, and K. Łatuszyński. “A framework for adaptive MCMC targeting multimodal distributions”. *The Annals of Statistics* 48.5 (2020), pp. 2930–2952.
- [RGG97] G. O. Roberts, A. Gelman, and W. R. Gilks. “Weak convergence and optimal scaling of random walk Metropolis algorithms”. *The Annals of Applied Probability* 7.1 (1997), pp. 110–120.
- [RR09] G. O. Roberts and J. S. Rosenthal. “Examples of adaptive MCMC”. *Journal of computational and graphical statistics* 18.2 (2009), pp. 349–367.
- [RS94] G. O. Roberts and A. F. Smith. “Simple conditions for the convergence of the Gibbs sampler and Metropolis-Hastings algorithms”. *Stochastic processes and their applications* 49.2 (1994), pp. 207–216.
- [RT96a] G. O. Roberts and R. L. Tweedie. “Exponential convergence of Langevin distributions and their discrete approximations”. *Bernoulli* (1996), pp. 341–363.
- [RT96b] G. O. Roberts and R. L. Tweedie. “Geometric convergence and central limit theorems for multidimensional Hastings and Metropolis algorithms”. *Biometrika* 83.1 (1996), pp. 95–110.
- [SFR10] C. Sherlock, P. Fearnhead, and G. O. Roberts. “The random walk Metropolis: linking theory and practice through a case study”. *Statistical Science* 25.2 (2010), pp. 172–190.
- [VR21a] G. Vasdekis and G. O. Roberts. “A Note on the Polynomial Ergodicity of the One-Dimensional Zig-Zag process”. *arXiv:2106.11357* (2021).
- [VR21b] G. Vasdekis and G. O. Roberts. “Speed Up Zig-Zag”. *arXiv:2103.16620* (2021).
- [YR17] J. Yang and J. S. Rosenthal. “Complexity Results for MCMC derived from Quantitative Bounds”. *arXiv:1708.00829* (2017).
- [YRR20] J. Yang, G. O. Roberts, and J. S. Rosenthal. “Optimal scaling of random-walk Metropolis algorithms on general target distributions”. *Stochastic Processes and their Applications* 130.10 (2020), pp. 6094–6132.
- [ZHCG18] E. Zappa, M. Holmes-Cerfon, and J. Goodman. “Monte Carlo on manifolds: sampling densities and integrating functions”. *Communications on Pure and Applied Mathematics* 71.12 (2018), pp. 2609–2647.